FAST CONVERGING ROBUST BEAMFORMING FOR DOWNLINK MASSIVE MIMO SYSTEMS IN HETEROGENEOUS NETWORKS

by

Malcolm Makomborero Sande

Submitted in partial fulfilment of the requirements for the degree
Master of Engineering (Electronic Engineering)

in the

Department of Electrical, Electronic and Computer Engineering
Faculty of Engineering, Built Environment and Information Technology

UNIVERSITY OF PRETORIA

February 2018

SUMMARY

FAST CONVERGING ROBUST BEAMFORMING FOR DOWNLINK MASSIVE MIMO SYSTEMS IN HETEROGENEOUS NETWORKS

by

Malcolm Makomborero Sande

Supervisor: Prof B.T. Maharaj

Department: Electrical, Electronic and Computer Engineering

University: University of Pretoria

Degree: Master of Engineering (Electronic Engineering)

Keywords: Massive MIMO, HetNet, macrocell, beamforming, matrix stuffing, ADMM algorithm.

Massive multiple-input multiple-output (MIMO) is an emerging technology, which is an enabler for future broadband wireless networks that support high speed connection of densely populated areas. Application of massive MIMO at the macrocell base stations in heterogeneous networks (HetNets) offers an increase in throughput without increasing the bandwidth, but with reduced power consumption. This research investigated the optimisation problem of signal-to-interference-plus-noise ratio (SINR) balancing for macrocell users in a typical HetNet scenario with massive MIMO at the base station. The aim was to present an efficient beamforming solution that would enhance inter-tier interference mitigation in heterogeneous networks. The system model considered the case of perfect channel state information (CSI) acquisition at the transmitter, as well as the case of imperfect CSI at the transmitter. A fast converging beamforming solution, which is applicable to both channel models, is presented.

The proposed beamforming solution method applies the matrix stuffing technique and the alternative direction method of multipliers, in a two-stage fashion, to give a modestly accurate and efficient solution. In the first stage, the original optimisation problem is transformed into standard second-order conic program (SOCP) form using the Smith form reformulation and applying the matrix stuffing technique for fast transformation. The second stage uses the alternative direction method of multipliers to solve the SOCP-based optimisation problem.

Simulations to evaluate the SINR performance of the proposed solution method were carried out with supporting software-based simulations using relevant MATLAB toolboxes. The simulation results of a typical single cell in a HetNet show that the proposed solution gives performance with modest accuracy, while converging in an efficient manner, compared to optimal solutions achieved by state-of-the-art modelling languages and interior-point solvers. This is particularly for cases when the number of antennas at the base station increases to large values, for both models of perfect CSI and imperfect CSI. This makes the solution method attractive for practical implementation in heterogeneous networks with large scale antenna arrays at the macrocell base station.

ACKNOWLEDGEMENTS

I would like to express my sincerest gratitude to the following people for their invaluable contribution during the course of this research work:

- My supervisor, Prof. B.T. Maharaj for his expert guidance and support.
- Prof. S. Hamouda, who is with Sup'Com in Tunisia, for her encouragement, expert insight and advice.
- The Sentech Chair in Broadband Wireless Multimedia Communications (BWMC) and the Mastercard Foundation Scholarship Fund for the resources and financial support.
- My fellow BWMC students for their technical advice and encouragement.
- My parents, my sisters, Ashiella Musindo and my close friends for their unending moral support and encouragement.

LIST OF ABBREVIATIONS

ABS	Almost blank subframes
ADMM	Alternative direction method of multipliers
AP	Access point
AWGN	Additive white Gaussian noise
BS	Base station
CoMP	Cooperative multi-point
CRE	Cell range expansion
CSG	Closed subscriber group
CSI	Channel state information
DAC	Digital-to-analogue converter
DPC	Dirty paper coding
eICIC	Enhanced inter-cell interference coordination
FDD	Frequency division duplexing
HIA	Hierarchical interference alignment
HMIA	Hierarchical multi-stage interference alignment
IA	Interference alignment
KKT	Karush-Kuhn-Tucker
LTE	Long-term evolution
MCM	Maximum correlation method
MIMO	Multiple-input multiple-output
MIMO-BC	Multiple-input multiple-output broadcast channel
ML	Maximum likelihood
MMSE	Minimum mean square error
MRT	Maximum ratio transmission
MS	Matrix stuffing
MUE	Macrocell user equipment

MU-MIMO	Multi-user multiple-input multiple-output
PA	Power amplifier
PISTA	Projected iterative shrinkage-thresholding algorithm
QEGT	Quantized equal gain transmission
QoS	Quality of service
RF	Radio-frequency
RTDD	Reversed time division duplexing
RZF	Regularised zero-forcing
SCA	Successive convex approximation
SCS	Splitting conic solver
SDP	Semi-definite program
SIN	Soft interference nulling
SINR	Signal-to-interference-plus-noise ratio
SISO	Single-input-single-output
SNR	Signal-to-noise ratio
SOCP	Second-order cone program
SUE	Small-cell user equipment
TDD	Time division duplexing
UE	User equipment
WMMSE	Weighted sum-minimum mean square error
WSRMax	Weighted sum rate maximization
ZF	Zero-forcing
ZFBF	Zero-forcing beamforming

TABLE OF CONTENTS

LIST OF TABLES

LIST OF FIGURES

CHAPTER 1 INTRODUCTION

1.1 PROBLEM STATEMENT

1.1.1 Context of the problem

The rapid growth and increasing demand for mobile access to the internet, cloud-based services and Big Data analytics presents a demand for very high data transmission rates. The next generation broadband wireless networks, commonly known as 5G, aim to support connection of the internet of people and internet of things (IoT), while providing high data rates and reduced latency for communication. The main key performance indicators for 5G networks are [1]:

- Increased capacity of up to 100-fold compared to current 4G technologies with peak data rates reaching up to 10Gbps, and minimum guaranteed user data rate ≥ 100Mbps,
- Massive connectivity with connection density ≥ 1M connections/ km2,
- Traffic density ≥ 10 Tbps/ km2,
- Reduced radio latency of less than 1 ms,
- Support for high mobility of up to 500km/h.

According to Shannon's channel capacity theorem, in order to increase the data rate, one has to increase either the transmission bandwidth or the signal-to-noise ratio (SNR) [2]. However, the limited radio-frequency (RF) spectrum restricts the maximum attainable bandwidth for wireless communication systems. On the other hand, increasing SNR is not always feasible because of transmission power constraints. The use of massive multiple-input multiple-output (MIMO) base stations (BSs) offers an increase in throughput without increasing the bandwidth, but with reduced power consumption [3].

In urban environments, a large proportion of data traffic is generated by large groups of users in a relatively small area, and with low mobility. Examples of such groups are found in restaurants, in stadiums, at stations and airports, and they are often known as hotspots. Use of traditional cellular networks in order to cope with high throughput demands of such

scenarios is expensive and practically infeasible [4]. The use of small-cells has been found effectively to increase the network capacity while reducing the total transmit power [5]. On the other hand, a large number of small-cells diminish network performance and quality of service (QoS) for the user [6]. The small-cell radii with BS antennas on and below rooftops cannot support highly mobile equipment and large area coverage is difficult. This has led to the introduction of the heterogeneous network (HetNet) structure. A typical HetNet comprises a macrocell with a high-power BS, which is overlaid by a number of small-cells with short range low-power access points (APs) [5]. These small-cells in HetNets are the so-called femtocells or picocells and they aim to serve the hotspots. The BSs serving femtocells and picocells are low-cost and are installed by the consumer, thus their distribution is time-varying.

Frequency reuse even for neighbouring cells in wireless communications has become a de facto standard in order to address the high throughput demand [7]. Although the HetNet structure leads to an improvement in the average spectral efficiency, its overlaid cell deployment with frequency reuse of one introduces severe inter-tier interference, especially for cell edge users in the macrocell [8]. This is because the macrocell users at the cell edges are further away from their serving BS and may be in close proximity to a small-cell BS. Although the small-cell BS transmits with lower power compared to the macrocell BS, it can cause significantly high interference with the macrocell users at the cell edges. The increased number of users in hotspots increases cell density and the classical resource management techniques based on frequency/space reuse and power control are incapable of curbing the additional interference.

Massive MIMO has been proposed to be applied at the macrocell BS in HetNets in order to enhance inter-tier interference mitigation further. Massive MIMO is a technique where arrays of hundreds of localised or distributed antennas serve many tens of users in the same time-frequency resource [9]. A massive MIMO system is also referred to as multi-user MIMO (MU-MIMO). Large-scale antenna arrays present a significant improvement in spectral efficiency and energy efficiency in wireless systems over the conventional MIMO used in long-term evolution (LTE) or 4G systems. Other benefits of massive MIMO

include reduced costs, reduced latency, increased reliability and high degrees of freedom [3], [10]. Use of massive MIMO presents a reduction in costs because it can be implemented with low-cost power amplifiers and there may not be need for other costly components such as large coaxial cables [5]. By virtue of having greater robustness to interference, massive MIMO systems are more reliable than conventional MIMO systems. The significantly large number of transmit antennas compared to user terminals in a massive MIMO system renders high degrees of freedom, which enables many users to be served simultaneously without increased use of transmission resources [8].

1.1.2 Research gap

A key enabler for the increased degrees of freedom in massive MIMO systems is the application of beamforming or precoding. For the downlink in massive MIMO systems, i.e. transmitting from BS to user terminal, precoding is the mapping of the message bearing signals for K users into M symbols for the M transmit antennas [9], and beamforming is achieved by combining elements into a phased array in order to create a certain required antenna directive pattern for a given required performance [11]. These two terms will be used interchangeably in this document.

Beamforming for downlink communication in massive MIMO networks that use the time division duplexing (TDD) protocol assumes channel reciprocity, i.e. identical uplink and downlink channels. This assumption, however, is not accurate, especially for users with high mobility and it diminishes their network performance, particularly the minimum achievable SNR. This is because channel reciprocity is highly sensitive to errors, which may be due to imperfect CSI acquisition or RF impairments.

With a large antenna array at the BS, it was shown that linear precoding techniques, such as zero-forcing beamforming (ZFBF) and minimum mean square error (MMSE) precoding, can achieve near optimum results in terms of sum rate performance [10], [12]. As a result, the less computationally complex linear precoding techniques have been found to be more practical to use [13]. The linear precoding schemes, however, cannot account for CSI acquisition errors and other factors that contribute to channel uncertainty. Linear

precoding techniques also become difficult to implement in hardware when the number of BS antennas grows to very large values.

To address the challenge of imperfect CSI acquisition at the transmitter, efficient robust beamforming techniques for massive MIMO downlink systems have been proposed. The key tool common to the proposed solutions is the application of robust optimisation theory. Robust beamforming is optimisation of the beamforming matrix for which the errors in CSI approximation are constrained to lie in an uncertainty set [14]. In other words, it is an uncertainty-based beamforming approach in which the uncertainty model is not stochastic, but rather deterministic and set-based [15].

Significant performance gains are expected from network topologies where massive MIMO BSs and HetNets coexist, and there are contributions that investigated how to best exploit the merits of massive MIMO with the main aim of interference nulling in HetNets [6], [16]-[18]. Thus, there is a need for a novel, uncertainty immune, massive MIMO beamforming method that significantly mitigates interference in heterogeneous wireless networks. The beamforming scheme should provide acceptable performance in terms of average maximum achievable user rate with relatively low complexity for practical implementation. In order to maximise the average user rate without increasing the bandwidth, one needs to maximise the worst-case signal-to-interference-plus-noise ratio (SINR).

1.2 RESEARCH OBJECTIVE AND QUESTIONS

The objective of this research was to investigate and address the optimisation problem of beamforming for massive MIMO in HetNets. In particular, the research focused on maximising the throughput and SINR performance of macrocell users for the case of imperfect CSI at the transmitter while considering power constraints. The focus was on investigating efficient methods to apply in order to solve the beamforming optimisation problems for massive MIMO downlink transmission in a typical HetNet scenario. The optimisation aims to maximise the performance of macrocell users in order to enhance inter-tier interference mitigation.

The research sought to find answers to the following questions:

- How can beamforming for massive MIMO be utilised to reduce interference in HetNets?
- To what extent should robustness in massive MIMO beamforming be accounted for while adhering to practical complexity?
- What is the cost, in terms of time-frequency resources needed and in terms of additional components needed, of implementing beamforming?
- Which optimisation techniques would be applicable to optimise beamforming for a relatively high sum rate or worst-case SINR with low complexity?
- Is there a suitable fast converging algorithm that can be applied to solve the optimisation problem? Is it perhaps necessary to design a new algorithm?
- What is the practical limit of the number of antennas at the BS for acceptable latency introduced by beamforming weight calculation?

1.3 APPROACH

In carrying out the research, a literature study of interference mitigation schemes in HetNets and prominent beamforming methods for massive MIMO systems was done. The focus of the literature study was on investigating the performance of the prominent beamforming schemes and applicability of robust beamforming in a HetNet scenario. An investigation into the performance of common optimal solvers for convex optimisation problems was also conducted. The investigation aimed to evaluate the performance of the solvers in terms of worst case SINR accuracy and time taken to converge to a solution. An efficient robust beamforming scheme for the downlink transmission for macrocell users in a HetNet was then designed. The performance of the proposed solution method was evaluated against the performance of the prominent optimal solvers and precoding schemes. The performance evaluation was carried out by performing simulations in MATLAB.

1.4 RESEARCH GOALS

Since "simultaneous, uncoordinated, communication in HetNets causes cross-tier interference and exacerbates the overall network performance" [9], the main goal of the research was to address this challenge. The aim was to design a robust beamforming scheme for the downlink transmission for macrocell users in a HetNet setup, where massive MIMO is employed at the macrocell BS. The beamforming scheme needed to account for imperfect CSI acquisition and RF impairments in order to model channel estimation error uncertainties. In addition, the beamforming scheme should converge to a solution quickly, with reduced complexity compared to optimal solvers, such that it can be implemented in practical low-latency applications.

1.5 RESEARCH CONTRIBUTION

From the research, a beamforming method that uses a solution based on a second-order cone program (SOCP) to solve beamforming optimisation problems for macrocell users in a HetNet scenario was proposed. The method was applied to solve the sum rate maximisation problem for the case of perfect CSI at the transmitter. The solution method was also adopted to solve the problem of maximising the minimum achievable SINR of the macrocell users in a HetNet scenario, for the case of imperfect CSI. The robust beamforming scheme accounts for channel error uncertainties at the transmitter, and it can be implemented in an uncoordinated network of BSs.

The proposed method was shown to present solutions with modest accuracy, while converging much faster than the typical optimal solution. The proposed two-stage method presented desirable convergence efficiency compared to the optimal solution method. In its first stage, the original non-convex optimisation problem is transformed into a standard SOCP using the Smith form reformulation and the matrix stuffing (MS) technique. The resulting SOCP is then solved by an efficient solver, which uses the alternative direction method of multipliers (ADMM).

1.6 PUBLICATIONS

The following articles have been submitted and/or published in the course of the research study; they have been derived from the work undertaken as part of the research process.

1.6.1 Conference papers

Details of papers that have been accepted to be published in proceedings of international conferences are given as follows:

- M. M. Sande, B. T. Maharaj, and S. Hamouda, "Fast Convergence for Efficient Beamforming in Massive MIMO Heterogeneous Networks," in *IEEE 12th International Conference on Wireless and Mobile Computing, Networking and Communications (WiMob)*, 2016, pp. 1-7.
- M. M. Sande and B. T. Maharaj, "Efficient Robust Beamforming for Downlink Transmission in Massive MIMO Systems," in *IEEE 87th Vehicular Technology Conference: VTC2018-Spring*, 2018, pp. 1-5.

1.6.2 Journal article

The following article was submitted to a peer-reviewed and ISI-accredited journal:

- M. M. Sande, S. Hamouda, and B. T. Maharaj, "Fast Converging Robust Beamforming for Massive MIMO in Heterogeneous Networks," *Mobile Networks and Applications*, under review, August 2017.

1.7 OVERVIEW OF STUDY

The rest of this dissertation is organised as follows:

Chapter 2 gives an overview of interference mitigation techniques that have been proposed for HetNets. More attention is paid to the use of massive MIMO in HetNets and the various models considered in literature. A literature review of beamforming schemes applicable to massive MIMO downlink transmission is also presented. These beamforming schemes include the prominent linear precoding schemes, which assume channel reciprocity, and robust beamforming schemes, which account for imperfect CSI. The

chapter ends with a summary of the common optimal solvers used to solve beamforming optimisation problems in literature.

Chapter 3 describes the system model that was used for analysis and performance evalution of the beamforming solutions considered for massive MIMO downlink transmission in HetNets. In the research, both CSI models were considered, that is, the perfect CSI model and the imperfect CSI model.

Chapter 4 presents the proposed fast converging beamforming solution method. The two-stage SOCP-based beamforming solution is applicable to both the perfect CSI case and the imperfect CSI case.

Chapter 5 presents and discusses the simulation results of the system model discussed in Chapter 3. The variable parameters in the system model are specified for each simulation result.

Chapter 6 gives a conclusion of the research findings, and in addition to the concluding remarks, it makes suggestions for future work that can be carried out to improve the research findings.

CHAPTER 2 LITERATURE STUDY

2.1 CHAPTER OBJECTIVES

This chapter presents findings from an investigation of interference mitigation techniques for heterogeneous wireless networks, paying particular attention to the use of massive MIMO at the macrocell BSs in HetNets for the case of imperfect CSI acquisition at the transmitter. Background on MIMO techniques and development to massive MIMO is firstly presented and the benefits of the use of massive MIMO BSs in classic networks are illustrated. Beamforming techniques for massive MIMO are investigated and a literature review of the prominent linear precoding schemes and robust beamforming techniques for massive MIMO is carried out. An evaluation of solution methods applicable to the robust optimisation problem is then carried out.

The HetNet setup is presented and an overview of the common inter-tier interference mitigation techniques for HetNets is given. A thorough literature study on the application of massive MIMO in HetNets is carried out, highlighting a comparison of the various methods presented in literature.

2.2 MIMO CONCEPTS

MIMO is a technique that is applied in modern cellular communication systems, where multiple antennas are used at both the transmitter and receiver sides [19]. Making use of multiple antennas at the transmitter and receiver allows next-generation cellular networks to provide high data transmission rates to a large number of users at longer ranges without consuming extra bandwidth and with reduced transmit power [20]. MIMO communication applies spatial diversity techniques that are based on exploiting the different fading experienced by the multiple independent paths. Leveraging this multipath phenomenon improves data rates for the users and it makes the system more robust.

A typical MIMO system consists of M transmit antennas and K receive antennas, and it is defined as an $M \times K$ system. Common configurations are the 2×1 and 2×2 systems, which apply the Alamouti scheme [21], and the 4×4 system. The 4×4 system forms the

basis of LTE-Advanced, while a maximum configuration of an 8 × 8 system is considered [19].

2.2.1 MIMO downlink transmission

Spatial multiplexing, a spatial diversity technique, allows a MIMO BS to transmit different data streams on the same resource block at the same time [22]. If all the transmitted data streams belong to one user, the system is known to operate in the single-user MIMO (SU-MIMO) mode, whereas if the data streams are intended for different users, the system is known to operate in the multi-user MIMO (MU-MIMO) mode. SU-MIMO makes it possible to achieve substantial peak data rates for a single user, and MU-MIMO offers good complexity/performance trade-off [19].

A typical MIMO configuration is shown in Figure 2.1, where the system is equipped with M transmit antennas and K receive antennas. Note that if $M = K = 1$, it will be a single-input single-output (SISO) system. Figure 2.1 shows that there are $M \times K$ independent paths. Let the channel response between transmitter i and receiver j be represented by h_{ij}. The MIMO channel matrix, **H**, is then given as

$$\mathbf{H} = \begin{bmatrix} h_{11} & h_{12} & \cdots & h_{1M} \\ h_{21} & h_{22} & \dots & h_{2M} \\ \vdots & \vdots & \ddots & \vdots \\ h_{K1} & h_{K2} & \dots & h_{KM} \end{bmatrix}. \tag{2.1}$$

The signal received by the antennas is given by

$$\mathbf{y} = \mathbf{Hx} + \mathbf{n}, \tag{2.2}$$

where **x** is the transmitted signal and **n** is the noise vector, which for additive white Gaussian noise (AWGN) consists of complex elements with zero mean and variance σ^2.

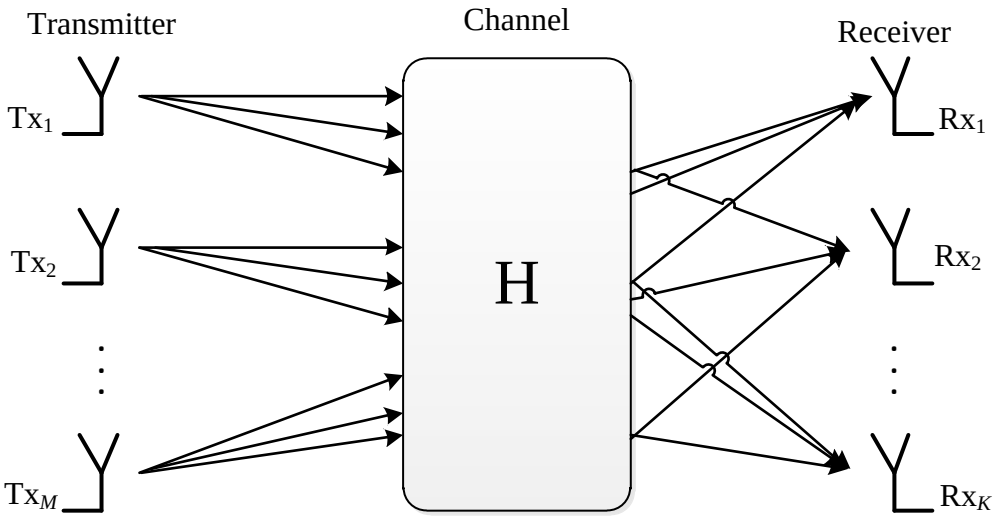

Figure 2.1. Configuration of an *M* x *K* MIMO system.

In addition to SU-MIMO and MU-MIMO, LTE-Advanced introduced the application of cooperative MIMO, which is a cooperative multi-point (CoMP) technique. This MIMO mode is an interference mitigation technique that improves cell-edge user throughput by enabling cooperation among MIMO BSs in cellular networks [19], [23]. In CoMP, BSs in multi-cell cellular networks coordinate to transmit data jointly to multiple users in the same time/frequency resource. CoMP coupled with MU-MIMO has been shown to improve SINR for users that receive relatively weak signals. This, in turn, provides higher data rates to the cell-edge users.

2.2.2 MIMO precoding

Precoding is an operation that enables spatial multiplexing for MIMO. This operation is achieved by multiplying the transmitted signal vector **x** with a precoding matrix **W** before transmission [21]. A predefined codebook that is known at both the transmitter and receiver is used to select the precoding matrix in MIMO precoding. The precoding matrices are unitary. That is, $\mathbf{W}^{H}\mathbf{W} = \mathbf{I}$, where $\mathbf{W}^{H}$ is the Hermitian transpose of the matrix **W** and **I** is an identity matrix. At the receiver side, the user equipment (UE) estimates the channel condition and selects the optimum precoding matrix that offers maximum capacity for the estimated channel. The UE then provides this information of the preferred precoding matrix to the BS via a feedback on the uplink control channel. Figure 2.2

illustrates this operation of precoding in a MIMO system. The receiver in Figure 2.2 is either a maximum likelihood (ML) receiver or an MMSE-based receiver.

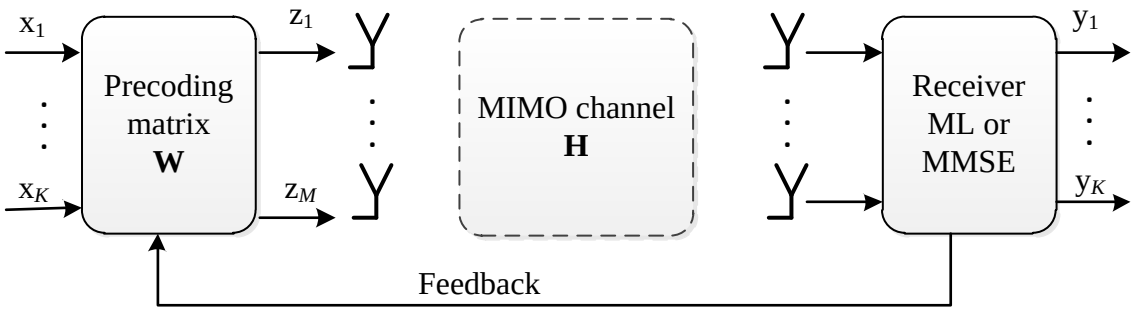

Figure 2.2. Illustration of MIMO precoding.

LTE-Advanced applies the concept of advanced precoding, which comprises a combination of single-user beamforming and spatial multiplexing or multi-user beamforming and spatial diversity [19]. This improves the range of transmission and, in addition, can either provide higher data rates for multiplexing or improve link reliability through diversity. LTE-Advanced also employs the technique of user-specific beamforming, which is a beamforming approach that does not use predefined precoder sets. This provides more degrees of freedom for the BS and it enables control or nearly nulling of intra-cell interference. The most common precoding techniques for such cases are zero-forcing (ZF) precoding, dirty paper coding (DPC), and maximisation of signal-to-leakage ratio. DPC achieves optimal performance; however, it suffers from intense computational complexity for a large number of users. These non-codebook precoding techniques require knowledge of the channel information between the BS and the user.

2.3 MASSIVE MIMO

Massive MIMO is a technique where MU-MIMO is scaled up by more than one order of magnitude. In massive MIMO systems, a BS equipped with an array of hundreds of antennas serves many tens of users in the same time-frequency resource [3]. The antennas at the BS can be localised or distributed, and the users are all equipped with a single antenna each. Although having multiple antennas for the UE would increase spectral

efficiency and data rate performance, the physical size of the UE would have to increase significantly as well. Reducing the separation between antennas in the same array decreases the achievable MIMO gain and it also increases power consumption to levels that may be too high for a single UE device [19].

Figure 2.3 shows a typical massive MIMO configuration for a classic multi-cell cellular network. The solid arrows in the figure indicate the intended downlink signal transmission, and the dashed arrows represent interference. Note that in a multi-cell massive MIMO system there are two forms of interference, that is, intra-cell interference and inter-cell interference. Intra-cell interference is when the transmitted signal from the BS is received by an unintended user in the same cell of the BS. On the other hand, inter-cell interference is when the transmitted signal is received by a user in different (usually adjacent) cell to the cell of the serving BS.

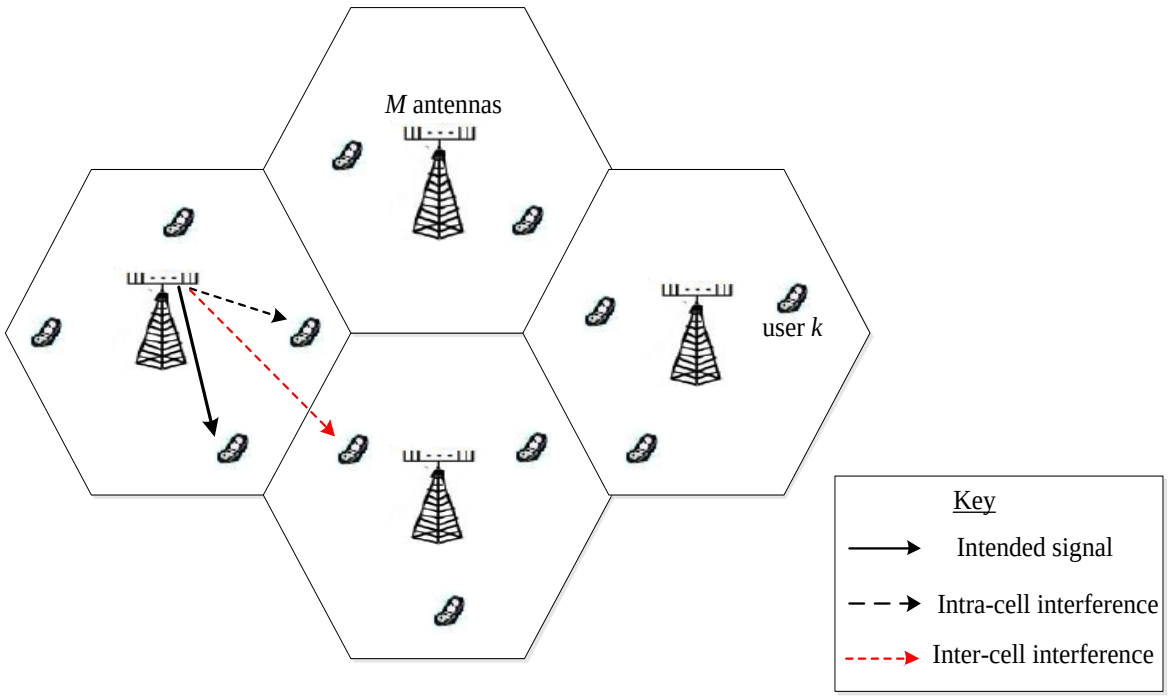

Figure 2.3. Typical structure of a classical massive MIMO cellular network.

2.3.1 Benefits of massive MIMO

The MU-MIMO setup of massive MIMO technology, where the single antenna users share the multiplexing gain, means that only the BS requires expensive equipment. Relatively cheap single-antenna devices can be used for the UE, and this reduces the overall costs of implementing massive MIMO systems [24]. In addition, because of multi-user diversity, massive MIMO systems are less sensitive to the propagation effects of the channel environment compared to point-to-point MIMO systems.

As the number of antennas in a MIMO system grows towards infinity, it has been shown that the effects of uncorrelated noise and small-scale fading diminish, and in addition, the power required to transmit a bit becomes negligible [25]. Assuming the number of antennas at the BS to be much larger than the number of users offers increased degrees of freedom, which enhances interference nulling through beamforming.

Single-antenna users in a massive MIMO system can scale down their transmit power proportional to the BS power for the case of perfect CSI or proportional to the square root of the number of BS antennas for the case of imperfect CSI [26]. This increases the energy efficiency in massive MIMO systems compared to SISO systems. Thus massive MIMO systems are essential for future generation networks that consume excessive power.

2.3.2 Massive MIMO challenges

Vast amounts of data are generated in typical massive MIMO systems with large antenna arrays. The data needs to be processed in an efficient manner and simple processing methods are therefore required. The simple methods can preferably be linear, but performance of linear processing may not be accurate enough in some cases [3]. This presents a need for fast converging non-linear precoding or beamforming algorithms.

Since massive MIMO relies on the law of large numbers, the large number of RF chains required presents increased costs and energy consumption. Thus the equipment is likely to be low-cost and hence relatively inaccurate. This means that massive MIMO systems are

more prone to errors in CSI acquisition due to hardware impairments. In addition, operation with the TDD scheme requires reciprocity calibration, which has to be performed regularly. In order to address these challenges, the concept of hybrid beamforming has been proposed for massive MIMO systems. Hybrid transceivers use analog beamformers in the RF chains, coupled with digital beamforming in the baseband through up/down converters [27]. A number of various structures for massive MIMO hybrid transceivers have been proposed in literature [28]-[31], which aim to provide a good trade-off between complexity and performance.

In a multi-cell massive MIMO system the number of available orthogonal pilot sequences used for channel estimation can easily be exhausted. The negative effects that result from the reuse of pilot sequences in adjacent cells in a multi-cell network are termed pilot contamination [32]. Using contaminated channel estimate results for downlink beamforming results in users using the same pilots experiencing interference. Many pilot contamination coordination techniques have been investigated and presented in literature. Some pilot contamination coordination techniques for large-scale antenna systems are based on BS coordination and applying pilot contamination precoding [33], [34]. Other novel blind pilot contamination techniques that avoid the use of pilots have been presented [35], [36].

2.4 CHANNEL ESTIMATION

Beamforming for downlink transmission in MU-MIMO systems requires knowledge of CSI at the BS. The time or frequency resources required for channel estimation in massive MIMO systems is proportional to the number of BS antennas and it is independent of the number of receive antennas [24]. The downlink transmission in massive MIMO can operate in either of two modes; frequency division duplexing (FDD) or TDD.

2.4.1 FDD

In FDD operation, the downlink and uplink use different frequency bands and the CSI for the uplink and downlink are thus different. Obtaining CSI for the downlink channel is a two-stage operation, where in the first stage the BS transmits pilots to the users, and in the

second stage the users send feedback of the CSI for the downlink channel [4]. The time required for this to occur is proportional to the number of BS antennas. Hence, as the number of BS antennas grows to large values, channel estimation for downlink transmission with FDD becomes infeasible.

2.4.2 TDD

Downlink transmission for massive MIMO systems operating in TDD assumes channel reciprocity for perfect CSI. In the TDD protocol, all users first send uplink data signals and pilot sequences. The BSs then use these pilots for CSI estimation and the estimated CSI is used to determine the users' beamforming vectors [24].

2.4.3 Channel estimation techniques

Channel estimation techniques that are applied in MIMO systems are mainly training-based. Training-based channel estimation, also known as pilot-based channel estimation, uses the pilots received from users during the uplink transmission to estimate the downlink channel [37], [38]. The most common training-based CE techniques are the least squares (LS) and the linear MMSE schemes. An investigation into the performance of these two schemes in a multipath fading channel showed that the linear MMSE scheme gave better performance than the LS scheme, in terms of the symbol error rate, for various values of SNR [37].

Channel estimation techniques based on compressed sensing have also been applied in massive MIMO systems. A compressive sensing CE technique that exploits the degrees of freedom of the channel matrix was shown to improve spectral efficiency in a massive MIMO system [39], [40]. Two other CE methods based on compressive sensing have been investigated for application in MIMO systems [41]. The first method minimises the largest element in a mutual coherence set, and the second method applies the genetic algorithm and a shifting mechanism. It was shown that both methods provide better bit error rate performance compared to the LS and MMSE schemes.

2.5 BEAMFORMING FOR MASSIVE MIMO DOWNLINK TRANSMISSION

2.5.1 Linear precoding techniques

Many linear precoding techniques for downlink transmission in massive MIMO systems have been presented in literature. In this study, three prominent schemes, namely ZF, MMSE and maximum ratio transmission (MRT) were considered.

2.5.1.1 ZF precoding

The ZF precoding technique eliminates inter-user interference by transmitting the signals to the intended user and forcing zeros in the direction of other users [12]. By assuming perfect CSI at the transmitter, the ZF precoding scheme ensures zero interference, although this comes at a cost of reduced power received by each user [13]. This results in the users having low QoS in terms of data transmission rate. The ZF precoding scheme makes use of a pseudo-inverse of the channel matrix to determine the precoding matrix, $\mathbf{W}_{\mathrm{ZF}}$, which is given by [12]

$$\mathbf{W}_{\mathrm{ZF}} = \mathbf{H}^{\mathrm{H}}(\mathbf{H}\mathbf{H}^{\mathrm{H}})^{-\mathbf{1}}, \tag{2.3}$$

where $\mathbf{H}^{\mathrm{H}}$ is the Hermitian inverse of the channel matrix $\mathbf{H}$.

2.5.1.2 MMSE precoding

MMSE precoding is an optimal precoding technique, which obtains the precoding matrix by minimising the mean square error (MSE) subject to a power constraint [42]. By applying the Lagrangian method with the average power constraint at each transmit antenna, the optimal MMSE precoding matrix is given by [15]

$$\mathbf{W}_{\mathrm{MMSE}} = \mathbf{H}^{\mathrm{H}}(\mathbf{H}\mathbf{H}^{\mathrm{H}} + \alpha\mathbf{I}_{\mathrm{K}})^{-1}, \tag{2.4}$$

where $\alpha = K/P_b$ with K being the number of users served by the BS with power limit P_b and $\mathbf{I}_{\mathrm{K}}$ being a K x K identity matrix. It is concluded that the MMSE precoding technique provides optimal precoding through a trade-off between interference suppression and energy efficiency.

2.5.1.3 MRT precoding

MRT is a linear precoding technique that maximises SNR for the users, and it is best suited to application in massive MIMO with low signal power transmission [43]. The ideal precoding matrix for MRT is given as

$$\mathbf{W}_{\mathrm{MRT}} = \alpha_{MRT}\mathbf{H}^{\mathrm{H}}, \tag{2.5}$$

where α_{MRT} is a normalisation constant, which ensures that the BS transmit power constraint is satisfied.

2.5.1.4 Performance analysis and comparison

In the literature, the performance of precoding or beamforming techniques is mainly evaluated in terms of the achievable single-user rate, the sum rate, and the energy and spectral efficiency. It was observed that employing massive MIMO at the BS in wireless communication networks increased the spectral and energy efficiency by significant orders of magnitude [26]. Simulation results have shown that increasing the number of transmit antennas at the BS in a MU-MIMO system improves the system performance in terms of both sum rate and energy efficiency [44]. Application of the prominent linear precoding techniques in MU-MIMO systems has been shown to improve spectral efficiency when the number of transmit antennas is increased or when the cell radii are reduced [45].

ZF and MMSE precoding techniques were shown to achieve sum rates of up to 98% of the capacity of the optimal DPC for only two users with single antennas and 20 antennas at the BS [12]. In general, MMSE precoding was observed to give the best performance for spectral and energy efficiency when compared with ZF and MRT [42]. In terms of spectral efficiency, MRT was shown to give better performance than ZF in low SNR conditions, e.g. when there is high pilot contamination. However, increasing the number of antennas at the BS improves the low SNR performance of ZF, which makes it applicable in low SNR conditions. It has been observed that there is a trade-off between spectral efficiency and energy efficiency and in scenarios with low spectral efficiency, MRT gives better

performance than ZF, and vice versa [26]. MRT has an additional advantage over ZF in that it can be implemented in a distributed massive antenna system.

It was shown that by increasing the number of antennas at the BS while keeping the number of users fixed, MMSE has the highest rate of increase of spectral efficiency, followed by ZF, and MRT gives the lowest increase rate [42]. Analysis of a single cell with the BS equipped with antennas ranging between 20 and 200 showed that ZF precoding gave a mean sum rate performance more than double that achieved by MRT precoding [9]. On the other hand, both precoding techniques require the same power to achieve a spectral efficiency of 1 bit/s/Hz when the sum rate is assumed to be equally distributed among all users. This concludes that ZF is more power-efficient than MRT when aiming to achieve high spectral efficiency.

2.5.2 Modified linear precoding techniques

A number of variations of the aforementioned linear precoding techniques have been presented in literature. For massive MIMO systems, it has been shown that as the number of BS antennas grows towards infinity, the effects of fading, interference and imperfect CSI are eliminated and the system performance is only constrained by pilot contamination [46]. Since it is impractical to have an unlimited number of antennas at the BS, these modified versions of linear precoders aim to reduce complexity while maintaining or improving performance.

2.5.2.1 Leakage-based precoding

Leakage-based precoding determines the beamforming vector of a user by applying the concept of signal leakage, which is defined as the interference introduced to other users by a signal meant for a certain user [47], [48]. Unlike the ZF precoding scheme, which forces zeros towards unintended users, leakage-based precoding does not constrain the number of users that can be served reliably by a given number of BS antennas [13]. However, when determining the coefficients of the beamforming vector, the leakage-based technique accounts for the noise in the system, and this results in an improvement in performance over the ZF precoding scheme [47].

2.5.2.2 Regularised zero-forcing

Regularised ZF (RZF) was developed with the aim to achieve the near optimal performance of ZF in practical applications [49]. It is a precoding technique that is applicable to distributed massive MIMO systems, where the overall beamforming calculations are broken down into smaller, less complex calculations carried out in groups [50]. RZF is different from ZF in that it introduces a regularising parameter and by properly selecting this parameter, a group of linear precoders can attain an RZF structure. The precoding matrix for the RZF technique is given by

$$\mathbf{W}_{\mathrm{RZF}} = (\mathbf{H}\mathbf{H}^{\mathrm{H}} + \mathbf{F} + \beta\mathbf{I}_{\mathrm{M}})^{-1}\mathbf{H}, \tag{2.6}$$

where **F** is a deterministic Hermitian nonnegative matrix and β is the regularising parameter. It has been shown that by reducing the multi-user interference, RZF significantly outperforms MRT and that they both achieve the same performance when RZF has an order of magnitude fewer antennas per user terminal [50].

2.5.2.3 Beamforming with PA non-linearity

The RF front end of the transmitter at the BS of a massive MIMO consists of high-power amplifiers (PAs), which amplify the signal before it is transmitted by the antennas. The PAs are usually assumed to operate in their linear region, but this is not what is encountered in practice [51]. When the PAs operate in the non-linear region, it causes amplitude and phase distortion in the transmitted signal, which either reduces the channel capacity or results in channel interference [52]. This results in the massive MIMO system losing its merits of diversity and multiplexing gain, hence it is imperative to consider ways to deal with these impairments. Beamforming techniques that account for PA non-linearity include the closed-loop MIMO transmit beamforming technique and the quantised equal gain transmission (QEGT) scheme [51]. By exploiting the constant modulus property of the beamforming weight vector elements, the QEGT scheme presents a less complex solution compared to the closed-loop transmit beamforming technique; however, it is less accurate.

2.5.2.4 *k*-Regular beamformer

The *k*-regular beamformer aims to reduce the hardware complexity required by the beamforming or precoding computations by varying the number of complex gains, *k*, and consequently proving a scalable trade-off between complexity and performance [53]. The hardware required by precoding includes multipliers to carry out multiplications, and digital-to-analog converters that are required in the RF front-end. Two beamforming matrix determination algorithms are presented, namely the maximum correlation method (MCM) and the projected iterative shrinkage-thresholding algorithm (PISTA). The MCM is a non-optimal two-step approach, which requires singular value decomposition, whereas the PISTA converges faster by avoiding combinatorial searching of the *k*-regular beamformer design problem.

2.6 HETNETS

BSs have traditionally been envisioned as large high-power consuming towers with large cell coverage. It is essential to realise that these high tower-mounted BSs, which are referred to as *macrocell BSs* in this dissertation, are just a single type of BS. A BS has three fundamental requirements. "First, it must be able to initiate and accommodate spontaneous requests for communication channels with mobile users in its coverage area. Secondly, it must provide a reliable backhaul connection into the core network through a wired or wireless connection. Thirdly, it must have a sustainable power source" [55].

With the high data rate demand of modern wireless communication, use of high-power BSs cannot provide high signal quality at the high data rates, particularly to cell-edge users in the macrocell. Use of short-range, low-power BSs in small cells reduces transmit power and achieves high SINR [5]. The reduced interference and increased capacity lead to increased spectral efficiency; that is, more users can be covered actively per Hertz per unit area.

The HetNet structure has been developed in order to reap the coverage benefits of both macrocells and small cells. The macrocells make it possible to support users with high

mobility, whereas the small cells provide better coverage for large groups of users with low mobility and concentrated in a small area. The typical structure of a single cell in a HetNet setup is shown in Figure 2.4. The HetNet structure consists of a macrocell BS that serves a set of macrocell user equipment (MUE). The macrocell is overlaid by a number of small cells that serve a varying number of small-cell user equipment (SUE). The main challenge to contend with in a HetNet setup is the problem of inter-tier interference, as shown in Figure 2.4. Weak interference can be experienced by SUE when they receive a signal from the macrocell BS that is meant for a MUE. On the other hand, MUE can experience strong interference from small cell APs, especially if the MUE is at the edge of the macrocell but in close proximity to a small-cell AP.

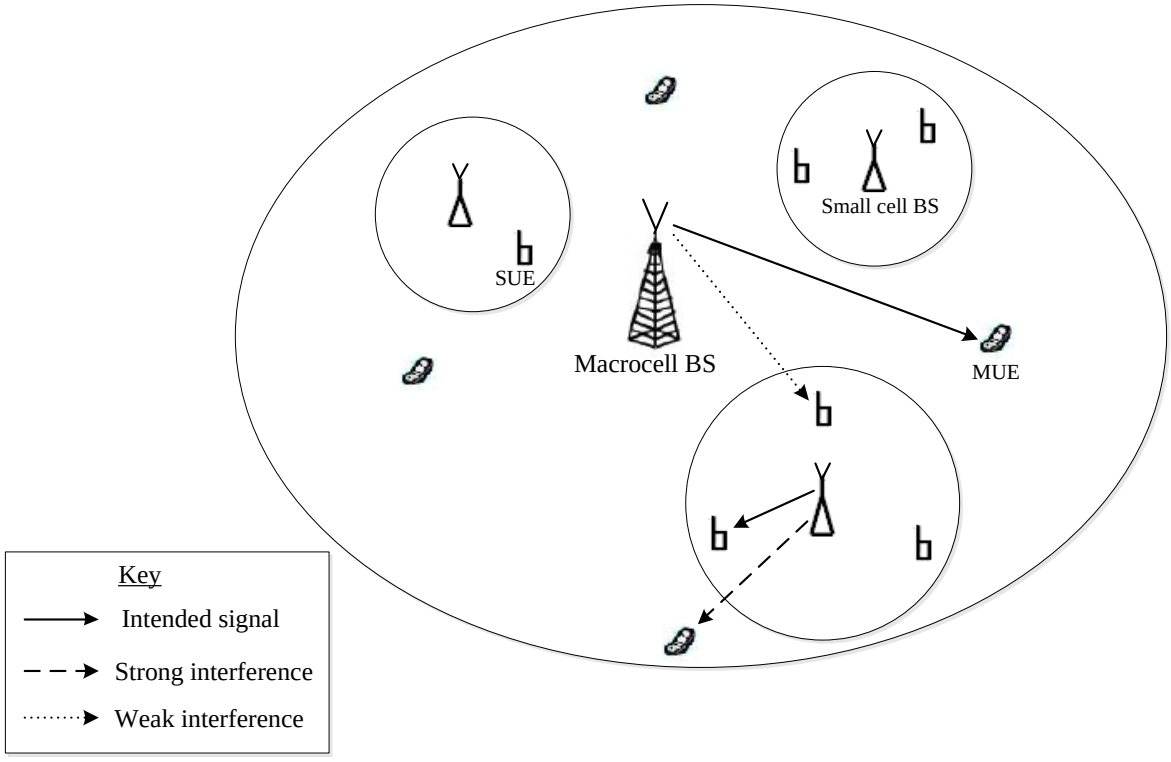

Figure 2.4. Structure of a single cell HetNet setup.

Small cell BSs or APs are typically installed by the consumer, thus their distribution is time-varying [55]. The small cells can be classified to operate in either of two modes: the closed subscriber group (CSG) mode or an open access mode. In the CSG mode, access

through the AP is restricted to known subscribers and non-subscribers cannot connect to the BS, although it may be the nearest BS [56].

Table 2.1 summarises the main aspects in which HetNets differ from traditional cellular networks [54].

Table 2.1. Summary of the main differences between traditional cellular networks and HetNets.

Aspect	Traditional Cellular Network	HetNet
Performance metrics	SINR performance to evaluate outage probability or spectral efficiency (bps/Hz)	Rate performance to evaluate outage probability or area spectral efficiency (bps/Hz/m^2)
Topology	BSs with distinct area of coverage, typically hexagonal in shape, spread out in a grid.	Macrocells overlaid by small cells, and the BS locations are modelled as random processes.
BS Association	Usually connect to the strongest serving BS.	Instead of connecting to the BS with highest signal strength, connect to one that provides highest data rate. Use of biasing in small cells.
Backhaul	BSs connect to the core network through (heavy-duty) wired backhaul.	BSs can have wireless connection to the core network in addition to lower speed wired connections.
Interference Management	Manage frequency reuse, particularly for cell-edge users. All BSs have open access.	Manage closed access interference through resource allocation. Users in "the same" cell may use different BSs. Some small cells may not have open access.

2.7 INTERFERENCE MITIGATION IN HETNETS

The overlaid cell deployment in HetNets creates a large number of cell boundaries and this causes strong inter-tier interference, especially for cell-edge users [59]. The ad hoc, unplanned deployment nature of small-cells in HetNets, makes it difficult to use traditional interference mitigation techniques to address the inter-tier interference between macrocells and small-cells. The operation of some small-cells in CSG mode also gives rise to strong inter-tier interference [55]. Thus, there is a need for new efficient interference mitigation techniques, which operate in a decentralised manner by only using local information, but enhancing overall network performance.

2.7.1 Subframe alignment

The almost blank subframes (ABS) scheme is a time-domain interference coordination technique that aims to reduce the backhaul requirement of enhanced inter-cell interference coordination (eICIC) schemes such as interference alignment. ABS is an uncoordinated transmit precoding scheme that manages both intra-cell interference and inter-cell interference [56]. In this interference mitigation technique, the small-cells classify their users as either cell-inner or cell-border. The macrocell BS is designed to stop transmission in selected time-domain subframes periodically, and the small-cells then use these subframes to serve the cell-edge users [57]. Since some information, such as pilots, is still transmitted by the macrocell user equipment, the subframes are thus referred to as *ABS*. This scheduling of cell-edge users during ABSs is also known as strict scheduling.

Figure 2.5 illustrates the operation of ABS for a macrocell that is overlaid by a picocell and a femtocell. In Figure 2.5(a) the femtocell transmits with ABSs during the even subframes and these subframes can be used to schedule transmission to MUE close to the femtocell. On the other hand, in Figure 2.5(b), the macrocell transmits with ABSs during the even subframes and these can be scheduled to serve the picocell's cell-edge users.

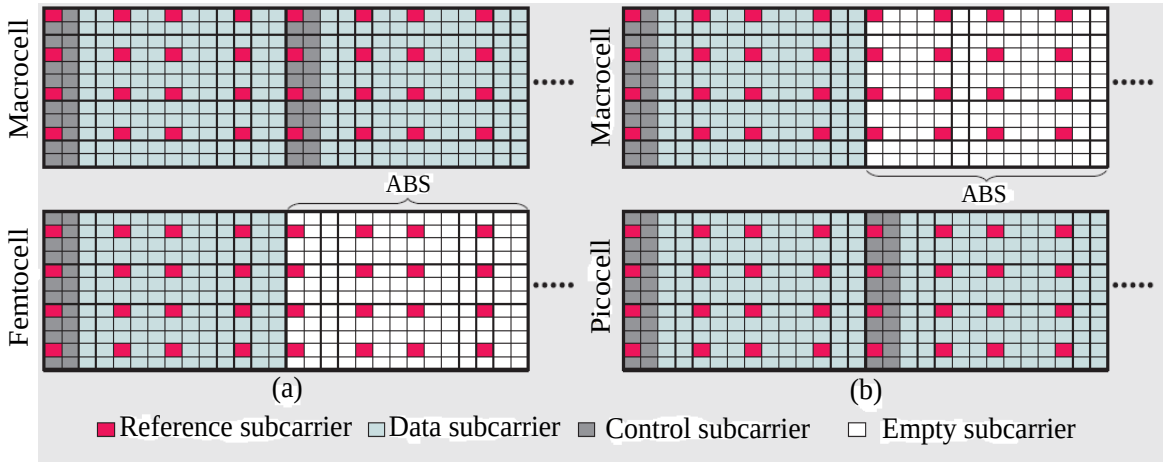

Figure 2.5. Illustration of operation of ABS between two tiers in a HetNet. (a) The ABSs of the femtocell can be used to schedule transmission to MUEs close to the femtocell; (b) the ABSs of the macrocell can be scheduled to serve the picocell's cell-edge users. (Taken from [56], © 2011 IEEE.)

2.7.2 Cell range expansion

Cell range expansion (CRE) is a concept applied where some traffic of the macro-tier is offloaded into the small-cell tier in order to achieve load balancing between the two tiers [57]. Since both the macro- and the small-cell layers typically use the same amount of bandwidth, this presents an unfair bandwidth distribution due to the smaller coverage area of small-cells. CRE aims to exploit the bandwidth allocation fairly by offloading macrocell traffic into the small-cell tier through cell biasing. Although CRE significantly mitigates inter-tier interference in the uplink, it results in very low SINR for the downlink transmission, especially for cell-edge users. To address this problem, the ABS interference mitigation scheme has been adopted to be applied in conjunction with CRE [58]. Another technique that can be used in conjunction with CRE is jointly serving the offloaded user through cooperation between the macrocell BS and small-cell access point, only if it suffers from high interference [59].

The concept of CRE is illustrated in Figure 2.6. The figure shows that the small-cell BS extends its coverage area to serve MUE_2. In other words, MUE_2 is offloaded from the macrocell BS to the small-cell BS.

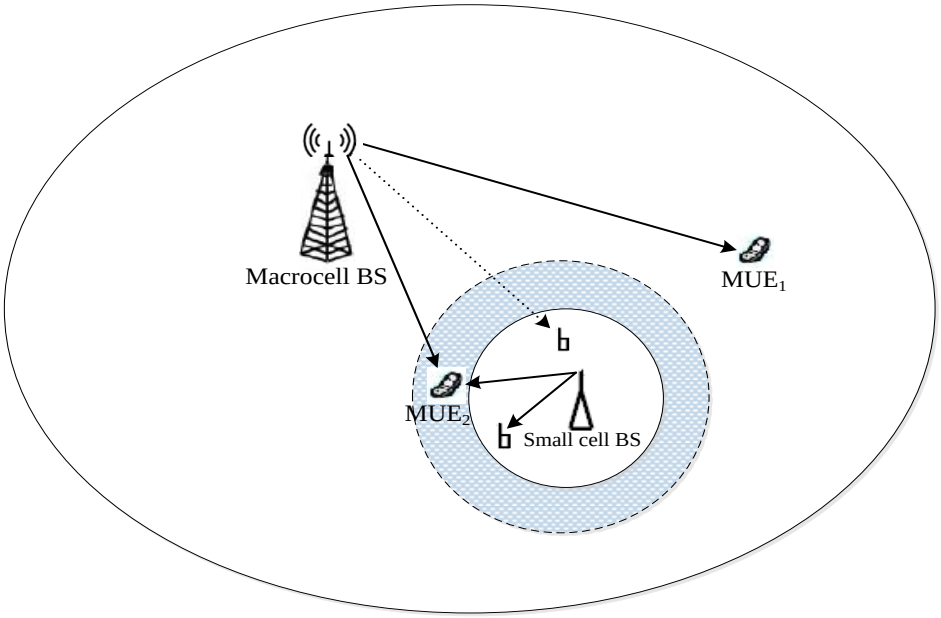

Figure 2.6. Illustration of CRE, where a macrocell user is offloaded to a small-cell BS after range expansion.

Performance analysis of HetNets with stochastic small-cells that employ CRE, and with large antenna arrays at the macrocell BSs, was presented by Wu *et al.* [60]. The authors investigated the use of interference nulling beamforming in order to improve the performance of offloaded users in HetNets implementing CRE. A tractable expression for the rate coverage probability of the interference nulling scheme was presented, and optimisation of the number of degrees of freedom was also considered in order to improve the rate coverage probability further.

2.7.3 Interference alignment

Interference alignment (IA) is an eICIC precoding technique that aims to maximise the degrees of freedom, also known as the multiplexing gain, of transmission over the interference channel [61]. IA techniques applicable to a HetNet with multiple antennas at the BSs were proposed [4]. It is proposed to apply hierarchical interference alignment (HIA) schemes to the two possible small-cell access modes in a HetNet, i.e. open subscriber groups and closed subscriber groups. The HIA schemes use a two-stage beamforming method to compute the beamforming matrices, based on the number of antennas at the BSs. The transmit beamforming matrix of the small-cell APs, which have fewer antennas compared to the macrocell BS, is designed in the first stage. The second stage then designs the beamforming matrix for the BS with the larger number of antennas. An optimisation method for maximising the sum rate for each cell in the network is also developed.

In contrast to the HIA schemes, a hierarchical multi-stage interference alignment (HMIA) scheme that designs the transmit beamforming matrices in descending order of signal strength was developed [62]. Although some weak interference signals are not aligned, this multi-stage design method allows it to provide significant interference mitigation for a macrocell with more than two picocells.

2.8 BEAMFORMING FOR MASSIVE MIMO IN HETNETS

Application of beamforming at massive MIMO BSs in HetNets is expected to present significant network performance gains. Having a massive MIMO BS for the macrocell in a HetNet enables it to concentrate its transmission power on the users or hotspots that it serves. This provides transmission opportunities to the small-cells located in other directions, and it is a technique known as spatial blanking.

Three interference coordination strategies that use the spatial blanking technique with reduced complexity have been developed [17]. In the first strategy, small-cells are turned off on the basis of the amount of inter-tier interference that they receive or that they present to the macrocell tier. The second strategy schedules transmission for small-cells such that the interference noise is optimised for the Gaussian interference channel. The third strategy applies CRE by offloading some of the macrocell users to small-cells. The strategies aim to address the problem of severe inter-tier interference, which results from the random geometry of hotspots using the technique of joint spatial division and multiplexing [63]. In addition, all three strategies aim to give insight into the best deployment of small-cells, which provides most benefits for a given performance metric; that is, either uniform deployment, deploying more cells towards the cell-interior, or deployment at the cell-edges.

2.8.1 TDD protocol

Employing the TDD protocol in a synchronised manner for both tiers in a HetNet scenario facilitates large-dimensional channel estimation at the BSs [18]. Operating with the TDD protocol also enables implicit coordination between both tiers without use of backhaul to exchange data. This in turn enables all the equipment in the network structure to obtain information about the interfering channels with no additional overhead. By employing massive MIMO at the macrocell BS and small scale MIMO at the small-cell AP, the BSs and APs can sacrifice some of their degrees of freedom to enhance interference mitigation.

Figure 2.7 shows the operation of the TDD protocol in a two-tier network. The figure shows that both tiers operate in the same mode in each interval of the channel coherence time, *T*.

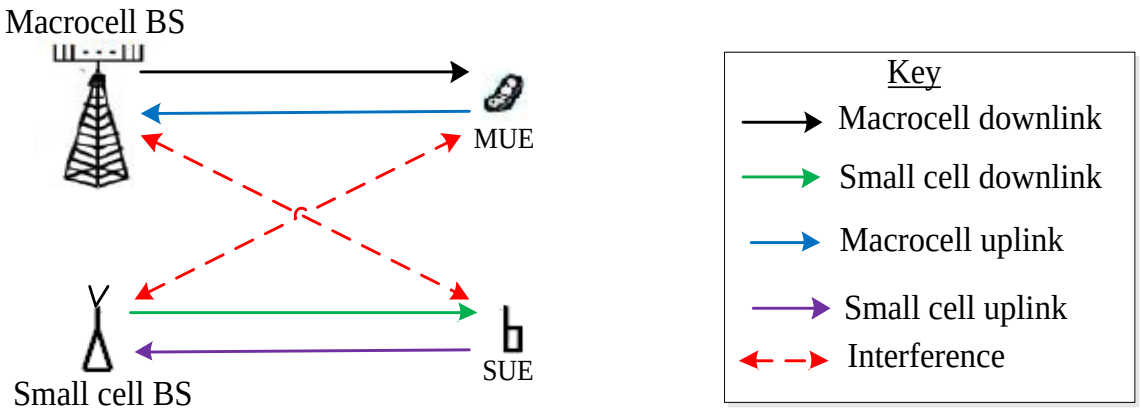

Figure 2.7. Operation of the TDD protocol in a two-tier network.

For a TDD-based network structure with a massive MIMO macrocell BS that is overlaid with small-cells, the coverage probability and spectral efficiency performance have been analysed for both tiers [7]. Analytical expressions that evaluate the optimal number of small-cells that can operate when the macrocell is in the uplink mode are provided. When the macrocell is in the downlink mode, interference mitigation in small-cells is enhanced by leveraging channel reciprocity and estimation of the interference covariance matrix. In addition, the authors of [7] showed how the macrocell BS can leverage the covariance matrix knowledge to improve the throughput of small-cells in a reverse TDD mode further.

2.8.2 RTDD protocol

The reversed TDD (RTDD) protocol is used when the two tiers in a HetNet operate in opposite modes during a time period. That is, when the macrocell is in uplink, the small-cells will transmit in downlink, and vice versa [16]. This enhances accurate estimation of the interference subspace for both tiers' BSs if they are fixed. It was observed that the RTDD scheme can outperform TDD in some cases, depending on the network structure. The performance of RTDD in the case of imperfect CSI at the transmitter was analysed in [64]. An RTDD-based beamforming scheme for the macrocell BS, which allows it to

manage both MUE and SUE by applying linear precoding techniques, was proposed. When the macrocell BS is in uplink mode, an MMSE receiver is used, and in downlink mode, a concatenated technique based on ZF is used. In contrast to [16], the authors of [64] make use of a wireless backhaul among the small-cells. Thus RTDD is applied not only between the two tiers, but also among the small-cell APs.

Operation of the RTDD protocol in a two-tier network is illustrated in Figure 2.8. Figure 2.8 shows that the two tiers operate in opposite modes during each interval of *T*, unlike the TDD operation shown in Figure 2.7.

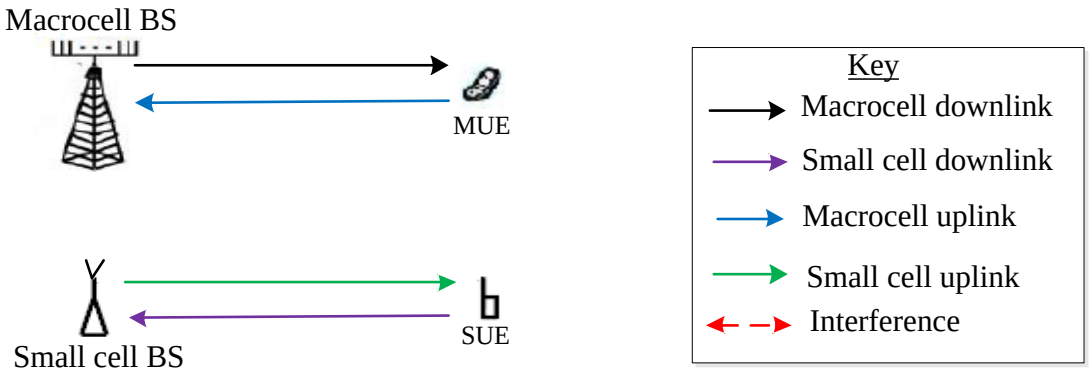

Figure 2.8. Operation of the RTDD protocol in a two-tier network.

2.8.3 Hybrid beamforming

Hybrid coordinated beamforming for massive MIMO in a HetNet has been proposed for the case where the massive MIMO macrocell BS employs an analogue beamformer coupled with a digital beamformer, and the small cell AP is equipped with multiple antennas and applies digital beamforming [65]. The authors a beamforming scheme that is robust to CSI uncertainty under conditions of pre-assigned outage probability constraints by applying semidefinite relaxation to reformulate the beamforming optimisation problem into an SDP. In addition, they develop a distributed antenna implementation of the digital coordinated beamformer by applying the ADMM.

A low complex hybrid transmit and receive beamforming technique for massive MIMO in ultra-dense HetNets that mitigates inter-cell and intra-cell interference was proposed [66].

The technique applies a hybrid beamforming architecture at the small cells, where the analog part is implemented at the small cell APs and the digital part is performed at a central unit for joint processing. The digital precoders that are employed at the SUEs are designed such that the inter-tier interference resides in a low dimension at the macrocell BS.

2.9 WEIGHTED SUM RATE MAXIMISATION TECHNIQUES

The weighted sum rate maximization (WSRMax) optimisation problem for massive MIMO downlink systems with power constraint at the BS is given by [67]

$$\begin{aligned} &\text{maximise} \sum_{k=1}^{K} \alpha_k \log_2(1+\gamma_k) \\ &\text{subject to } \textstyle\sum_{k\in U_b} \|\mathbf{w}_k\|_2^2 \le P_b, \end{aligned} \tag{2.7}$$

where the decision variable, $\mathbf{w}_k$, is the beamforming vector for user k, γ_k is the SINR of user k, and U_b is the set of all users served by the BS. The WSRMax problem is known to be non-deterministic polynomial-hard and various methods have been proposed and presented in literature, which solve the non-convex problem with near optimum results. A common goal of the proposed methods or algorithms is to present a solution with low complexity of the beamformer design but which converges in relatively few iterations.

2.9.1 Weighted sum rate maximisation via branch and bound

The WSRMax problem has been solved using the branch-and-bound (BRB) optimisation technique with definitive accuracy using efficient bounding methods which are based on conic optimisation. Relaxing the SINR requirement in equation (2.7) and changing the sign of the objective function, the optimisation problem is reformulated as [68]

$$\begin{aligned} &\text{maximise} \sum_{k=1}^{K} -\alpha_k \log_2(1+\gamma_k) \\ &\text{subject to } \gamma_k \le \frac{P_b|\mathbf{h}_k\mathbf{w}_k|^2}{1+P_b\sum_{i=1}^{K}|\mathbf{h}_k\mathbf{w}_i|^2} \end{aligned}$$

$$\sum_{k\in U_b}\|\mathbf{w}_k\|_2^2 \leq P_b, \tag{2.8}$$

It has been shown that applying BRB optimisation techniques to solve the non-convex minimisation problem over an L-dimensional rectangle presents efficient bounding methods that are based on conic optimisation. In addition to solving WSRMax problems, the solution is capable of handling other systems with Lipschitz continuous performance metrics that are increasing functions of SINR [68].

2.9.2 Soft interference nulling

Soft interference nulling (SIN) is a linear precoding technique, which is based on solving a sequence of convex optimisation problems about some given point in order to determine the precoding matrices [69]. In this method, the inequality constraints in equation (2.8) are approximated by the first-order Taylor series expansion of the log-determinant function about the operating point. For a cooperative MU-MIMO downlink system, the results have shown that with partial network coordination, SIN precoding can outperform ZF operating with full network coordination, at moderate SNR values. SIN precoding is particularly useful for clusters that overlap, where the coordination clusters comprise a limited number of cooperating BS. In such cases, optimal precoding techniques such as DPC and ZF cannot be applied directly.

2.9.3 Weighted MMSE

With the aim to design a linear filter for the transmitter in a MIMO broadcast channel (MIMO-BC), a relationship between the WSRMax problem and weighted sum-minimum MSE (WMMSE) was established [70]. It was shown that the WSRMax problem can be solved as a WMMSE problem with optimized MSE weights. An algorithm that updates the beamforming weights and the transmit or receive filters' weights simultaneously in one loop was proposed. Numerical results showed that the proposed algorithms achieve relatively good performance in a few iterations. This makes the method favourable for practical low-complexity implementation.

2.10 ROBUST BEAMFORMING

Robust beamforming is optimisation of the beamforming matrix for which the errors in channel estimation are constrained to lie in an uncertainty set [14], [71]. In other words, it is "an approach to optimisation under uncertainty in which the uncertainty model is not stochastic, but rather deterministic and set-based" [15]. Robust optimisation provides essential tools for dealing with various uncertainty types, whether model error or noisy data. However, the robust counterpart of an optimisation problem may potentially be intractable or a tractable solution becomes significantly complex. Solution methods thus aim to contend with this complexity challenge. When designing uncertainty immune beamforming matrices, increased complexity is further enhanced when some of the parameters involved in the system take up very large values [72], as in the case of massive MIMO BSs.

2.10.1 SDP-based robust optimisation

The traditional approaches to introducing robustness in the precoder design can end up requiring semi-definite programming (SDP). SDP is the optimisation of a function over the intersection of an affine set and the cone of positive semi-definite matrices [72]. The robust solution of the non-convex WSRMax problem is highly dependent on the type of uncertainty set, and the SDP design assumes an ellipsoidal uncertainty model where the channel error vectors are bounded in an ellipsoid defined by the ellipsoid's parameter, ρ [71]. That is, the norm involved in the uncertainty set is simply an l_2 norm. This assumption is an accurate estimation for channels with errors that follow a Gaussian distribution [73]. In such cases, the WSRMax problem can be solved using SDP approximations after appropriately relaxing some of the constraints in order to make them tractable.

To solve the problem of maximising the minimum sum secrecy rate for multi-user MIMO networks with imperfect CSI, an efficient approximation algorithm based on Taylor expansion was developed [74]. The beamforming design scheme transforms the original problem into a convex approximation problem by applying semi-definite relaxation and a

first-order Taylor expansion approximation. In addition to the Taylor expansion approximation-based algorithm, the authors of [74] also propose a ZF-based beamforming scheme, which is applied in cases when the BS is able to nullify the eavesdroppers' rate. Joint robust optimisation algorithms for the worst-case weighted sum rate maximization in multicell massive MIMO networks, which are based on the SDP approach, have been presented [75]. The algorithms have different levels of complexity and consider variations in coordination among BSs.

The complexity of the SDP optimisation scheme is highly sensitive to the size of the beamforming matrix and the SDP-based solutions may incur appreciable computational cost or in certain circumstances the digital resources may not be sufficient to cater for the memory requirements of an SDP-based solution [15]. In addition, the SDP approach has a limited choice of solvers, and another limitation is that it is unable to handle various types of uncertainty sets.

2.10.2 SOCP-based robust optimization

In solving a convex SOCP, a linear function of the optimisation variables is minimized over the intersection of an affine linear manifold with the Cartesian product of quadratic (second-order) Lorenz cones [72]. SOCP-based optimisation is generally more computationally efficient compared to SDP-based methods. SOCPs provide a viable alternative to designing algorithms for large-scale antenna arrays [67]. SOCP problems can be solved in polynomial-time by interior point methods; however, it is difficult to develop simplex methods to solve SOCP problems.

A fast converging, iterative beamforming algorithm, which locally solves the WSRMax problem for a massive MIMO system, was proposed [67]. The beamforming design is based on the concept of successive convex approximation (SCA), where the original non-convex problem is approximated by an efficiently solvable convex problem. The variables of concern are then updated on each iteration, until convergence. Each step of the SCA method approximates the WSRMax problem as an SOCP by performing relevant transformations.

The problem of SINR balancing in a MU-MIMO downlink system for the case of imperfect CSI acquisition at the transmitter was addressed. The worst-case design approach was followed for a system of coordinated BSs. The robust counterpart of the SINR maximisation problem was relaxed to an SDP, and then it was sub-optimally solved in conjunction with a bisection search [71]. A robust beamforming design which is merely based on solving SOCPs is also proposed.

The maximum SINR balancing problem for the case of perfect CSI was presented as [71]

$$\begin{aligned} &\text{maximise} \quad \min \alpha_k \gamma_k \\ &\text{subject to} \quad \textstyle\sum_{k\in U_b} \|\mathbf{w}_k\|_2^2 \leq P_b \end{aligned} \tag{2.9}$$

where α_k are positive weighting factors and γ_k is the SINR of user k. In order to account for imperfect CSI for the TDD massive MIMO system, the channel vectors were modelled as

$$\mathbf{h}_k = \hat{\mathbf{h}}_k + \mathbf{v}_k \mathbf{A}_k \tag{2.10}$$

where $\mathbf{h}_k$ represents the known channel vector for user k, $\mathbf{A}_k$ comprises the channel perturbation direction vectors and $\mathbf{v}_k$ is the channel error row vector for user k. The channel error vectors are determined to lie in an affine uncertainty set S given as

$$S_k = \{\mathbf{v}_k : \|\mathbf{v}_k\| \leq \rho_k\}, \forall k. \tag{2.11}$$

For worst case robust optimisation, by introducing a new variable, t for the objective function, the robust counterpart of (2.9) was formulated as

$$\begin{aligned} &\text{maximise } t \\ &\text{s.t.} \quad \frac{\alpha_k}{t} |\mathbf{h}_k \mathbf{w}_k|^2 \geq \sum_{i\in U_{b\setminus k}} |\mathbf{h}_k \mathbf{w}_k|^2 + \sigma^2, \quad \forall k, \forall \{\mathbf{v}_k \mathbf{A}_k : \mathbf{v}_k \in S_k\} \\ &\qquad \textstyle\sum_{k\in U_b} ||\mathbf{w}_k||_2^2 \leq \mathrm{P}_b. \end{aligned} \tag{2.12}$$

The proposed method further reduces complexity in comparison to the original version of the SINR balancing problem. This is accomplished by exploiting various properties of the constraints in the robust optimisation problem. An additional advantage of the proposed SOCP-based design is that it can be applied to various uncertainty models, whereas the SDP-based design formulations commonly used in literature are only applicable to the cases where the channel errors lie in an ellipsoid.

2.10.3 Uncertainties for robust optimisation

The robust counterpart of a linear optimisation problem is generally written as [15]

$$\begin{aligned} &\text{minimise } \mathbf{c}^T\boldsymbol{x} \\ &\text{subject to } \mathbf{A}\boldsymbol{x} \leq \mathbf{b} \quad \forall\, \boldsymbol{a}_1 \in \cup_1, \ldots, \boldsymbol{a}_m \in \cup_m \end{aligned} \tag{2.13}$$

where $\mathbf{c}^T$ is the transpose of $\mathbf{c}$, $\boldsymbol{a}_i$ represents the i^{th} row of the matrix $\mathbf{A}$, whose uncertainties are contained in the set $\cup_i \subseteq \mathbb{R}^n$. The constraint $\boldsymbol{a}_i^T\boldsymbol{x} \leq \boldsymbol{b}_i, \forall\, \boldsymbol{a}_i \in \cup_i$ is satisfied if and only if $\max_{\{\boldsymbol{a}_i \in \cup_i\}} \boldsymbol{a}_i^T\boldsymbol{x} \leq \boldsymbol{b}_i, \forall\, i$. It was shown that this robust linear programming problem is always tractable for most practical uncertainties, although the resulting robust problem may no longer be a linear programming problem [76]. There are various types of uncertainties that can be considered for robust optimisation problems which include:

- Ellipsoidal uncertainty
- Polyhedral uncertainty
- Cardinality constrained uncertainty
- Norm uncertainty.

Considering ellipsoidal uncertainty presents a trade-off between robustness and performance, which is controlled by the size of the ellipsoidal set. Polyhedral uncertainty is considered as a special case of ellipsoidal uncertainty, where the size of the resultant robust optimisation problems grows polynomially in the dimensions of the uncertainty set and in the size of the nominal problem. Cardinality constrained uncertainty is when a family of polyhedral uncertainty sets encode a budget of uncertainty in terms of cardinality constraints [77]. The cardinality constraints are the parameters of the problem that are allowed to vary from the nominal points.

It was shown that robust optimisation problems with uncertainty sets described by general norms result in convex problems with constraints related to the norm of the dual problem [78], [79]. In particular, the l_2 norm of a linear programming problem results in an SOCP, whereas those for the l_2 and l_∞ norms remain as linear programs. The robust counterparts of most choices of the uncertainty sets for linear programming under norm uncertainty were observed to be tractable.

2.11 OPTIMAL SOLVERS

In order to solve convex optimisation problems, two main approaches are generally used in literature. The first approach makes use of a parser to canonicalise the original problem to obtain an SOCP, which is then solved by a solver. Examples of parsers/solvers that use such an approach are CVX [17], YALMIP [80], and SeDuMi [81]. These commonly used optimal solvers are not computationally efficient for problems with large dimensions, e.g. with massive antenna arrays at the BS. This is because the transformations required in order to deploy the algorithms onto embedded systems are time-consuming.

The second approach makes use of a parser and generator combination. Here the original problem is analysed in advance, before the generator generates a custom SOCP solver. The parameters of the problem are mapped to the custom solver to give a solution. An example of a parser/generator that uses this approach is CVXGEN [82]. Although this approach reduces the transformation overhead of the aforementioned approach, the code generation step is also time-consuming and this makes it unsuitable for rapid prototyping [83]. Moreover, CVXGEN and similar frameworks, such as FORCES [84] and ACADO [85], are limited to solving quadratic programs.

CHAPTER 3 SYSTEM MODEL

Use of a massive MIMO BS for the macrocell in a HetNet scenario allows the system to achieve significant performance improvement as discussed in Section 2.8. Although beamforming for massive MIMO in HetNets helps mitigate inter-tier interference, the notion of operating in TDD mode does not give accurate solutions. Hence there is need for a novel uncertainty immune massive MIMO beamforming method that achieves acceptable performance in terms of SINR maximization with relatively low complexity for practical implementation. The beamforming scheme needs to account for imperfect CSI acquisition and RF impairments in order to model channel uncertainties for downlink transmission in HetNets with massive MIMO BSs.

In this work, a single cell of a typical HetNet was considered. The macrocell BS is equipped with M transmit antennas transmitting to K single-antenna MUE. The macrocell is overlaid with S small-cells, which contain a single-antenna BS serving a few single-antenna SUE. The setup is illustrated in Figure 3.1 and typically one would have $M >> K$. The K users and the small-cells are served in the same time-frequency resource and the channel is considered to be Rayleigh-fading.

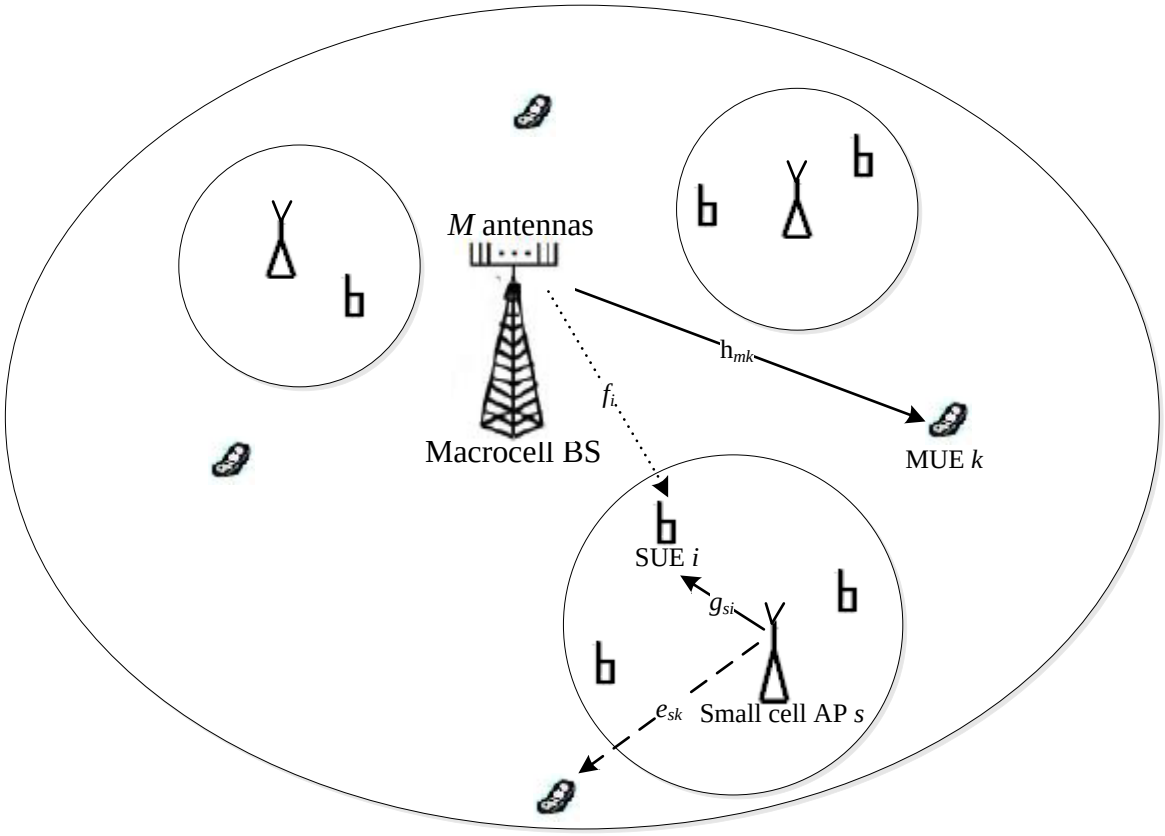

Figure 3.1. Typical single cell of a HetNet with massive MIMO at the macrocell BS.

3.1 DOWNLINK TRANSMISSION

The received signals at MUE k and at SUE i in Figure 3.1 are modelled as [16]

$$y_{MUE,k} = \sqrt{P_b}\mathbf{h}_k^{\mathrm{H}}\mathbf{s} + z_{MUE,k} \tag{3.1}$$

$$y_{SUE,i} = g_{ii}^{*}x_{SCA,i} + z_{SUE,k} \tag{3.2}$$

where P_b is the total downlink transmit power, $\mathbf{h}_k$ is the channel vector between MUE k and the macrocell BS, $\mathbf{s} = \mathbf{W}\mathbf{x}$ is the transmitted vector with $\mathbf{x} \in \mathbb{R}^K$ containing the data symbols for the K users. Let $\mathbf{H} = [\mathbf{h}_1, \mathbf{h}_2, \ldots, \mathbf{h}_K]$ be the $M \times K$ channel matrix, and $\mathbf{W}$ be the $M \times K$ precoding matrix. g_{ji} expresses the channel gain between small-cell BS j and SUE i, and $x_{SCA,i}$ is the data symbol transmitted to SUE i from its associated BS. The interference and noise terms are defined as

$$z_{MUE,k} = \sum_{i \in S} \check{e}_{ik} x_{SCA,i} + n, \tag{3.3}$$

$$z_{SUE,k} = \sum_{i \in S} g_{ik} x_{SCA,i} + \mathbf{f}_i^{\mathrm{H}} \mathbf{s} + n, \tag{3.4}$$

where $\check{e}_{ik}$ represents the channel from MUE k to small-cell BS i, $S = \{1, 2, \ldots S\}$ is the set of small-cell BSs, and $\mathbf{f}_i$ denotes the M-dimensional channel vector between the macrocell BS and SUE i, and n is AWGN, which consists of complex elements with zero mean and variance σ^2.

3.2 PERFECT CSI MODEL

For the case of perfect CSI, that is, in the absence of CSI acquisition errors, the WSRMax problem given in equation (2.7) can be solved by a bi-section method. By setting a threshold for the minimum achievable rate for each user, γ, the optimisation problem can be recast as

$$\begin{gathered} \text{minimise } \|\mathbf{w}\|_2 \\ \text{subject to } \alpha_k \log_2(1+\gamma_k) \geq \gamma, \forall k \\ \sum_{k \in B_u} \|\mathbf{w}_k\|_2^2 \leq P_b, \end{gathered} \tag{3.5}$$

where P_b is the transmit power limit of the corresponding BS, α_k is a positive weighting factor for user k, B_u is the set of all macrocell users served by the BS, and $\mathbf{w}_k$ is the beamforming vector for user k. γ_k is the SINR of macrocell user k as given by

$$\gamma_k = \frac{P_b \left|\mathbf{h}_k^T \mathbf{w}_k\right|^2}{\sigma^2 + P_b \sum_{i \neq k} \left|\mathbf{h}_i^T \mathbf{w}_i\right|^2 + P_{SCA} \sum_{i=1}^{S} |\check{g}_{ik}|^2}, \tag{3.6}$$

where P_{SCA} is the transmit power of the small cell APs.

The optimisation problem given by equation (2.5) can be reformulated as an SOCP and the resulting problem is solved by applying the max-min fairness algorithm [86]. This solution method is based on determining the upper bound of the users' sum rate using the uplink-downlink duality theory before applying the max-min fairness algorithm to solve the SOCP problem [87]. By applying Jensen's inequality after noting that the log function is concave,

the rate upper bound of user *k* for the case of perfect CSI acquisition at the transmitter is determined by [88], [89]

$$C_k \leq \log_2\left(\det\left[\mathbf{I}_k + \frac{1}{\sigma^2}E[\mathbf{h}_k^H\mathbf{h}_k]\right]\right), \forall k, \tag{3.7}$$

where $\mathbf{I}_k$ is a $K \times K$ identity matrix and $E[(\mathbf{h}_k^T\mathbf{h}_k)]$ is the autocorrelation matrix of the channel vector $\mathbf{h}_k$.

3.3 IMPERFECT CSI MODEL

The premise of the TDD protocol is that the channel is assumed to remain constant during the channel coherence time. This can be valid for cases where the user remains in the same vicinity relative to the BS during the channel coherence interval; however, this is practically inaccurate for users with high mobility. This work focused on investigating and optimising the SINR performance of a massive MIMO system for macrocell users in a HetNet scenario. Although the RTDD protocol addresses the problem of imperfect CSI in HetNets with massive MIMO base stations, its backhaul requirement for coordination increases overhead and latency. In this work, the channel estimation was modelled to account for uncertainty in the CSI acquisition, and consequently the channel vector for each user *k* takes the form

$$\mathbf{h}_k = \hat{\mathbf{h}}_k + \mathbf{e}_k, \tag{3.8}$$

where $\hat{\mathbf{h}}_k$ is the estimated channel vector for user *k*, and $\mathbf{e}_k$ is the corresponding downlink channel error vector. The channel estimation error vectors for user *k* are assumed to be bounded and to lie in an uncertainty set U_k, defined as

$$U_k = \{\mathbf{e}_k : \|\mathbf{e}_k\| \leq \rho_k, \forall k\}, \tag{3.9}$$

where $\|\mathbf{e}_k\|$ is an appropriate absolute norm for the vector $\mathbf{e}_k$, described by the parameter ρ_k, which is chosen based on the desired channel uncertainty model [90].

Imperfect CSI for robust optimisation can be modelled either statistically or by using the worst case design, and selection of the modelling design depends on the source of CSI errors at the BS [71]. Statistical modelling guarantees a certain system performance based on averages obtained over a number of channel realisations, whereas the worst case design guarantees a certain system performance for channels sufficiently close to the estimated values.

Uncertainty in CSI acquisition is a result of either estimation error or quantisation error [90]. Considering that current and next generation channel estimation methods provide accurate estimates, and that massive MIMO systems rely on the law of large numbers where the RF chains are built with low-cost components in order to achieve economic production, the dominant source of uncertainty in our model is assumed to be the quantisation errors. Taking into account that the quantisation errors are bounded, it can be justified to adopt the worst case design model for imperfect CSI, which is based on the bounded channel error model.

In order to account for the imperfect CSI, a new capacity upper bound is used, assuming that the channel error statistics are known. Considering the channel errors for each user *k* to be i.i.d. Gaussian entries, with zero mean and variance $\sigma_{e,k}^2$, which is customary for conventional channel estimation schemes [91], the new capacity upper bound is determined by

$$C_k \leq \log_2\left(\det\left[\mathbf{I}_k + \frac{1}{\sigma^2}E[\mathbf{h}_k^H\mathbf{h}_k + \sigma_{e,k}^2\mathbf{I}_k]\right]\right), \forall k. \tag{3.10}$$

Comparing equations (3.7) and (3.10), one can see the effect that the channel errors have on the capacity upper bound. This reduction in the capacity upper bound negatively affects the solution that is given by applying the max-min fairness algorithm. The same applies to other solution methods that make use of the rate upper bound, such as the ADMM algorithm.

Given the capacity upper bound under channel uncertainty conditions as given by equation (3.10), an effective robust beamforming solution method that makes best use of the erroneous channel vector estimation needs to be designed. It is essential, under such conditions, to provide the best model for the channel errors in order to obtain proper error statistics.

CHAPTER 4 FAST CONVERGING ROBUST BEAMFORMER DESIGN

The robust counterpart of any optimisation problem is usually either intractable or more complex to solve because the robust optimisation problem's set of constraints becomes infinite. "Commonly employed approximation schemes usually increase the complexity of the original problem by one degree; that is, a linear program becomes an SOCP, and an SOCP transforms to an SDP" [71]. It is essential for the robust counterpart of an optimisation problem to be computationally tractable. Possibilities of converting the robust counterpart to tractable form do not only depend on the analytical structure of the generic problem, but also on the geometry of the uncertainty set [14].

4.1 SOCP-BASED ROBUST OPTIMISATION

To obtain the robust counterpart of an optimisation problem, it is imperative to linearize the objective function by introducing a new variable if necessary [90]. To obtain the robust counterpart of the SINR balancing problem given by problem (3.5), a new variable, *t*, is introduced and is then minimised as the objective. The resultant robust formulation of problem (3.5) is written as

$$\begin{aligned} & \text{minimise } t \\ \text{subject to } & \|\mathbf{w}\|_2 \leq t \\ & \alpha_k \log_2(1+\gamma_k) \geq \gamma, \forall k \\ & \textstyle\sum_{k\in\cup_b} \|\mathbf{w}_k\|_2^2 \leq P_b, \end{aligned} \tag{4.1}$$

where **w** represents the vectorised precoding matrix.

In order to solve the robust beamforming optimisation problem efficiently, a robust beamforming design which is based on iteratively solving SOCPs, is proposed. By not specifying any particular norm for the uncertainty set of the channel error vectors, the SOCP-based scheme is capable of handling a wide variety of uncertainties. A tractable robust formulation which incorporates uncertainty with second order cone constraints, is obtained. The solution method is designed to account for imperfect CSI by using the

channel vector model given in equation (3.8) and the capacity upper bound given by equation (3.10).

To solve the robust optimisation problem for massive MIMO beamforming in a HetNet scenario, it was proposed to follow the parser/generator approach of [83], where a problem family is canonicalised, and lightweight code for mapping the parameters into an SOCP is generated. The canonicalisation is done using the Smith Form reformulation [91] and the MS technique is used for the mapping. The ADMM is then adopted to solve the SOCP-based optimisation problem. It was shown that use of the MS technique and the ADMM algorithm provides an efficient near-optimum solution of the WSRMax problem for macrocell users in a HetNet scenario [92]. The flexibility of the solution allows for easy scaling of the network structure for very large antenna arrays at the BS without much increase in computational overhead.

The solution method that uses the MS technique and the ADMM algorithm is based on a two-stage technique, as illustrated in Figure 4.1. The first stage first transforms the original optimisation problem P, given in equation (3.5), into an ADMM-compliant form, PADMM. The second stage applies the operator splitting method [93] to obtain an ADMM-based solution to the problem.

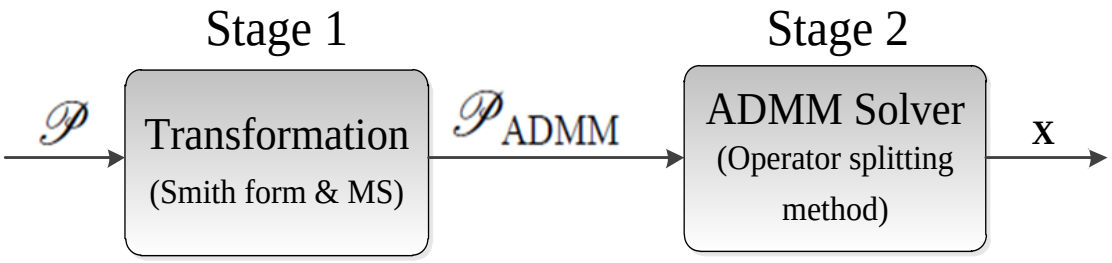

Figure 4.1. Two-stage approach of the proposed solution method.

4.2 SOCP PROBLEM FORMULATION

The aim of the transformation stage in Figure 4.1 is to give the ADMM-compliant form representation of the original optimisation problem. The ADMM-compliant form of an optimisation problem is the standard form of an SOCP, which is given as [73]

$$\begin{aligned} \mathscr{P}_{\text{ADMM}}: \quad & \text{minimise } \mathbf{c}^T\mathbf{x} \\ & \text{subject to } \mathbf{A}\mathbf{x} + \mu = \mathbf{b} \\ & (\mathrm{x}, \mu) \in \mathbb{R}^n \times \mathrm{V}, \end{aligned} \tag{4.2}$$

where $\mathbf{x} \in \mathbb{R}^n$ is the optimisation variable, $\mu \in \mathbb{R}^m$ denotes the slack variable, $\mathrm{V} = \{0\}^r \times S^{m_1} \times \ldots \times S^{m_q}$ with S^p as the standard second-order cone of dimension p. $\mathbf{A} \in \mathbb{R}^{m \times n}$ and $\mathbf{b} \in \mathbb{R}^m$ contain the original problem's constraints data, and $\mathbf{c} \in \mathbb{R}^n$ contains the objective function's scalar coefficients.

4.2.1 Smith form reformulation

The Smith form reformulation involves the introduction of new variables for each sub-expression of the objective function and all the constraints. The sub-expressions for the objective function and the constraints are first described by a set of given atoms, which are built-in functions such as norm, square, or sum [94]. A full list of the atoms is given in Table 4.1. Each atom has three characteristic properties, namely

- the sign of its output (positive, negative, or unknown),
- its monotonicity (increasing, decreasing, or neither), and
- its curvature (convex, concave, or affine).

Given a threshold, γ, for the SINR, the SINR balancing problem introduced in problem (2.9) is recast as

$$\begin{aligned} & \text{minimise } \|\mathbf{w}\|_2 \\ \text{subject to} \quad & \gamma_k \geq \gamma, \forall k \\ & \textstyle\sum_{k \in B_u} \|\mathbf{w}\|_2^2 \leq P_b, \end{aligned} \tag{4.3}$$

where γ_k is the SINR for user k, which is given by equation (3.6).

Table 4.1. Library of atoms used for Smith form reformulation.

Atom	Definition	Curvature	Implementation
Parametric atoms			
$\varphi^{\text{smult}}(x;a)$	ax	Affine	$t = ax$
$\varphi^{\text{mmult}}(x;\text{A})$	$\text{A}x$	Affine	$t = \text{A}x$
$\varphi^{\text{const}}(;a)$	a	Affine	$t = a$
Scalar atoms			
$\varphi^{\text{plus}}(x;y)$	$x+y$	Affine	$t = x + y$
$\varphi^{\text{minus}}(x;y)$	$x - y$	Affine	$t = x - y$
$\varphi^{\text{negate}}(x)$	$-x$	Affine	$t = -x$
$\varphi^{\text{pos}}(x)$	$\max(x,0)$	Convex	$t \in \mathbb{Q}^1,\ t - x \in \mathbb{Q}^1$
$\varphi^{\text{neg}}(x)$	$\max(-x,0)$	Convex	$t \in \mathbb{Q}^1,\ t + x \in \mathbb{Q}^1$
$\varphi^{\text{square}}(x)$	x^2	Convex	$t \geq \varphi^{\text{quad\_over\_lin}}(x, 1)$
$\varphi^{\text{inv\_pos}}(x)$	$1/x$	Convex	$t \geq \varphi^{\text{quad\_over\_lin}}(1, x)$
$\varphi^{\text{abs}}(x)$	$\lvert x\rvert$	Convex	$(t, x) \in \mathbb{Q}^2$
$\varphi^{\text{geo\_mean}}(x,y)$	$\sqrt{xy}$	Concave	$((1/2)(y + x), (1/2)(y - x), t) \in \mathbb{Q}^{n+2}, y \in \mathbb{Q}^1$
$\varphi^{\text{sqrt}}(x)$	$\sqrt{x}$	Concave	$t \leq \varphi^{\text{geo\_mean}}(x, 1)$
Vector atoms			
$\varphi^{\text{sum}}(x)$	$\mathbf{1}^T x$	Affine	$t = \mathbf{1}^T x$
$\varphi^{\text{max}}(x)$	$\max\{x_1, x_2, \ldots, x_n\}$	Convex	$t - x_i \in \mathbb{Q}^1,\ i = 1,\ldots,n$
$\varphi^{\text{quad\_over\_lin}}(x,y)$	$x^T x/y$	Convex	$((1/2)(y + t), (1/2)(y - t), x) \in \mathbb{Q}^{n+2}, y \in \mathbb{Q}^1$
$\varphi^{\text{norm}}(x)$	$\lVert x\rVert_2$	Convex	$(t, x) \in \mathbb{Q}^{n+1}$
$\varphi^{\text{norm1}}(x)$	$\lVert x\rVert_1$	Convex	$t \geq \varphi^{\text{sum}}(\varphi^{\text{abs}}(x))$
$\varphi^{\text{norm\_inf}}(x)$	$\lVert x\rVert_\infty$	Convex	$t \geq \varphi^{\text{max}}(\varphi^{\text{abs}}(x))$
$\varphi^{\text{min}}(x)$	$\min\{x_1, x_2, \ldots, x_n\}$	Concave	$x_i - t \in \mathbb{Q}^1,\ i = 1,\ldots,n$

Using the atoms in Table 4.1, the Smith form of the optimisation problem given in (4.3) is expressed as

$$\text{minimise } t_0$$

subject to

$$t_0 \geq \varphi^{norm}(\mathbf{w}), \tag{4.4}$$

$$\frac{\varphi^{smult}(P_b(\varphi^{square}(\varphi^{abs}(\varphi^{mmult}(\mathbf{h}_k\mathbf{w}_k)))))}{\varphi^{plus}(\varphi^{square}(\sigma),\varphi^{smult}(P_{SCA};\varphi^{square}(\varphi^{abs}(\check{e}_{ik}))))} \geq \gamma, \tag{4.5}$$

$$\varphi^{norm}(\mathbf{w}_m \leq \sqrt{P_m}), \tag{4.6}$$

where equation (4.6) represents the per-antenna power constraint.

4.2.1.1 Relaxed Smith form

Although the Smith form is equivalent to the original problem, it is not necessarily convex, unless all atoms used are affine. The reformulated problem is convex if all expressions used are affine. Thus, all equality constraints for atoms that are not affine are relaxed to inequality constraints, based on their curvature, in order to make them affine. If an atom φ is concave, its equality constraint $t = \varphi(x)$ is replaced with $t \leq \varphi(x)$. On the other hand, if φ is convex, the equality constraint is replaced by $t \geq \varphi(x)$.

4.2.1.2 Representative form

To represent the atoms of the reformulated problem, graph implementations are used, particularly for the non-linear functions. Affine atoms do not require any special representation. Each atom in the relaxed Smith form is replaced by its graph implementation, where each graph implementation is a small SOCP. The definitions of atoms, their curvature, and their equivalent conic implementations are given in Table 4.1.

By introducing new variables, t_0 and $\mathbf{t}_1$, for the sub-expressions problem's (4.3) objective function, $\min \|\mathbf{w}\|_2$, the representative Smith form is given as

$$\begin{aligned} & \text{minimise } t_0 \\ \text{subject to} \quad & (t_0, \mathbf{t}_1) \in \mathbb{Q}^{N+1}, \\ & \mathbf{t}_1 = \mathbf{w} \in \mathbb{R}^N, \end{aligned} \tag{4.7}$$

where $N = KM$.

For the per-antenna power constraint $\mathbf{w}_m \leq \sqrt{P_m}$, introducing new variables, v_0 and $\mathbf{v}_1$, results in the representative formulation

$$\begin{aligned} (v_0^m, \mathbf{v}_1^m) &\in \mathbb{Q}^{K+1} \\ v_0^m = \sqrt{P_m} &\in \mathbb{R} \\ \mathbf{v}_1^m = \mathbf{w}_m &\in \mathbb{R}^K. \end{aligned} \tag{4.8}$$

With the aim to make the QoS constraint in (4.1) convex, i.e., for all sub-expressions to be affine, let $\theta_k = 2^{\gamma/\alpha_k} - 1$. The QoS constraint is then given by the expression

$$\frac{P_b|\mathbf{h}_k^T\mathbf{w}_k|^2}{\sigma^2+P_b\sum_{i\neq k}|\mathbf{h}_i^T\mathbf{w}_i|^2+P_{SCA}\sum_{i=1}^{S}|\breve{g}_{ik}|^2} \geq \theta_k, \tag{4.9}$$

which is equivalent to the l_2 norm representation

$$\|\mathbf{C}_k\mathbf{w} + \mathbf{q}_k\|_2 \leq \beta_k\mathbf{r}_k^T\mathbf{w}, \tag{4.10}$$

where

$$\mathbf{q}_k = [\mathbf{0}_k^T, \sigma_k]^T \in \mathbb{R}^{K+1}, \tag{4.11}$$

$$\beta_k = \sqrt{1 + 1/\theta_k} \in \mathbb{R}, \tag{4.12}$$

$$\mathbf{r}_k = \left[\mathbf{0}_{(k-1)M}^T, \mathbf{h}_k^T, \mathbf{0}_{(K-k)M}^T\right]^T \in \mathbb{R}^N, \tag{4.13}$$

and $\mathbf{C}_k$ is given by

$$\mathbf{C}_k = \begin{bmatrix} \boldsymbol{h}_k^T & & \\ & \ddots & \\ & & \boldsymbol{h}_k^T \\ \hline & \mathbf{0}_N^T & \end{bmatrix} \in \mathbb{R}^{(K+1)\times N}. \tag{4.14}$$

By introducing new variables y_0^k, $\mathbf{y}_1^k$, $\mathbf{y}_2^k$, and $\mathbf{y}_3^k$ and using the representative form given in Table 4.1 the relaxed Smith form representation of equation (4.10) is given as

$$\begin{aligned} (y_0^k, \mathbf{y}_1^k) &\in \mathbb{Q}^{K+1} \\ y_0^k &= \beta_k\mathbf{r}_k^T\mathbf{w} \in \mathbb{R} \\ \mathbf{y}_1^k &= \mathbf{y}_2^k + \mathbf{y}_3^k \in \mathbb{R}^{K+1} \\ \mathbf{y}_2^k &= \mathbf{C}_k\mathbf{w} \in \mathbb{R}^{K+1} \\ \mathbf{y}_3^k &= \mathbf{q}_k \in \mathbb{R}^{K+1}. \end{aligned} \tag{4.15}$$

The resultant relaxed Smith form reformulation of the original problem in (4.1) is represented as

$$\begin{aligned} &\text{minimise } t_0 \\ &\text{subject to } \mathcal{G}_0,\ \mathcal{G}_1(m),\ \mathcal{G}_2(k),\ \forall k, m, \end{aligned} \tag{4.16}$$

where $\mathcal{G}_0$ is the relaxed Smith form representation of the objective function, which is given by

$$\mathcal{G}_0 : \begin{Bmatrix} (t_0, \mathbf{t_1}) \in \mathbb{Q}^{N+1} \\ \mathbf{t}_1 = \mathbf{w} \in \mathbb{R}^N \end{Bmatrix}. \tag{4.17}$$

$\mathcal{G}_1(m)$ is the relaxed Smith form representation of the power constraint given as

$$\mathcal{G}_1(m) : \begin{Bmatrix} (v_0^m, \mathbf{v}_1^m) \in \mathbb{Q}^{K+1} \\ v_0^m = \sqrt{P_b} \in \mathbb{R} \\ \mathbf{v}_1^m = \mathbf{w}_m \in \mathbb{R}^K \end{Bmatrix}, \tag{4.18}$$

and $\mathcal{G}_2(k)$ represents the relaxed Smith form reformulation for the QoS constraint of MUE_k, given as

$$\mathcal{G}_2(k) : \begin{Bmatrix} \left(y_0^k, \mathbf{y}_1^k\right) \in \mathbb{Q}^{K+1} \\ y_0^k = \beta_k \mathbf{r}_k^T \mathbf{w} \in \mathbb{R} \\ \mathbf{y}_1^k = \mathbf{y}_2^k + \mathbf{y}_3^k \in \mathbb{R}^{K+1} \\ \mathbf{y}_2^k = \mathbf{C}_k \mathbf{w} \in \mathbb{R}^{K+1} \\ \mathbf{y}_3^k = \mathbf{q}_k \in \mathbb{R}^{K+1} \end{Bmatrix}. \tag{4.19}$$

The standard SOCP (ADMM-compliant) representation of the reformulated problem is represented by the vector of variables **x**, which includes the original variables and the new variables, and the problem data, which are defined in **A**, **b**, and **c**. The optimisation variables are given by

$$\mathbf{x} = [t_0; v_0^1; \dots; v_0^M; y_0^1; \dots; y_0^K; \mathbf{w}] \in \mathbb{R}^n, \tag{4.20}$$

and the vector of coefficients is consequently given by

$$\mathbf{c} = [\mathbf{0}_{n-1}; 1]. \tag{4.21}$$

The standard SOCP problem's structure is characterised by the cone dimensions and the matrices that represent the problem data. The cone dimensions of the reformulated problem, n, m, and V, are given by

$$n = 1 + M + K + N, \tag{4.22}$$

$$m = (M + K) + (M + 1) + M(K + 1) + K(K + 2), \tag{4.23}$$

$$\mathsf{V} = (\mathbb{Q}^1)^{M+K} \times \mathbb{Q}^{N+1} \times (\mathbb{Q}^{K+1})^L \times (\mathbb{Q}^{K+2})^K, \tag{4.24}$$

where V is the Cartesian product of $2(M + K) + 1$ closed convex cones. The matrices that contain the original problem's constraints data, **A** and **b**, are given as follows:

$$\mathbf{A} = \left[\begin{array}{cccc|c}
1 & & & & \\
& \ddots & & & \\
& & 1 & & \\
\hline
& & 1 & & -\beta_1 \mathbf{r}_1^T \\
& & & \ddots & \vdots \\
& & & 1 & -\beta_k \mathbf{r}_k^T \\
\hline
-1 & & & & \\
& & & & -\mathbf{I}_N \\
\hline
& -1 & & & -\mathbf{I}_K^m \\
\hline
& \vdots & & & \vdots \\
& -1 & & & \\
& & & & -\mathbf{I}_K^M \\
\hline
& & -1 & & \\
& & & & -\mathbf{C}_1 \\
\hline
& \vdots & & & \vdots \\
\hline
& & & -1 & \\
& & & & -\mathbf{C}_K
\end{array}\right] \in \mathbb{R}^{m \times n}, \tag{4.25}$$

where the number of columns of **A** is equal to the total number of variables, i.e. the original variables plus the new variables introduced by the reformulation. The rows of **A** are composed of from the atoms of the reformulation, where each atom is a block that is underlined.

$$\mathbf{b} = \begin{bmatrix} \sqrt{P_1} \\ \vdots \\ \sqrt{P_M} \\ \hline 0 \\ \vdots \\ 0 \\ \hline \mathbf{0}_N \\ \hline 0 \\ \mathbf{0}_K \\ \hline 0 \\ \mathbf{q}_1 \\ \hline \vdots \\ \hline 0 \\ \mathbf{q}_K \end{bmatrix} \in \mathbb{R}^{m \times 1}. \tag{4.26}$$

4.2.2 Matrix stuffing for fast transformation

MS is a technique that provides significantly faster transformation for convex optimisation problems compared to other modelling and transformation frameworks such as CVX [95]. The canonicalisation procedure carried out through the Smith form reformulation simply creates the SOCP structure of the original problem. For a given set of the HetNet's parameters, i.e. the number of BS antennas, MUEs and SUEs, the SOCP structure is fixed. Since the parameters for a given scenario of a HetNet setup can be assumed to remain constant for a long period, the structures of **A**, **b**, **c** and the description of $\mathcal{V}$ can be generated and stored offline.

For any specific network realisation of the HetNet scenario, the problem data are then copied to the corresponding positions in the standard SOCP structure. These data comprise the maximum per-antenna transmit power of the macrocell BS, which is represented by the $\sqrt{P_m}$'s in **b**; the per-user SINR thresholds γ_k, which are copied to the β_k's in **A**; and the channel realisations $\mathbf{h}_k$'s, which are copied to the $\mathbf{r}_k$'s and $\mathbf{C}_k$'s in **A**. This MS technique presents a fast transformation solution for non-convex optimisation problems such as the WSRMax problem for macrocell users in a HetNet scenario.

4.3 ADMM-BASED SOLUTION

To solve the formulated standard SOCP for a given problem to optimise the user rate or SINR performance for macrocell users in a HetNet scenario, it was proposed to apply a first-order method for solving very large cone programs. The solution of the method is a result of solving the homogeneous self-embedding of a primal-dual pair of the optimisation problem by using an operator splitting method known as the ADMM algorithm. This approach scales favourably to convex conic problems with very large dimensions, and it is well suited for a distributed antenna setup since it can be applied in parallel across multiple processors [86]. This makes the method converge to reliable, modestly accurate solutions faster than interior-point methods, at the cost of lower accuracy.

4.3.1 Homogeneous self-embedding

Homogeneous self-embedding is a single convex feasibility problem, which results from encoding the primal and dual pair of an optimisation problem into a single feasible problem. The process of obtaining homogeneous self-embedding entails finding a feasible (non-zero) point in the intersection of a convex set and a subspace, and it has been widely used in inter-point methods. A non-zero solution of the original pair is taken as the optimal solution otherwise a certificate of infeasibility is generated that proves that either the primal or dual optimisation problem is infeasible.

The primal and dual pair, $\mathscr{P}_{\text{ADMM}}$ and $\mathscr{D}_{\text{ADMM}}$, of the ADMM-compliant problem is represented as

$$\begin{aligned} \mathscr{P}_{\text{ADMM}}\text{: } & \text{minimise } \mathbf{c}^T\mathbf{x} \\ & \text{subject to } \mathbf{A}\mathbf{x} + \mu = \mathbf{b} \\ & (\mathbf{x}, \mu) \in \mathbb{R}^n \times \mathrm{V}, \end{aligned} \tag{4.27}$$

$$\begin{aligned} \mathscr{D}_{\text{ADMM}}\text{: } & \text{minimise } -\mathbf{b}^T\boldsymbol{\eta} \\ & \text{subject to } -\mathbf{A}^T\boldsymbol{\eta} + \boldsymbol{\lambda} = \mathbf{c} \\ & (\boldsymbol{\eta}, \boldsymbol{\lambda}) \in \{0\}^n \times \mathrm{V}^*, \end{aligned} \tag{4.28}$$

where $\boldsymbol{\eta} \in \mathbb{C}^m$ is the dual's optimisation variable, and $\boldsymbol{\lambda} \in \mathbb{C}^n$ is the dual slack variable. V^* is the dual cone of the non-empty closed convex cone V and $\{0\}^n$ is the dual cone of $\mathbb{R}^n$.

To ensure that strong duality holds, the Karush-Kuhn-Tucker (KKT) conditions are necessary and sufficient, in order to solve the optimisation problem optimally. The pair in (4.87) and (4.28) satisfies the KKT conditions and is primal-dual optimal when

$$\mathbf{A}\mathbf{x} + \boldsymbol{\mu} = \mathbf{b}, \tag{4.29}$$

$$\mathbf{A}^T\boldsymbol{\eta} + \mathbf{c} = \boldsymbol{\lambda}, \tag{4.30}$$

$$\mathbf{c}^T\mathbf{x} + \mathbf{b}^T\boldsymbol{\eta} = \mathbf{0}, \tag{4.31}$$

with $(\mathbf{x}, \boldsymbol{\mu}, \boldsymbol{\lambda}, \boldsymbol{\eta}) \in \mathbb{R}^n \times V \times \{0\}^n \times V^*$. The primal-dual pair can be converted into a single problem by embedding the KKT conditions into a single system of equations and including the optimal points that the primal and dual problems must jointly satisfy. This embedding gives

$$\begin{bmatrix} \boldsymbol{\lambda} \\ \boldsymbol{\mu} \\ \mathbf{0} \end{bmatrix} = \begin{bmatrix} \mathbf{0} & \mathbf{A}^{\mathrm{T}} \\ -\mathbf{A} & \mathbf{0} \\ \mathbf{c}^{\mathrm{T}} & \mathbf{b}^{\mathrm{T}} \end{bmatrix} \begin{bmatrix} \mathbf{x} \\ \boldsymbol{\eta} \end{bmatrix} + \begin{bmatrix} \mathbf{c} \\ \mathbf{b} \\ \mathbf{0} \end{bmatrix}, \tag{4.32}$$

$$(\mathbf{x}, \boldsymbol{\mu}, \boldsymbol{\lambda}, \boldsymbol{\eta}) \in \mathbb{R}^n \times V \times \{0\}^n \times V^*.$$

In this case, if the primal optimization problem in (4.27) or the dual problem in (4.28) is infeasible, (4.32) has no solution. Homogeneous self-dual embedding addresses this shortcoming by introducing two new nonnegative variables τ and κ, which encode the different possible outcomes of the solution [96]. The homogeneous self-dual embedded system of equations is then given as

$$\begin{bmatrix} \boldsymbol{\lambda} \\ \boldsymbol{\mu} \\ \kappa \end{bmatrix} = \begin{bmatrix} 0 & \mathbf{A}^T & \mathbf{c} \\ -\mathbf{A} & 0 & \mathbf{b} \\ -\mathbf{c}^T & -\mathbf{b}^T & 0 \end{bmatrix} \begin{bmatrix} \mathbf{x} \\ \boldsymbol{\eta} \\ \tau \end{bmatrix}. \tag{4.33}$$

The system of equations in (4.33) is homogeneous because if $(\mathbf{x}^*, \boldsymbol{\mu}^*, \boldsymbol{\lambda}^*, \boldsymbol{\eta}^*)$ is a solution to the embedded problem, then $(a\mathbf{x}^*, a\boldsymbol{\mu}^*, a\boldsymbol{\lambda}^*, a\boldsymbol{\eta}^*)$ is also a solution for any $a \geq 0$. The

embedded problem is also self-dual, and the proof is given in Appendix A. To simplify the representation of the embedded problem, let

$$\mathbf{r} = \begin{bmatrix} \boldsymbol{\lambda} \\ \boldsymbol{\mu} \\ \kappa \end{bmatrix}, \tag{4.34}$$

$$\mathbf{Q} = \begin{bmatrix} 0 & \mathbf{A}^T & \mathbf{c} \\ -\mathbf{A} & 0 & \mathbf{b} \\ -\mathbf{c}^T & -\mathbf{b}^T & 0 \end{bmatrix}, \tag{4.35}$$

$$\mathbf{p} = \begin{bmatrix} \mathbf{x} \\ \boldsymbol{\eta} \\ \tau \end{bmatrix}, \tag{4.36}$$

where $(\mathbf{p}, \mathbf{r}) \in \mathbb{R}^{n+m+1}$, $\mathbf{Q} \in \mathbb{R}^{(n+m+1)\times(n+m+1)}$. The homogeneous self-embedding problem is thus given as

$$\begin{aligned} &\text{find } (\mathbf{p}, \mathbf{r}) \\ &\text{subject to } \mathbf{r} = \mathbf{Q}\mathbf{p} \\ &(\mathbf{p}, \mathbf{r}) \in \mathbb{C} \times \mathbb{C}^* \end{aligned} \tag{4.37}$$

where $\mathbb{C} = \mathbb{R}^n \times \mathrm{V}^* \times \mathbb{R}^+$ is a cone with dual cone $\mathbb{C}^* = \{0\}^n \times \mathrm{V} \times \mathbb{R}^+$.

4.3.2 ADMM algorithm

The ADMM algorithm is a first-order method for solving optimisation problems, which is based on the operator splitting method [97]. The method is well-suited for large-scale convex optimisation problems. The algorithm has been applied to solve optimisation problems in cloud computing environments because it can handle complex problems fairly, while it is scalable enough to process data with large parameters. It was proposed to adopt this algorithm to solve the homogeneous self-dual embedded problem for robust beamforming optimisation for macrocell users in a typical HetNet.

The basic operator splitting method solves convex problems of the form

$$\begin{aligned} &\text{minimise } [\, f(y) + g(z) \,] \\ &\text{subject to } Ay + Bz = c, \end{aligned} \tag{4.38}$$

where $A \in \mathbb{R}^{p \times n}$, $B \in \mathbb{R}^{p \times m}$. Here the variable of the original problem $x \in \mathbb{R}^n$, is split into two parts, which are $y \in \mathbb{R}^n$ and $z \in \mathbb{R}^n$ in this case, provided the objective function of the original problem is separable across the splitting. It is assumed that *f* and *g* are convex, and they may be non-smooth or may take on infinite values to encode implicit constraints.

The iterations of the ADMM algorithm consist of the steps

$$y^{k+1} \equiv \text{argmin } L_\rho(y, z^k, d^k), \tag{4.39}$$

$$z^{k+1} \equiv \text{argmin } L_\rho(y^{k+1}, z, d^k), \tag{4.40}$$

$$d^{k+1} \equiv d^k + \delta(Ay^{k+1} + Bz^{k+1} - c), \tag{4.41}$$

where *d* is the dual variable, and $\delta > 0$ is a penalty multiplier of the augmented Lagrangian, L_ρ, defined as

$$L_\rho(x, z, y) = f(x) + g(z) + d^T(Ax + Bz - c) + (\delta/2)\|Ax + Bz - c\|_2^2. \tag{4.42}$$

The initial points of the iterations, z^0 and d^0, are arbitrary but they are usually assumed to be zero. From equations (4.39) – (4.41), it is observed that the algorithm comprises a *y*-minimisation step, a *z*-minimisation step, and a step to update the dual variable. This is basically similar to the method of multipliers, which takes the form

$$(y^{k+1}, z^{k+1}) \equiv \text{argmin } L_\rho(y, z^k, d^k), \tag{4.43}$$

$$d^{k+1} \equiv d^k + \delta(Ay^{k+1} + Bz^{k+1} - c). \tag{4.44}$$

The main difference to note is that in the ADMM, the variables are updated in an alternating manner as given in equations (4.39) and (4.40), unlike in the method of multipliers where the augmented Lagrangian for the two variables is jointly minimised as given in (4.43). This gives rise to the term *alternating direction* in ADMM.

4.3.2.1 Scaled form

The ADMM can be written in a more convenient scaled form. This is achieved by combining the linear and quadratic terms in the augmented Lagrangian and scaling the dual variable. After defining $r = Ay + Bz - c$ as the residual, part of equation (4.42) can be written as

$$\begin{aligned} d^T r + (\delta/2)\|r\|_2^2 &= (\delta/2)\|r + (1/\delta)d\|_2^2 - (1/2\delta)\|d\|_2^2 \\ &= (\delta/2)\|r + u\|_2^2 - (\delta/2)\|u\|_2^2 \end{aligned} \tag{4.45}$$

where $u = (1/\delta)y$ is the scaled dual variable. With this scaled dual variable, the ADMM is then given as

$$x^{k+1} \equiv \text{argmin}\ (f(x) + (\delta/2)\|Ax + Bz^k - c + u^k\|_2^2, \tag{4.46}$$

$$z^{k+1} \equiv \text{argmin}\ (g(x) + (\delta/2)\|Ax^{k+1} + Bz - c + u^k\|_2^2, \tag{4.47}$$

$$u^{k+1} \equiv u^k + Ax^{k+1} + Bz^{k+1} - c. \tag{4.48}$$

The scaled form of the ADMM given by Equations (4.46) – (4.48) is equivalent to the unscaled form in Equations (4.39) – (4.41). The formulas in the scaled form are, however, often shorter to implement and are thus used more often.

In order to apply the operator splitting method, the embedded problem in Equation (4.37) is transformed into the form

$$\begin{aligned} &\text{minimise } I_{\mathbb{C}\times\mathbb{C}^*}(p, r) + I_{\mathrm{Q}\tilde{\mathrm{x}}}(\tilde{p}, \tilde{r}) \\ &\text{subject to } (p, r) = (\tilde{p}, \tilde{r}), \end{aligned} \tag{4.49}$$

where I_S denotes the indicator function of the set S. Directly applying the ADMM to the self-dual embedding in Equation (4.49) yields the following algorithm

$$(\tilde{p}^{k+1}, \tilde{r}^{k+1}) = \prod_{Qp=r} (p^k + \lambda^k, r^k + \mu^k)$$

$$p^{k+1} = \prod_{\mathbb{C}} (\tilde{p}^{k+1} - \lambda^k)$$

$$r^{k+1} = \prod_{\mathbb{C}^*} (\tilde{r}^{k+1} - \mu^k)$$

$$\lambda^{k+1} = \lambda^k - \tilde{p}^{k+1} + p^{k+1}$$

$$\mu^{k+1} = \mu^k - \tilde{r}^{k+1} + r^{k+1},$$

where $\prod_S(x)$ denotes the Euclidean projection of x onto the set S, and λ and μ are dual variables for the equality constraints on p and r, respectively.

4.3.2.2 Convergence

The ADMM algorithm has been found to converge very slowly to high accuracy; however, it converges to modest accuracy in a few tens of iterations [97]. This corresponds with the results that were obtained in this research, as will be shown in Chapter 5. The convergence efficiency of the ADMM-based solution makes it practically useful in scenarios where modest accuracy is sufficient while solve time is critical, as in the case of beamforming for massive MIMO.

4.4 RUN TIME ANALYSIS

To achieve the reduced latency requirement for the 5G networks, it is imperative that the proposed beamforming schemes for massive MIMO be computationally efficient. That is, in addition to optimal accuracy, they need to converge to a solution much faster compared to the current schemes applied in 4G and LTE. Thus, it is essential to evaluate the efficiency of the proposed robust beamforming technique, which uses MS and the ADMM algorithm, in terms of the run time or the time it takes to converge to a solution. In order to analyse and compare the convergence rate of the proposed beamforming solution method with other optimal solutions, various techniques were considered.

4.4.1 Big O notation

Big O notation is a complexity analysis technique that represents the growth rate of an algorithm for the worst-case scenario in mathematical notation [98]. Big O notation characterises algorithms in terms of their growth rates, where algorithms with the same growth order are represented with the same function. It is worth noting that a representation of an algorithm in terms of big O notation usually only provides an upper bound on the growth rate of the algorithm.

For the beamforming optimisation solutions analysed in this research, it was challenging to perform analysis of algorithm run time in terms of big O notation, since the number of iterations for each algorithm to converge to a solution varies widely. It is thus difficult to indicate the worst-case growth rate for the algorithms. It was considered to compare the convergence efficiency of the optimisation solutions using the run time for the various simulated cases.

4.4.2 Platform independence

Analysis of algorithm convergence efficiency in terms of run time or other empirical methods does not give a comprehensive comparative analysis of the performance of the algorithms considered. In addition to convergence time, the convergence efficiency of the optimisation solutions analysed in this research was compared in terms of empirical local orders of growth. This provides a platform-independent comparative performance analysis for the algorithms, since a given algorithm can be implemented on an arbitrary computer running an arbitrary operating system using an arbitrary programming language. For run times t_1 and t_2, with their corresponding input parameters n_1 and n_2, the local order of growth, d, is given by

$$d = \frac{\log(t_2/t_1)}{\log(n_2/n_1)} \tag{4.50}$$

To illustrate the significance of comparing any two given algorithms in terms of their empirical local orders of growth behaviour, consider as an example a program that looks up a specific entry in a sorted list of size n. Suppose the program was implemented on

Computer A (a state-of-the-art machine) using a linear search algorithm, and on Computer B (a much slower machine) using a binary search algorithm. Table 4.2 gives the typical results of both convergence time and local growth order comparison for the two computers running their respective programs.

By only considering the run time for the first few rows in Table 4.2, one can easily conclude that Computer A is running an algorithm that is much superior in efficiency compared to that of Computer B. However, as the list size, *n*, grows to very large values, Computer B will inevitably surpass Computer A in terms of run-time, although Computer A is a faster machine. This is because Computer B runs an algorithm with a much slower growth rate, as can be seen from the results in Table 4.2.

Table 4.2. Typical results of run time analysis for two computers running their respective programs for the same search.

n	**Computer A run time (nanoseconds)**	**Local order of growth**	**Computer B run time (nanoseconds)**	**Local order of growth**
15	7		100 000	
65	32	1.04	150 000	0.28
250	125	1.01	200 000	0.21
1 000	500	1.00	250 000	0.16
…	…		…	
1 000 000	500 000	1.00	500 000	0.10
4 000 000	2 000 000	1.00	550 000	0.07
16 000 000	8 000 000	1.00	600 000	0.06

It can be seen that the algorithm implemented by Computer A exhibits a linear order of growth, whereas that for Computer B follows another rule of growth, where the empirical values of local growth order diminish rapidly as *n* increases. The algorithm of computer B has much lower local orders of growth than that of Computer A, and they improve further as *n* increases to very large values.

To further illustrate the platform independence significance of comparing algorithm convergence using the local order of growth, Table 4.3 shows the results of running the binary search algorithm on Computer A, and running the linear search algorithm on Computer B. Table 4.2 and Table 4.3 show that although Computer A is 100 times faster than Computer B, the local growth order analysis of the algorithms do not change after switching the search programs between the two computers.

Table 4.3. Results of run time analysis for the two computers running with the programs switched for the same search.

n	**Computer A run time (nanoseconds)**	**Local order of growth**	**Computer B run time (nanoseconds)**	**Local order of growth**
15	1 000		700	
65	1 500	0.28	3 200	1.04
250	2 000	0.21	12 500	1.01
1 000	2 500	0.16	50 000	1.00
…	…		…	
1 000 000	5 000	0.10	50 000 000	1.00
4 000 000	5 500	0.07	20 000 0000	1.00
16 000 000	6 000	0.06	80 000 0000	1.00

CHAPTER 5 RESULTS AND DISCUSSION

5.1 INTRODUCTION

This chapter presents the simulation results for the performance evaluation of the beamforming solution method, which uses the MS technique and the ADMM algorithm. The simulations were executed in MATLAB on a 64-bit Intel CORE i5 desktop computer with 8 GB RAM. For all the simulation scenarios, a single cell of a typical HetNet, where the macrocell is overlaid with four small-cells (S = 4), each serving one uniformly distributed user within 10 m was considered. The focus of the results was on evaluating the performance of the macrocell users, which were uniformly distributed within the macrocell with a radius of 60 m. The simulated channels were assumed to exhibit small-scale Rayleigh fading and they are modelled similar to Case 1 for heterogeneous deployments in the 3GPP LTE standard [99].

The performance of the proposed solution method, which uses the MS technique and the ADMM algorithm to solve the convex optimisation problem, was compared with an optimal solution which uses CVX and the BRB algorithm. The ADMM algorithm was implemented using the splitting conic solver (SCS) toolbox in MATLAB [93], whereas the solution method that uses the BRB algorithm was implemented with the SeDuMi solver. The beamforming solutions of the optimisation solutions were also compared with solutions given by the ZFBF and MMSE linear precoding techniques.

Section 5.2 presents simulation results for the case of perfect CSI, which is described in Section 3.3. The focus is on investigating how the average SINR performance of the proposed solution that uses MS and the ADMM algorithm compares to the performance of the other aforementioned beamforming methods.

Section 5.3 presents simulation results for the case of imperfect CSI discussed in Section 3.4. In this case, the focus is on evaluating the efficiency of the proposed solution in terms of robustness to channel error uncertainty, worst-case SINR maximisation accuracy, and

convergence efficiency of the optimisation algorithm compared to the solution method that uses CVX and the BRB algorithm.

5.2 PERFECT CSI MODEL

For the case of perfect CSI at the transmitter, the performance of the proposed beamformer design method was analysed by evaluating how the average SINR of all MUEs varies with the BS transmit power. The simulation environment and some parameters of the system model used to obtain the results are as described in Section 5.1.

Figure 5.1, Figure 5.2, and Figure 5.3 show results of how the average SINR of K = 20 users varies with the BS power for cases of M = 100, M = 150, and M = 200 antennas, respectively.

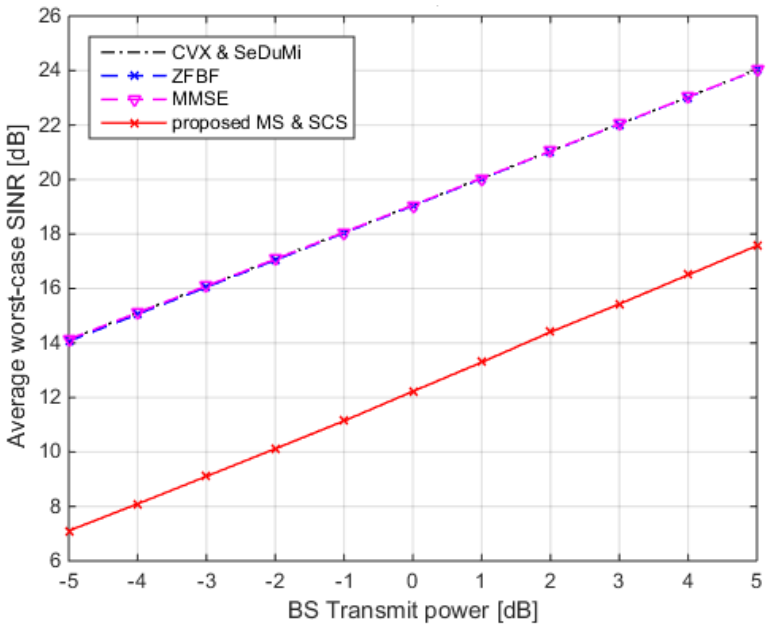

Figure 5.1. Average SINR performance for varying BS transmit power for K = 20 users, M = 100 antennas.

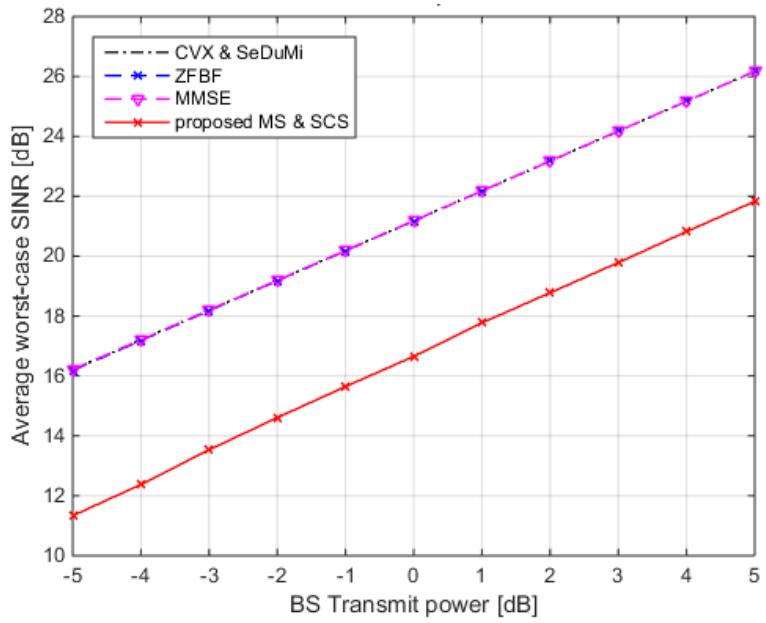

Figure 5.2. Average SINR performance for varying BS transmit power for K = 20 users, M = 150 antennas.

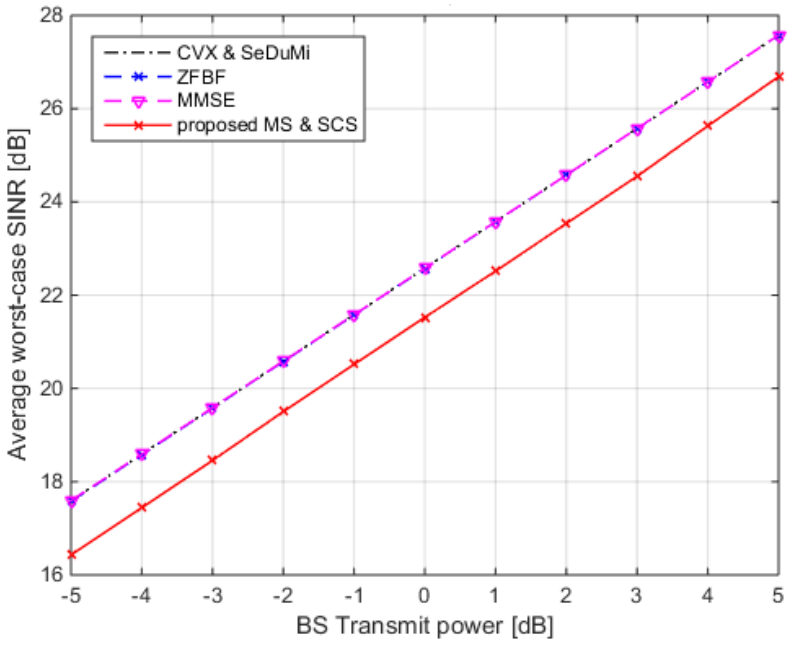

Figure 5.3. Average SINR performance for varying BS transmit power for K = 20 users, M = 200 antennas.

The results of the perfect CSI case show that the SINR performance of the MS and SCS solution method increases linearly, similar to that of the ZFBF, MMSE and the CVX and SeDuMi methods, although with reduced accuracy. The accuracy of the MS and SCS solution method improves significantly as the number of antennas, M, is increased, to achieve near optimum performance of the other beamforming methods. This can be seen from the reduction in the gap between the performance of the proposed method and that of the other methods as the number of antennas at the BS is increased from 100, through 150, to 200, as shown in Figure 5.1, Figure 5.2 and Figure 5.3.

5.3 IMPERFECT CSI MODEL

For the case of imperfect CSI acquisition at the transmitter, the performance of the proposed beamforming solution method was evaluated by analysing the average worst case SINR of all the MUEs. Maximising the average worst case SINR is the objective of the SINR balancing problem discussed in Section 4.2.1. The simulation scenario and solution methods used to compare the performance of the proposed solution are as described in Section 5.1. To generate the channel error vectors for the different uncertainty sets considered, the randomised algorithms control toolbox for MATLAB was used [100].

5.3.1 l_2 norm

Figure 5.4, Figure 5.5 and Figure 5.6 depict the accuracy and robustness performance of the proposed beamforming solution, which uses MS and SCS, by comparing it to the other aforementioned beamforming solution methods. The figures show plots of the average worst case SINR against the radius of the channel errors' uncertainty set, ρ, where the error uncertainty is bounded by the l_2-norm. The worst case SINR was averaged over 10 channel realisations for K = 20 MUEs with transmit power for the BS set at 1 dB.

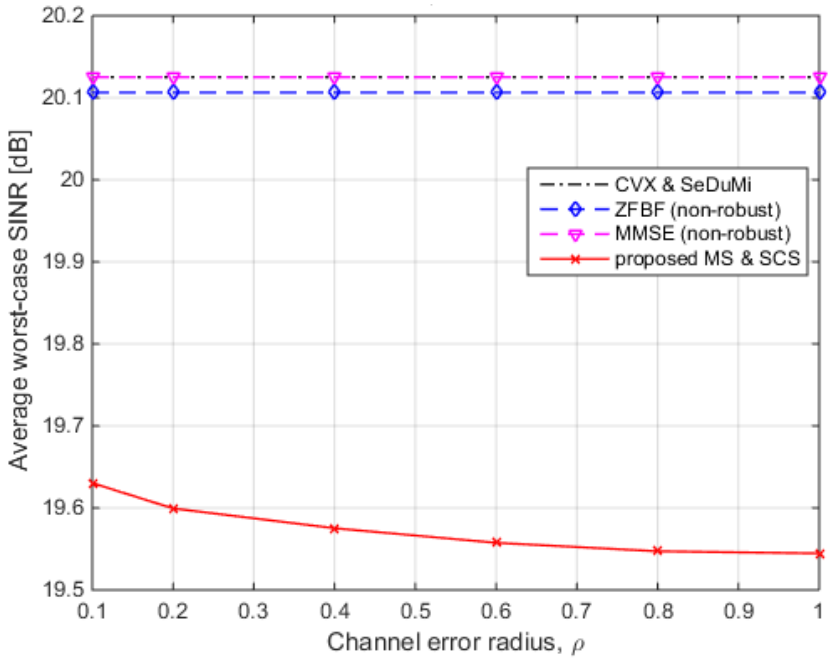

Figure 5.4. Average worst-case SINR performance against error uncertainty set radius, ρ, bounded by l_2-norm for number of BS antennas, M = 100, number of macrocell users, K = 20, and BS power, P_b = 1dB.

Figure 5.4 shows the result for the case when the number of antennas at the macrocell BS, M was set to be 100. It can be seen from the result of Figure 5.4 that for this case of M = 100, the MS and SCS solution method is outperformed by the optimal method, which uses SeDuMi and CVX, and also by methods that use ZFBF and MMSE. The robustness of the MS and SCS solution can be seen by the small degradation of the SINR as the uncertainty set radius, ρ, increases.

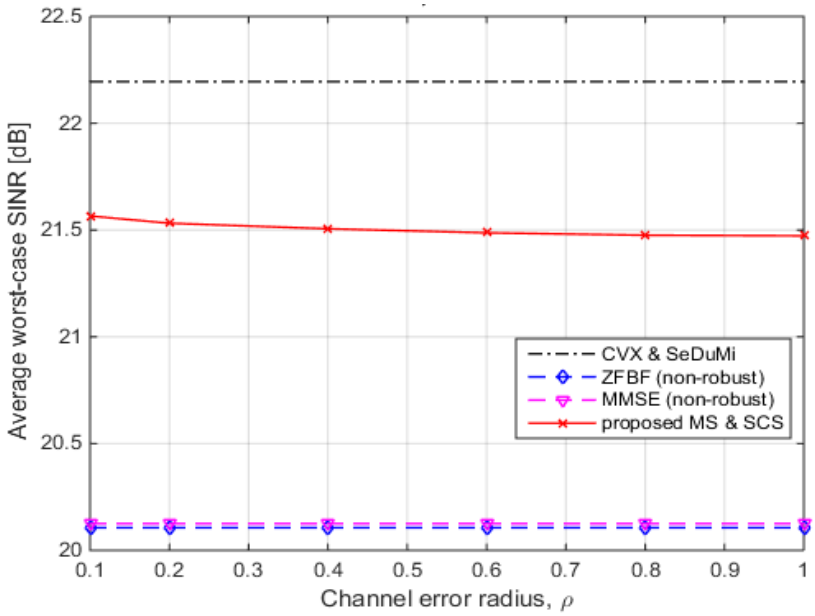

Figure 5.5. Average worst-case SINR performance against error uncertainty set radius, ρ, bounded by l_2-norm for number of BS antennas, M = 150, number of macrocell users, K = 20, and BS power, P_b = 1dB.

In Figure 5.5, the number of antennas at the macrocell BS, M, was increased to 150 while all the other parameters remained the same as for the simulation scenario of Figure 5.4. Comparing Figure 5.4 and Figure 5.5 shows that the worst-case SINR performance of all four solution methods, in terms of the average worst case SINR for a given ρ value, improved as M was increased. In addition, the MS and SCS method outperformed the ZFBF and MMSE solutions in this case of M = 150, unlike in the case of M = 100 shown in Figure 5.4.

Figure 5.6 shows the result for the case when the number of antennas at the macrocell BS, M was further increased to 200. The results of Figure 5.4, Figure 5.5 and Figure 5.6 show that increasing the number of BS antennas for the same number of macrocell users increases the average worst-case SINR performance of all the beamforming methods.

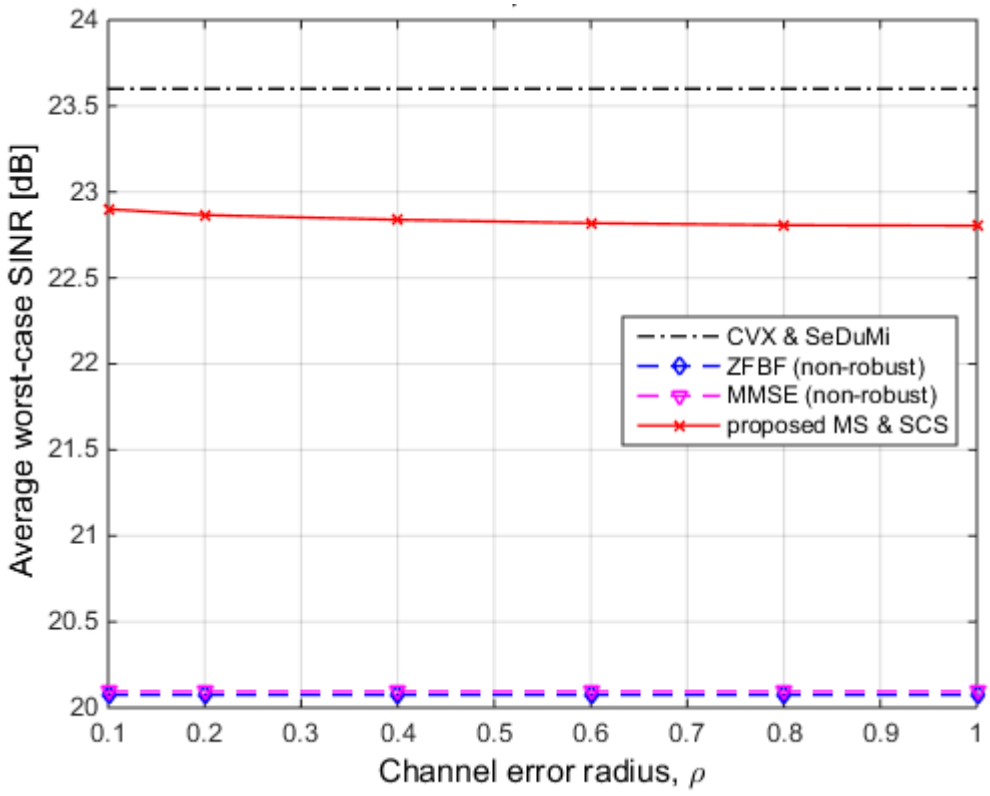

Figure 5.6. Average worst-case SINR performance against error uncertainty set radius, ρ, bounded by l_2-norm for number of BS antennas, M = 200, number of macrocell users, K = 20, and BS power, P_b = 1dB.

Figure 5.7, Figure 5.8 and Figure 5.9 show the results of investigating the effect of increasing the number of MUEs while the number of BS antennas remains the same as in Figure 5.4, Figure 5.5 and Figure 5.6, respectively. The number of macrocell users, K, was increased to 40 in this case. The results show that the average worst-case SINR performance of all the beamforming methods diminishes when the number of users is increased. The trend, however, remains the same as in the case of K = 20 users, with the MS and SCS method significantly outperforming the ZFBF and MMSE solutions but being outperformed by the CVX and SeDuMi method for the case of M = 150 and M = 200. As the number of BS antennas M is increased, the SINR accuracy of the proposed solution improves to approach that of the optimal solution given by the BRB algorithm closely.

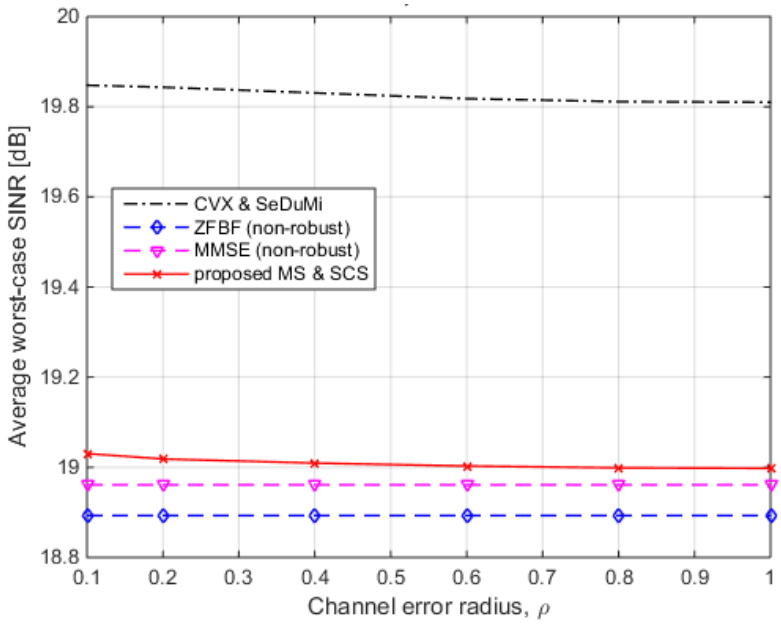

Figure 5.7. Average worst-case SINR performance against error uncertainty set radius, ρ, bounded by l_2-norm for number of BS antennas, M = 100, number of macrocell users, K = 40, and BS power, P_b = 1dB.

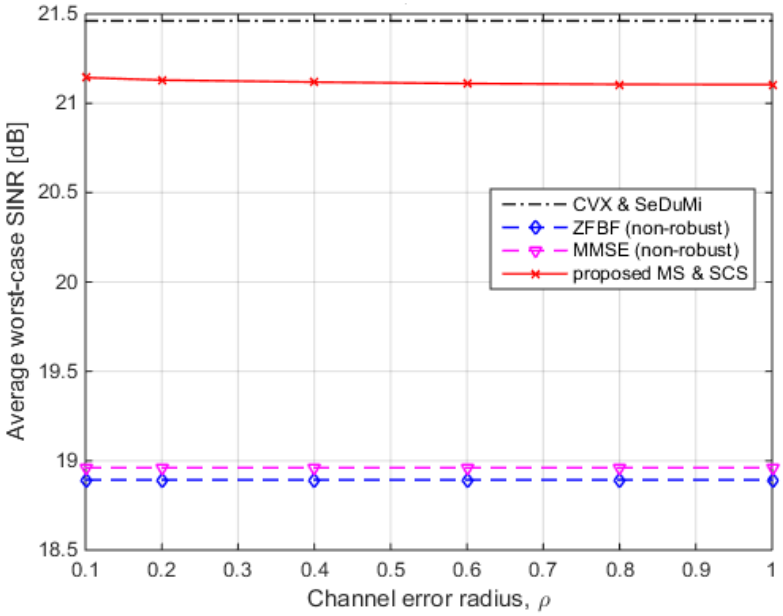

Figure 5.8. Average worst-case SINR performance against error uncertainty set radius, ρ, bounded by l_2-norm for number of BS antennas, M = 150, number of macrocell users, K = 40, and BS power, P_b = 1dB.

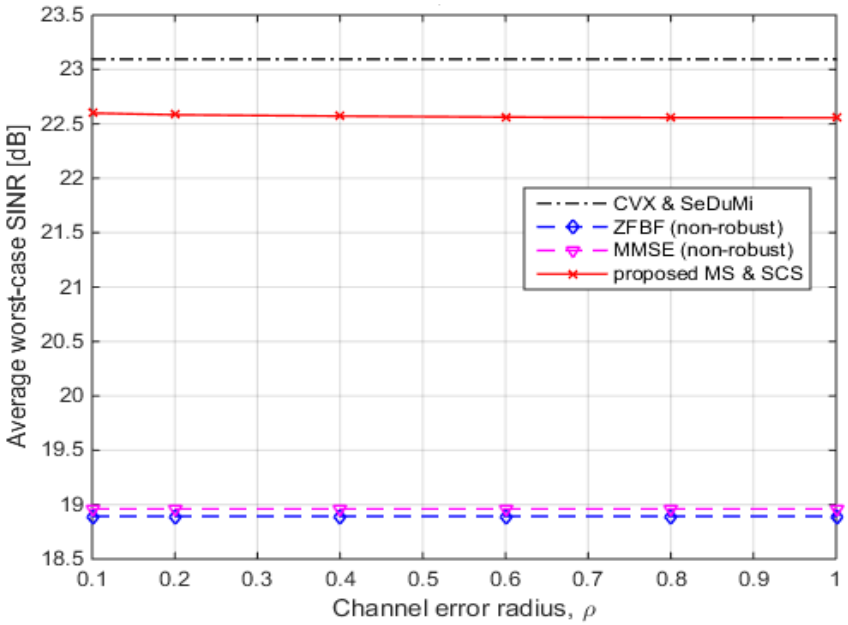

Figure 5.9. Average worst-case SINR performance against error uncertainty set radius, ρ, bounded by l_2-norm for number of BS antennas, M = 200, number of macrocell users, K = 40, and BS power, P_b = 1dB.

5.3.2 l_∞ norm

To evaluate the performance of the proposed solution method further in terms of robustness to channel error uncertainty, a different type of uncertainty was considered. In this case, the channel error vectors are bounded within a multi-dimensional box of size ρ. That is, $\|\mathbf{e}_k\|_\infty \leq \rho$ and in this case the channel error uncertainty is said to be bounded by the l_∞ norm. Figure 5.10, Figure 5.11 and Figure 5.12 show results of the SINR performance for K = 20 users, for the case of M = 100, M = 150, and M = 200, respectively.

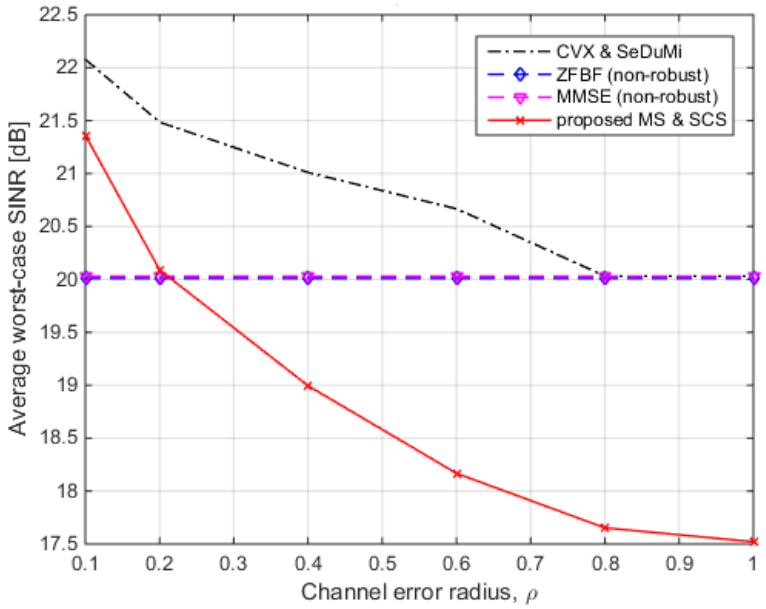

Figure 5.10. Average worst-case SINR performance against error uncertainty set radius, ρ, bounded by l_∞-norm for number of BS antennas, M = 100, number of macrocell users, K = 20, and BS transmit power, P_b = 1dB.

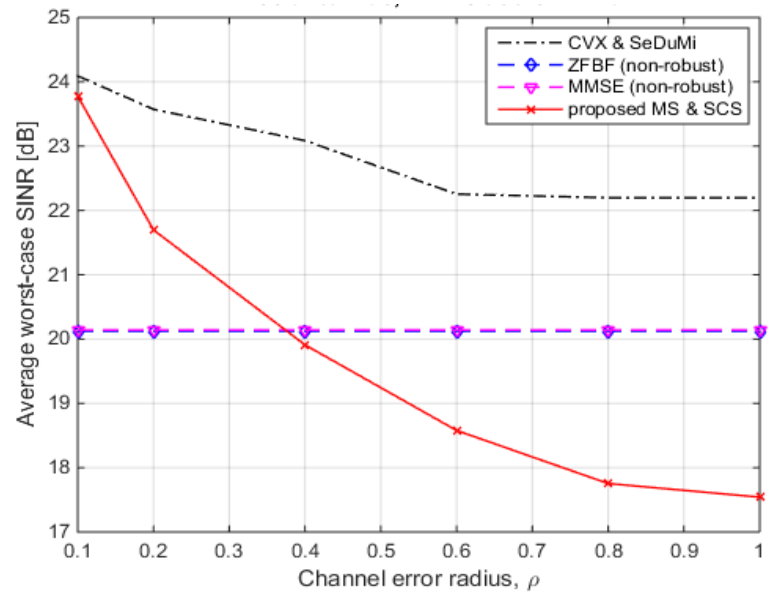

Figure 5.11. Average worst-case SINR performance against error uncertainty set radius, ρ, bounded by l_∞ norm for number of BS antennas, M = 150, number of macrocell users, K = 20, and BS transmit power, P_b = 1dB.

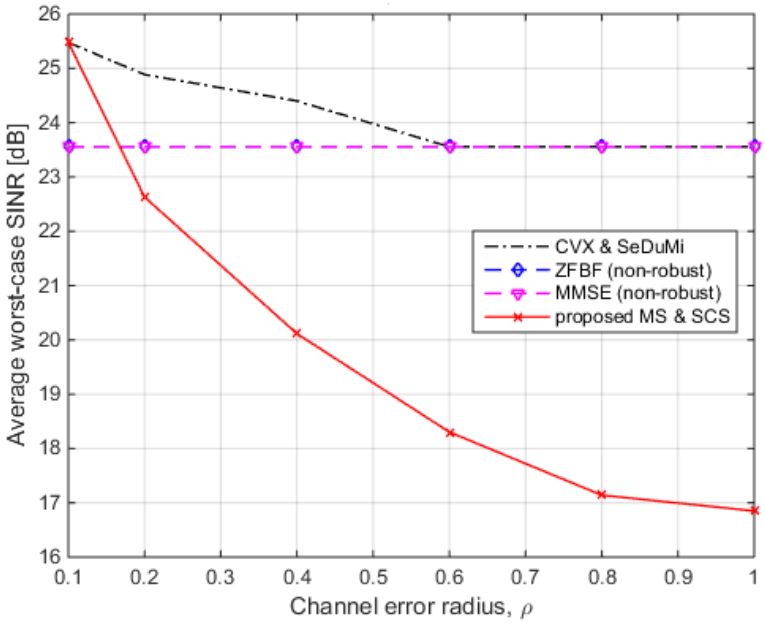

Figure 5.12. Average worst-case SINR performance against error uncertainty set radius, ρ, bounded by l_∞ norm for number of BS antennas, M = 200, number of macrocell users, K = 20, and BS transmit power, P_b = 1dB.

It is observed that the average worst case SINR performance for both MS and SCS method and the CVX and SeDuMi method is lower than that for the case when the error uncertainty set radius is bounded by the l_2 norm, for the same value of ρ. This is because the l_∞ norm defines a smaller feasible set than the l_2 norm for the same ρ [18], which leads to a degradation in performance. This also explains the worse robustness performance of the two optimisation methods for this case of l_∞ norm, compared to the case of l_2 norm in Figure 5.4, Figure 5.5, and Figure 5.6. This is observed from the greater range of worst-case SINR variations with ρ, particularly for the MS and SCS solution method.

The effect of increasing the number of users for the same number of antennas at the BS was also investigated for the case when the error uncertainty is bounded by the l_∞ norm. Figure 5.13, Figure 5.14, and Figure 5.15 show the SINR performance result for K = 40 users when M is set to be 100, 150, and 200, respectively.

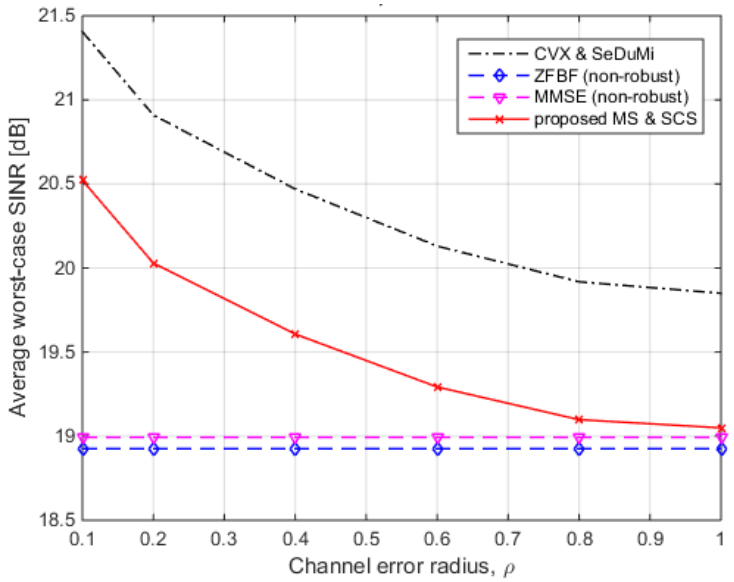

Figure 5.13. Average worst-case SINR performance against error uncertainty set radius, ρ, bounded by l_∞ norm for number of BS antennas, M = 100, number of macrocell users, K = 40, and BS transmit power, P_b = 1dB.

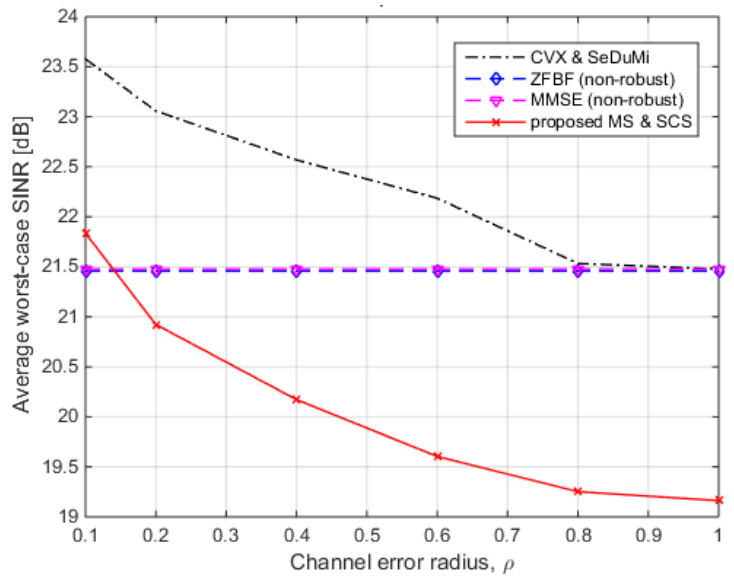

Figure 5.14. Average worst-case SINR performance against error uncertainty set radius, ρ, bounded by l_∞ norm for number of BS antennas, M = 150, number of macrocell users, K = 40, and BS transmit power, P_b = 1dB.

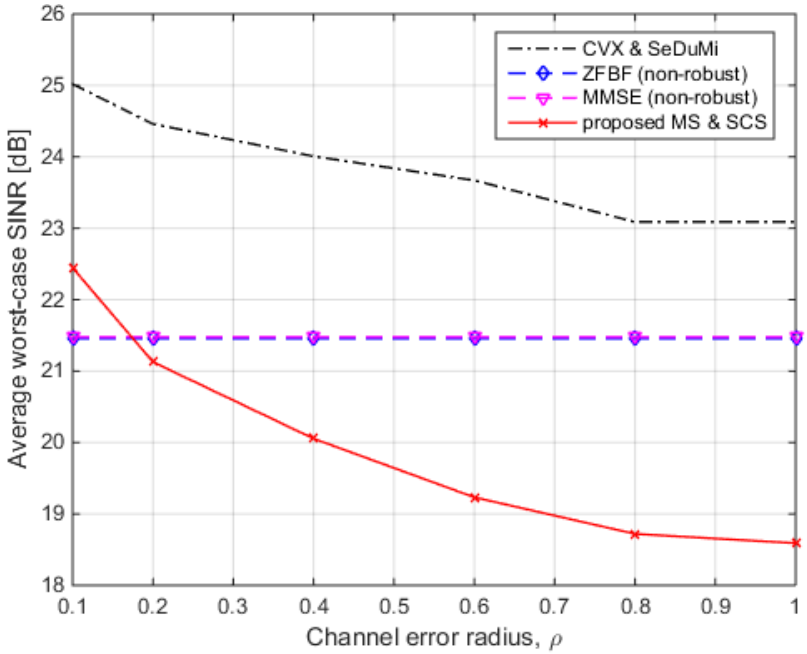

Figure 5.15. Average worst-case SINR performance against error uncertainty set radius, ρ, bounded by l_∞ norm for number of BS antennas, M = 200, number of macrocell users, K = 40, and BS transmit power, P_b = 1dB.

The results show that the average worst-case SINR performance of all the beamforming methods diminishes when the number of users is increased. The trend, however, remains the same as in the case of K = 20 users, where the average worst case SINR performance for both the MS and SCS method and the CVX and SeDuMi method is lower than that for the case when the error uncertainty set radius is bounded by the l_2 norm, for the same value of ρ.

5.3.3 BS power analysis

The performance of the proposed solution method was also evaluated in terms of how the average worst-case SINR scales with BS transmit power, P_b. The performance was compared with that of the optimal method, which uses CVX and SeDuMi, together with the other two non-robust methods. The results are shown in Figure 5.16, Figure 5.17, and Figure 5.18 for a simulation setup with K =20 users for the case of M = 100, M = 150, and M = 200, respectively. The figures show that the SINR performance of the MS and SCS

solution method increases linearly, similar to that of the ZFBF, MMSE and the CVX and SeDuMi methods, although with reduced accuracy. The accuracy of the MS and SCS solution method improves significantly as the number of BS antennas, *M*, is increased to achieve near optimum performance of the other beamforming methods. This can be seen from the reduction in the gap between the performance of the proposed method and the other beamforming methods as the number of antennas at the BS is increased from 100, through 150, to 200 as shown in Figure 5.16, Figure 5.17, and Figure 5.18.

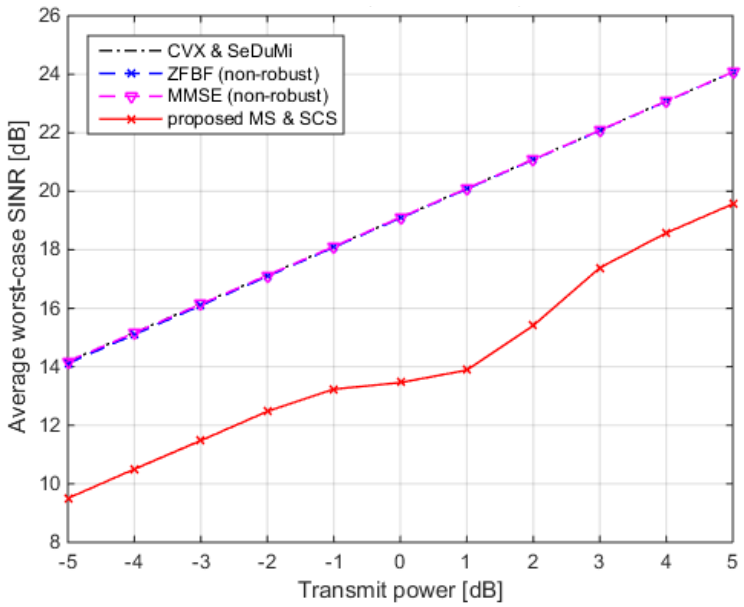

Figure 5.16. Average worst-case SINR performance against BS transmit power for number of BS antennas, $M = 100$, number of macrocell users, $K = 20$, and error uncertainty set radius, $\rho = 0.8$, bounded by l_2-norm.

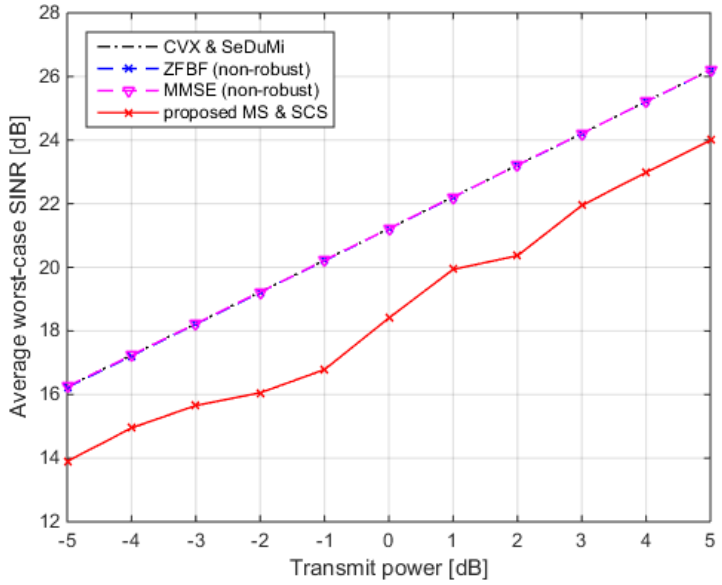

Figure 5.17. Average worst-case SINR performance against BS transmit power for number of BS antennas, M = 150, number of macrocell users, K = 20, and error uncertainty set radius, ρ = 0.8, bounded by l_2-norm.

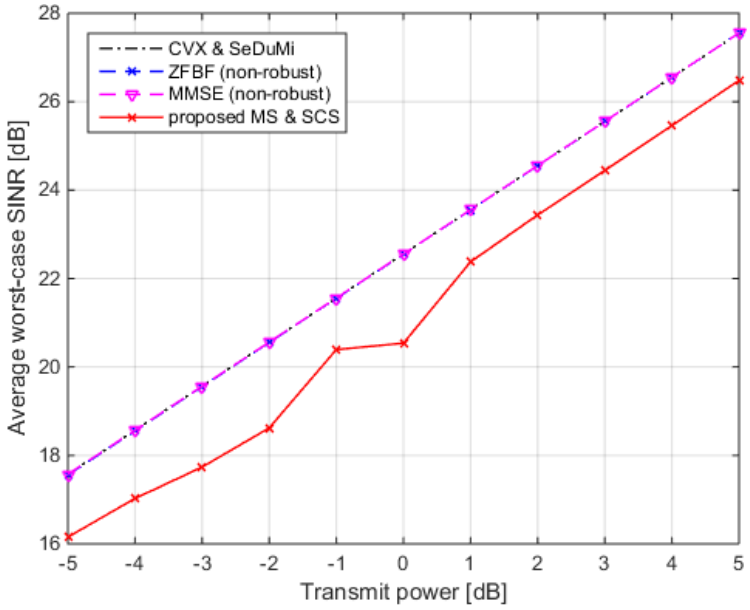

Figure 5.18. Average worst-case SINR performance against BS transmit power for number of BS antennas, M = 200, number of macrocell users, K = 20, and error uncertainty set radius, ρ = 0.8, bounded by l_2-norm.

From Figure 5.16, Figure 5.17, and Figure 5.18, it can be seen that the SINR performance of the proposed scheme achieves very good performance, comparable to the optimal method, which uses CVX and SeDuMi when the number of antennas at the BS is increased to very large values. This makes the method applicable to massive MIMO systems with large antenna arrays at the BS, in conditions of channel uncertainty.

5.3.4 Convergence efficiency analysis

To evaluate the convergence efficiency of the proposed solution method, which uses MS and SCS, an investigation of how the average worst-case SINR and the average convergence time scales with the number of antennas at the BS and the number of MUEs was carried out. The performance of the proposed solution is compared with that of the optimal solution, which uses CVX and SeDuMi.

5.3.4.1 Variation of macrocell BS antennas

Figure 5.19 depicts how the average worst-case SINR scales with the number of antennas at the BS. For this simulation, the varying number of antennas was serving K = 20 macrocell users, with the transmit power, P_b, set to be 1dB, and the uncertainty set radius, ρ, being 0.4 for channel errors bounded by the l_2-norm. It can be seen that the MS and SCS method is outperformed by the CVX and SeDuMi methods for all antenna cases, although it closely follows their average worst-case SINR. The results of the analysis of the efficiency of the proposed method, with comparison to the optimal method, which uses CVX and SeDuMi are given in Table 5.1.

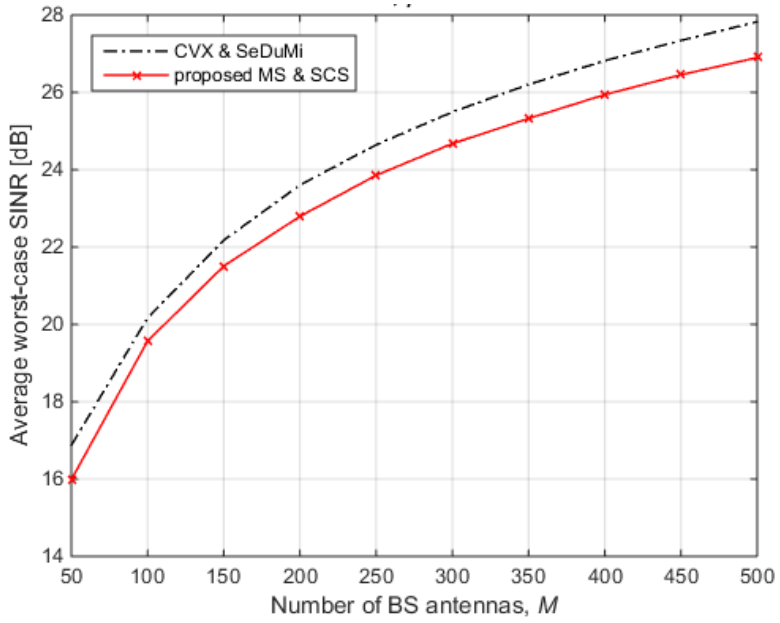

Figure 5.19. Average worst-case SINR performance for varying number of BS antennas, with error uncertainty set radius, ρ = 0.4, bounded by l_2-norm for number of macrocell users, K = 20, and BS power, P_b = 1dB.

Table 5.1 gives a comparison of the average worst-case SINR and the time taken to converge to a solution for various numbers of antennas at the BS. The convergence time includes both the time taken to transform the original problem and the time taken by the solver to reach a solution. The bisection procedure for both solution methods was set to terminate when the difference between the objective's values of two bisection steps, $\epsilon \leq 0.001$. The maximum number of iterations was set to be 2 500 for both iterative solvers. The results of Table 5.1 show that the MS and SCS method converges more than twice faster, with the average worst case SINR less than 1 dB in all cases, compared to the solution that uses CVX and SeDuMi.

In addition to the convergence time, the run-time efficiency of the two optimisation solutions was analysed by considering the local growth order of the respective solutions. This was done in order to account for platform independence of algorithms, as discussed in Section 4.4. The local growth order gives an indication of how the run-time of an algorithm increases as the input parameter increases. In this case, the input parameter is the number

of antennas at the BS, and the local growth orders of the two optimisation solutions for the various number of BS antenna cases are also given in Table 5.1.

Table 5.1. Comparison of SINR performance and convergence efficiency for the two optimisation solutions for various BS antenna cases with $K = 20$ users.

No. of BS antennas	SINR [dB]		Convergence time [s]		Local growth order	
	CVX + BRB	MS + SCS	CVX + BRB	MS + SCS	CVX + BRB	MS + SCS
50	16.8934	15.9472	27.3516	1.4780		
100	20.1081	19.6042	38.6138	2.0304	0.4974	0.4581
150	22.2393	21.5002	47.7635	4.5101	0.5244	1.9683
200	23.5986	22.8178	58.5188	8.7485	0.7059	2.3030
250	24.6431	23.8083	71.6505	14.4775	0.9072	2.2573
300	25.5000	24.6085	77.3890	20.8652	0.4225	2.0046
350	26.2029	25.3361	88.5346	28.5974	0.8728	2.0449
400	26.7980	25.8784	104.080	36.0553	1.2114	1.7354
450	27.3167	26.4306	119.968	44.3111	1.2061	1.7505
500	27.8233	26.9173	137.292	52.5670	1.2802	1.6215

Figure 5.20 gives a picture of how the local growth orders of the two solution methods vary as the input parameter, i.e. number of BS antennas, increases. The figure shows that the growth orders of both solution algorithms initially show an increasing trend as the number of BS antennas, M, increases. Although the local growth order of the MS and SCS method initially shows a higher rate of increase, it begins to show a decreasing trend as M increases beyond 250. The CVX and SeDuMi method, on the other hand, continues to show an increasing trend for the local growth rate as M increases.

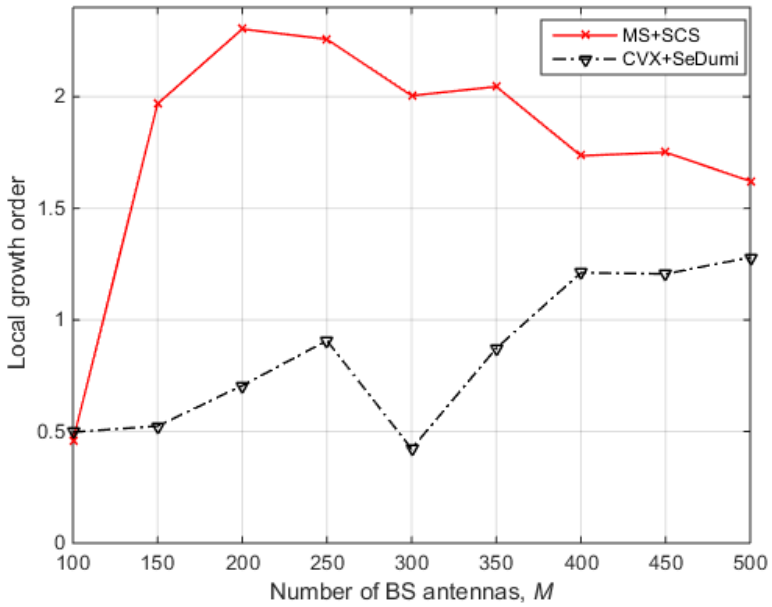

Figure 5.20. Variation of local growth order with increase in number of BS antennas for the two optimisation algorithms for K = 20.

The convergence efficiency was analysed for the case of K = 40 as well. Figure 5.21 shows the result of this simulation, and a summary of the results is given in Table 5.2.

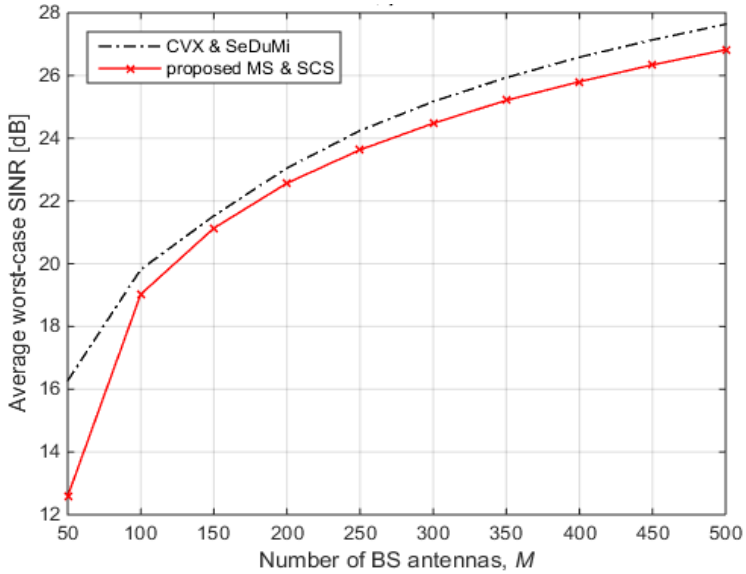

Figure 5.21. Average worst-case SINR performance for varying number of BS antennas, with error uncertainty set radius, ρ = 0.4, bounded by l_2-norm for number of macrocell users, K = 40, and BS power, P_b = 1dB.

Table 5.2. Comparison of SINR performance and convergence efficiency for the two optimisation solutions for various BS antenna cases with K = 40 users.

No. of BS antennas	SINR [dB]		Convergence time [s]		Local growth order	
	CVX + BRB	MS + SCS	CVX + BRB	MS + SCS	CVX + BRB	MS + SCS
50	16.2675	12.5833	195.0454	11.1545		
100	19.8187	19.0268	272.1324	15.1059	0.4805	0.4375
150	21.5289	21.1348	296.9940	16.3840	0.2156	0.2003
200	23.0515	22.5686	354.0629	29.4799	0.6110	2.0418
250	24.2428	23.6312	456.7951	46.7276	1.1416	2.0643
300	25.1697	24.4746	542.3982	68.4973	0.9421	2.0977
350	25.9339	25.2091	633.1217	94.3152	1.0033	2.0749
400	26.5845	25.8023	733.9028	121.212	1.1062	1.8789
450	27.1350	26.3390	839.4090	150.577	1.1404	1.8418
500	27.6346	26.8211	952.3769	179.720	1.1984	1.6792

Figure 5.22 shows the variation of the local growth orders for the case of K = 40 users as given in Table 5.2. Comparing Figure 5.20 and Figure 5.22 shows that the general trends of the variation in local growth order for the two optimization methods are not affected by a change in other parameters such as the number of users K. This corresponds to the results discussed in Section 4.4.2.

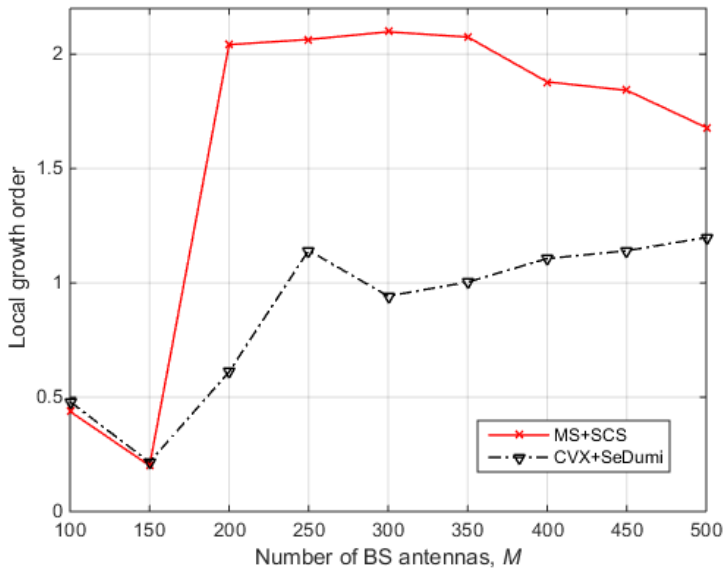

Figure 5.22. Variation of local growth order with increase in number of BS antennas for the two optimisation algorithms for K = 40.

5.3.4.2 Variation of MUEs

Figure 5.23 depicts how the average worst-case SINR scales with the number of MUEs for a fixed number of BS antennas M = 150. The transmit power, P_b, was set to be 1dB with the uncertainty set radius, ρ, being 0.4 for channel errors bounded by the l_2-norm. The figure shows that as the number of MUEs increases whilst the number of BS antennas is kept constant, the average worst-case SINR decreases for the two optimization beamforming methods. This is as expected since increasing the number of MUEs whilst keeping the number of macrocell BS antennas constant reduces the degrees of freedom for beamforming and thus a decrease in SINR performance.

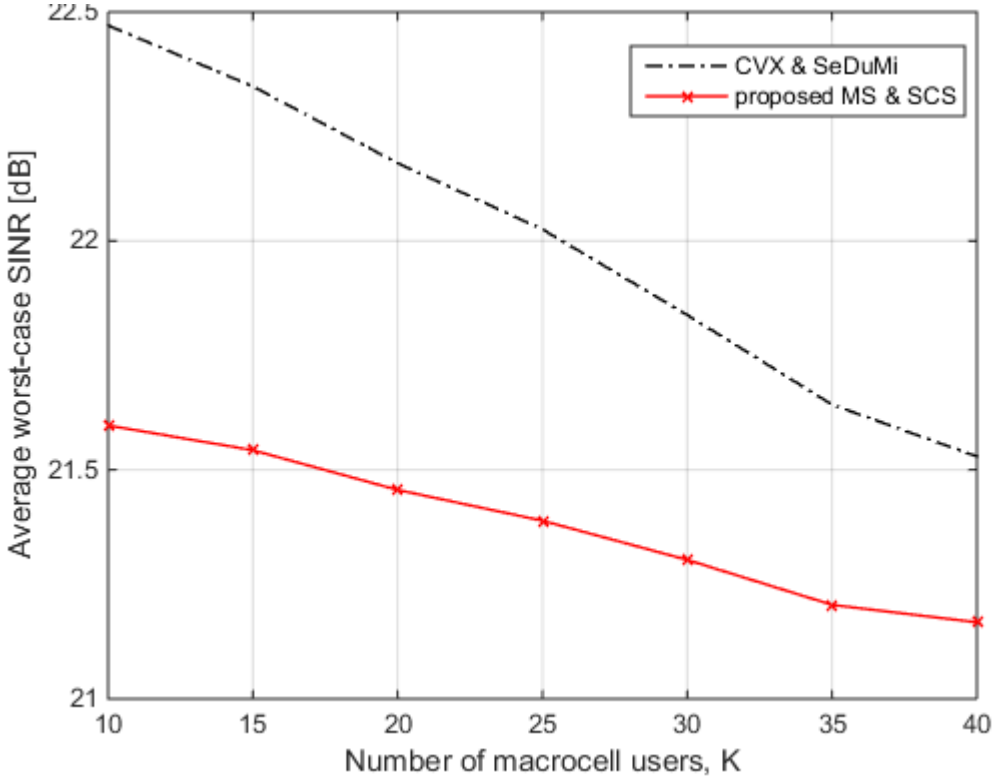

Figure 5.23. Average worst-case SINR performance for varying number of MUEs, with error uncertainty set radius, ρ = 0.4, bounded by l_2-norm, number of macrocell BS antennas, M = 150, and BS power, P_b = 1dB.

Table 5.3 gives a comparison of the average worst-case SINR, the time taken to converge to a solution, and the local growth order for various numbers MUEs for the fixed number of BS antennas, M = 150. The other simulation parameters are the same as for the results in Table 5.1. Figure 5.24 gives depicts how the local growth orders of the two optimisation solutions vary as the number of MUEs increases. The figure shows that the local growth orders of both solution algorithms generally increases as the number of MUEs increases. The local growth order of the CVX & SeDuMi method, however, increases more rapidly compared to that of the MS & SCS method.

Table 5.3. Comparison of SINR performance and convergence efficiency for the two optimisation solutions for various numbers of MUEs with M = 150.

No. of MUEs	SINR [dB]		Convergence time [s]		Local growth order	
	CVX + BRB	MS + SCS	CVX + BRB	MS + SCS	CVX + BRB	MS + SCS
10	22.597	21.536	12.369	1.6680		
15	22.365	21.563	27.534	2.8882	1.973505	1.354011
20	22.250	21.452	49.445	4.6681	2.034959	1.66882
25	22.125	21.317	83.269	7.0793	2.335753	1.866206
30	21.804	21.361	132.142	9.7269	2.533133	1.742662
35	21.722	21.286	201.922	13.127	2.750304	1.944801
40	21.540	21.135	308.007	16.775	3.162123	1.836316

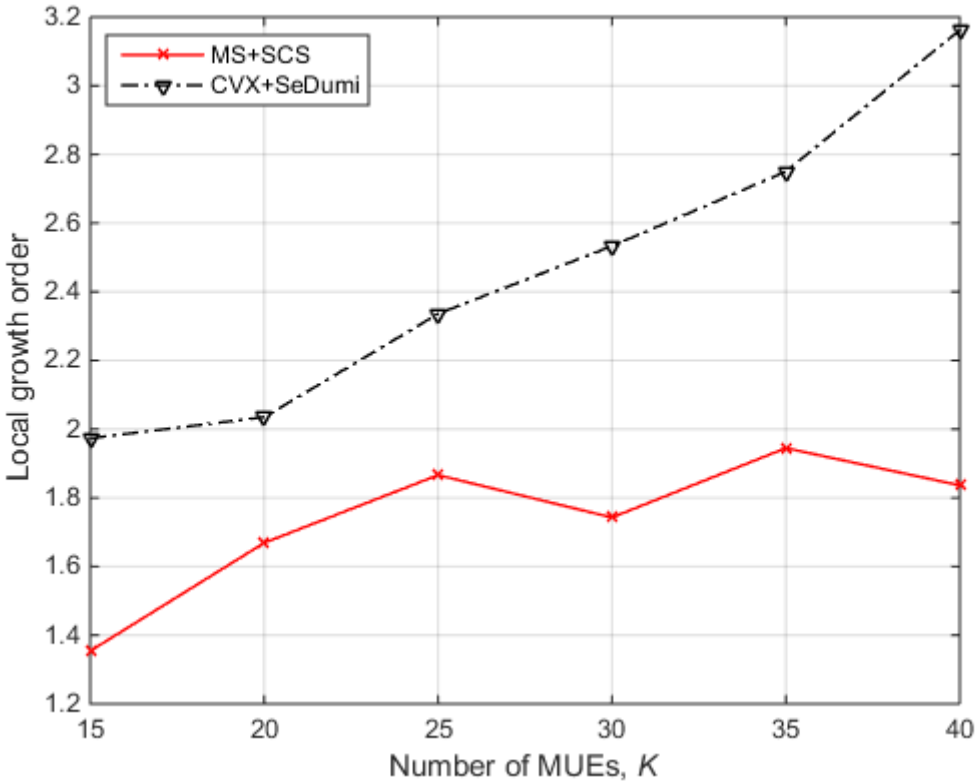

Figure 5.4. Variation of local growth order with increase in number of MUEs for the two optimisation algorithms for M = 150.

5.4 CONCLUDING REMARKS

The performance of the proposed beamforming solution method applicable to massive MIMO at the macrocell BS of a typical HetNet scenario was evaluated in terms of the average SINR of all the MUEs, for the cases of both perfect CSI and imperfect CSI at the transmitter. It is worth noting that for the case of imperfect CSI, the performance becomes the average worst-case SINR performance for a given channel error uncertainty norm type and its associated radius. It was found that the proposed solution method, which uses the MS technique and the ADMM algorithm, yields performance with reduced accuracy particularly for a few BS antennas, compared to the optimal solution that uses CVX and the SeDuMi solver. The performance of the proposed scheme was observed to increase to near-optimal performance for cases when the number of BS antennas was increased to very large values.

The proposed beamforming solution method that uses MS and the ADMM algorithm achieved solutions with about 97% accuracy, in terms of SINR performance, while it converged to a solution more than twice faster compared to the optimal solution of CVX and SeDuMi. The results of convergence analysis showed that the complexity of the SCS solution algorithm was observed to decrease as the number of antennas at the BS was increased, unlike that of the SeDuMi solution algorithm, which showed an increasing trend. This makes the proposed solution favourable for low latency applications of future generation networks that make use of massive MIMO as the BSs.

The practical limit of the number of antennas at the BS for acceptable latency depends on the trade-off between required performance and sensitivity to the delay introduced by beamforming for various applications. Although for applications that are not sensitive to the delay contribution of beamforming for massive MIMO systems in wireless networks it is ideal to use an infinite number of antennas as the BS, this is not cost effective and hence not practical.

CHAPTER 6 CONCLUSION AND FUTURE WORK

6.1 CONCLUDING REMARKS

This dissertation provides a report on findings from research carried out on beamforming for massive MIMO base stations at the macrocell of heterogeneous wireless networks. The focus of the research was on investigating the performance of the beamforming solutions for macrocell users in a typical HetNet scenario, served by a large array of antennas at their BS.

Chapter 2 gives an overview of the beamforming techniques that have been proposed in literature for massive MIMO beamforming in HetNets. Beamforming techniques that have been applied to traditional cellular networks are also summarised. These techniques include linear precoding schemes and robust optimisation methods. In addition to the beamforming techniques, an overview of the prevalent optimal solvers used to solve beamforming optimisation problems in literature is given.

In Chapter 3, the system model that was considered for the analysis and simulation to investigate the performance of the proposed beamforming solution method is presented and described. Two models are considered. One is the perfect CSI model, where TDD is envisaged. The other model is the imperfect CSI model, which aims to account for CSI acquisition errors that are usually encountered in practice.

Chapter 4 presents the proposed solution method for the beamforming for macrocell users in a typical HetNet configuration. The proposed solution method provides a fast transformation of the original optimisation into a convex SOCP by employing the Smith form reformulation and the MS technique. A fast converging solution of the transformed problem, which comes at the cost of reduced accuracy, is obtained by applying homogeneous self-embedding and the ADMM algorithm. A technique to analyse the

convergence efficiency of the proposed method and compare it to the optimal solution is described.

In Chapter 5, simulation results of the proposed beamforming method, with comparison to other prominent methods used in literature, are presented and discussed. Results of the performance analysis for both the perfect CSI case and the case of imperfect CSI are given. The solution method is based on applying the MS technique and the ADMM algorithm to transform and solve the original optimisation problem. Simulation results showed that this method gives average worst-case SINR performance with reduced accuracy compared to the optimal method which uses CVX and the BRB, but with near optimum accuracy for cases where the macrocell BS is equipped with a large number of antennas. The proposed solution method was shown to give better converge efficiency compared to the second-order method, which uses CVX and SeDuMi, particularly when the number of antennas at the macrocell BS grows to large values. This is because the proposed method converges to a solution much faster than the interior-point method, and the local growth order of the algorithm generally decreases with increasing BS antennas at the macrocell. This makes the proposed solution method attractive for practical application in HetNets with large antenna arrays at the macrocell BS in scenarios with channel uncertainty.

6.2 FUTURE WORK

Other research areas that can be explored further to build onto the work carried out for this research may include:

- Extend the system model to a multicell model and evaluate how the proposed solution method performs for both coordinated and uncoordinated systems of BSs.
- Investigate the application of cell range expansion together with the robust beamforming method to enhance interference mitigation for macrocell users in a HetNet scenario.
- Investigate the performance of small-cell users to see how the use of robust beamforming with massive MIMO for macrocell users affects the performance. Use of conventional MIMO can be applied at the small-cell access point.

- Analyse a distributed massive MIMO scenario, for example where the large array of antennas is modelled to be scattered around a building rooftop, typically in small groups of a few antennas each.
- Investigate application of massive MIMO BSs in cognitive radio networks, and the most suitable beamforming method for maximising rate performance in such networks.

REFERENCES

[1] M.G. Kachhavay and A.P. Thakare, "5G Technology-Evolution and Revolution," *International Journal of Computer Science and Mobile Computing*, vol. 3, no. 3, pp. 1080 – 1087, March 2014.

[2] P. Tebe, K. Yujun, J. Kponyo, "Performance Analysis and Comparison of ZF and MRT Based Downlink Massive MIMO Systems," in *IEEE Sixth International Conference on Ubiquitious and Future Networks (ICUFN)*, 2014, pp. 383-388.

[3] E.G. Larsson, O. Edfords, F. Tufvesson and L. Marzetta, "Massive MIMO for Next Generation Wireless Systems," *IEEE Communications Magazine*, vol 52, no. 2, pp. 187-195, Feb. 2014.

[4] L. Liu, J. Zhang, Y. Yi, H. Li, and J. Zhang, "Combating Interference: MU-MIMO, CoMP, and HetNet," *Journal of Communications*, vol. 7, no. 9, pp. 646-655, Sept. 2012.

[5] V. Chandrasekhar and J. G. Andrews, "Femtocell Networks: A Survey," *IEEE Communications Magazine*, vol 46, no. 9, pp. 59-68, Sept. 2008.

[6] C. Li, J. Zhang, S. H. Song, and K. B. Letaief, "Analysis of Area Spectral Efficiency and Link Reliability in Multiuser MIMO HetNets," in *IEEE International Conference on Communications (ICC)*, 2015, pp. 2839 – 2844.

[7] M. Kountouris and N. Pappas, "HetNets and Massive MIMO: Modeling, Potential Gains, and Performance Analysis," in *IEEE-APS Conference on Antennas and Propagation in Wireless Communications (APWC)*, pp. 1319-1322, Sep. 2013.

[8] W. Shin, W. Noh, K. Jang, and H. Choi, "Hierarchical Interference Alignment for Downlink Heterogeneous Networks," *IEEE Transactions on Wireless Communications*, vol. 11, no. 12, pp. 4549-4560, Dec. 2012.

[9] H. Yang and T.L. Marzetta, "Performance of Conjugate and Zero-Forcing Beamforming in Large-Scale Antenna Systems," *IEEE Journal on Selected Areas in Communications*, vol. 31, no. 2, pp. 172-179, Feb. 2013.

[10] C. Park, Y. Byun, A.M Bokiye and Y. Lee, "Complexity Reduced Zero-forcing Beamforming in Massive MIMO Systems," in *IEEE Conference on Information Theory and Applications Workshop (ITA)*, 2014, pp. 1-5.

[11] B.D. van Veen, K.M. Buckley, "Beamforming: A Versatile Approach to Spatial Filtering," *IEEE ASSP Magazine*, vol. 5, no. 2, pp. 4-24, Apr. 1988.

[12] X. Gao, O. Edfords, F. Rusek, and F. Tufvesson, "Linear Pre-coding Performance in Measured Very Large MIMO Channels," in *IEEE Vehicular Technology Conference (VTC Fall)*, 2011, pp. 1-5.

[13] M. Rao, A. Kazerouni, and O. Aryan, "Precoding Schemes for MIMO Downlink Transmission," Stanford University, Stanford, CA, EE360 Paper Summary.

[14] A. Ben-Tal and A. Nemirovski, "Robust Convex Optimisation," *Mathematics of Operations Research*, vol. 23, no. 4, pp. 769–805, Nov. 1998.

[15] D. Bertsimas, D.B. Brown, and C. Caramanis, "Theory and Applications of Robust Optimisation," *SAIM Review*, vol. 53, no. 3, pp. 464-501, Aug. 2011.

[16] K. Hosseini, J. Hoydis, S. ten Brink, and M. Debbah, "Massive MIMO and Small-cells: How to Densify Heterogeneous Networks," in *IEEE International Conference on Communications*, 2013, pp. 5442-5447.

[17] A. Adhikary, H.S. Dhillon, and G. Caire, "Massive-MIMO Meets HetNet: Interference Coordination through Spatial Blanking," *IEEE Journal on Selected Areas in Communications*, vol. 33, no. 6, pp. 1171-1186, Jun. 2015.

[18] J. Hoydis, K. Hosseini, S. ten-Brink, and M. Debbah, "Making Smart Use of Excess Antennas: Massive MIMO, Small-Cells, and TDD," *Bell Labs Technical Journal*, vol. 18, no. 2, pp. 5 – 21, 2013.

[19] I.F. Akyildiz, D.M. Gutierrez-Estevez and E.C. Reyes, "The Evolution to 4G Cellular Systems: LTE-Advanced," *Physical Communication*, vol. 3, no. 4, pp. 217-244, Dec. 2010.

[20] M. Ergen, *Mobile Broadband Including WiMax and LTE*. Berkely, CA: Springer, 2009.

[21] S.M. Alamouti, "A Simple Transmit Diversity Technique for Wireless Communications," *IEE Journal on Selected Areas in communications*, vol. 16, no. 8, pp. 1451-1458, Oct. 1998.

[22] Rhode & Schwarz, "UMTS Long Term Evolution (LTE) Technology Introduction," Application Note 1MA111, 2007.

[23] I. Ben Chaabane, S. Hamouda, and S. Tabbane, "Fair and Energy-Aware Power Allocation Scheme in Multi-cell MIMO Cooperative Networks," in *IEEE Vehicular Technology Conference (VTC Spring)*, 2014, pp. 1-5.

[24] L. Lu, G.Y. Li, A.L. Swindlehurst, A. Ashikhmin, and R. Zhang, "An Overview of Massive MIMO: Benefits and Challenges," *IEEE Journal of Selected Topics in Signal Processing*, vol. 8, no. 5, pp. 742-758, Oct. 2014.

[25] T.L. Marzetta, "Noncooprative Cellular Wireless with Unlimited Numbers of Base Stations," *IEEE Transactions on Wireless Communications*, vol. 9, no. 11, pp. 3590-3600, Nov. 2010.

[26] H.Q. Ngo, E.G. Larson, and T.L. Marzetta, "Energy and Spectral Efficiency of Very Large Multiuser MIMO Systems," *IEEE Transactions on Communications*, vol. 61, no. 4, pp. 1436-1449, Apr. 2013.

[27] A. F. Molisch et al., "Hybrid beamforming for massive MIMO: A survey", *IEEE Communications Magazine*, vol. 55, no. 9, pp. 134-141, Sept. 2017.

[28] S. Payami, M. Ghoraishi, and M. Dianati, “Hybrid Beamforming for Large Antenna Arrays with Phase Shifter Selection,” *IEEE Transactions on Wireless Communications*, vol. 15, no. 11, pp. 7258-7271, Nov. 2016.

[29] F. Sohrabi and W. Yu, ``Hybrid digital and analog beamforming design for large-scale MIMO systems," in *Proceedings of IEEE International Conference on Acoustics, Speech and Signal Processing (ICASSP)*, Brisbane, Australia, Apr. 2015, pp. 2929-2933.

[30] S. Han, I. Chih-Lin, Z. Xu, and C. Rowell, “Large-Scale Antenna Systems with Hybrid Analog and Digital Beamforming for Millimeter Wave 5G,” *IEEE Communications Magazine*, vol. 53, no. 1, pp. 186-194, Jan. 2015.

[31] A. Liu andV. K. N. Lau, “Impact of CSI Knowledge on the Codebook-Based Hybrid Beamforming in Massive MIMO,” *IEEE Transactions on Signal Processing*, vol. 64, no. 24, pp. 6545-6556, Dec. 2016

[32] H.Q. Ngo, T.L. Marzetta, and E.G. Larsson, “Analysis of the Pilot Contamination Effect in Very Large Multicell Multiuser MIMO Systems for Physical Channel Models,” in *IEEE International Conference on Acoustics, Speech and Signal Processing(ICASSP)*, 2011, pp. 3464-3468.

[33] A. Ashikhmin and T. Marzetta, “Pilot Contamination Precoding in Multi-Cell Large Scale Antenna Systems,” in *Proceedings of IEEE International Symposium on Information Theory*, 2012, pp. 1137-1142.

[34] L. Li, A. Ashikhmin, and T. Marzetta, “Pilot Contamination Precoding for Interference Reduction in Large Scale Antenna Systems,” in *Fifty-First Annual Allerton Conference*, 2013, pp. 226-233.

[35] R.R. Muller, L. Cottatellucci, and M. Vehkapera, “Blind Pilot Decontamination,” *IEEE Journal of Selected Topics on Signal Processing*, vol. 8, no. 5, pp. 773-786, Oct. 2014.

[36] R.R. Muller, M. Vehkapera, and L. Cottatellucci, "Analysis of Blind Pilot Decontamination," in *Asilomar Conference on Signals, Systems and Computers*, 2013, pp. 1016-1020.

[37] O.K. Ozdemir and H. Arslan, "Channel Estimation for Wireless OFDM Systems," *IEEE Communications Surveys and Tutorials*, vol. 9, no. 2, pp. 18-48, July 2007.

[38] O.O. Oyerinde and S.H. Mneney, "Review of Channel Estimation for Wireless Communication Systems," *IETE Technical Review Journal*, vol. 29, no. 4, pp. 282-298, Sept. 2014.

[39] S. Nguyen and A. Ghrayeb, "Compressive Sensing-Based Channel Estimation for Massive Multiuser MIMO Systems," in *Proceedings of IEEE Wireless Communications and Networking Conference (WCNC)*, 2013, pp. 2890-2895.

[40] L. Dai, Z. Wang, and Z. Yang, "Spectrally Efficient Time-Frequency Training OFDM for Mobile Large Scale MIMO systems," *IEEE Journal on Selected Areas in Communications*, vol. 31, no.2, pp. 251-263, Feb. 2013.

[41] X. He, R. Song, and W.P. Zhu, "Pilot Allocation for Sparse Channel Estimation in MIMO-OFDM Systems," *IEEE Transactions on Circuits and Systems II: Express Briefs*, vol. 60, n0. 9, pp. 612-616, Spt. 2013.

[42] E. Pakdeejit, "Linear Precoding Performance of Massive MU-MIMO Downlink System," M.S. thesis, Linkoping University, Linkoping, Sweden, May 2013.

[43] H.Q. Ngo, E.G. Larsson, and T.L. Marzetta, "Massive MU-MIMO Downlink TDD Systems with Linear Precoding and Downlink Pilots," in *51st Annual Allerton Conference on communication, Control and Computing*, 2013, pp. 293-299.

[44] F. Russek, D. Persson, B.K. lau, E.G. Larsson, T.L. Marzetta, O. Edfords, and F. Tufvesson, "Scaling up MIMO: Opportunities and Challenges with Very Large Arrays," *IEEE Signal Processing Magazine*, vol. 30, no. 1, pp. 40-60, Jan. 2013.

[45] L. Zhao, K. Zheng, H. long, H. Zhao, "Performance Analysis for Downlink Massive MIMO System with ZF Precoding," *Transactions on Emerging Telecommunications Technologies*, vol. 8, no. 3, pp. 390-398, Oct. 2014.

[46] J. hoydis, S. Brink, and M. Debbah, "Comparison of Linear Precoding Schemes for Downlink Massive MIMO," in *IEEE International Conference on Communications (ICC)*, 2012, pp. 2135-2139.

[47] M. Sadek, A. Tarighat, and A.H. Sayed, "Active Antenna Selection in Multi-User MIMO Communications," *IEEE Transactions on Signal processing*, vol. 55, no. 4, pp. 1498-1510, Apr. 2007.

[48] M. Sadek, A. Tarighat, and A.H. Sayed, "A Leakage-Based Precoding Scheme for Downlink Multi-User MIMO Channels," *IEEE Transactions on Wireless Communications*, vol. 6, no. 5, pp. 1711-1721.

[49] C. Peel, B. Hochwald, and A. Swindlehurst, "A VectorPerturbation Technique for Near-Capacity Multiantenna Multiuser Communication-Part I: Channel Inversion and Regularisation," *IEEE Transactions on Communications*, vol. 53, no. 1, pp. 195-202, Jan. 2005.

[50] C.K. Wen, J.C. Chen, K.K. Wong, and P. Ting, "Message Pasing Algorithm for Distributed Downlink Regularised Zero-Forcing Beamforming with Cooperative Base Stations," *IEEE Transactions on Wireless communications*, vol. 13, no. 5, pp. 2920-2930, May. 2014.

[51] J. Qi and S. Aissa, "Optimal Beamforming in MIMO Systems with HPA Nonlinearity," in *IEEE 21st International Sysmposium on Personal Indoor and Mobile Radio Communications*, 2010, pp. 911-915.

[52] J. Qi and S. Aissa, "On the Power Amplifier Non-Linearity in MIMO Transmit Beamforming Systems," *IEEE Transactions on Communications*, vol. 60, no. 3, pp. 876-887, Mar. 2012.

[53] G. lee, J. Park, Y. Sung, and J. Seo, "A New Approach to Beamformer Design for Massive MIMO Systems Based on *k*-Regularity," in *IEEE International Workshop on Emerging technologies for LTE-Advanced and Beyond 4G,* 2012, pp. 686-690.

[54] J.G. Andrews, "Seven Ways that HetNets are a Celluler Paradigm Shift," *IEEE Coummunications Magazine,* vol. 51, no. 3, pp. 136-144, Mar. 2013.

[55] D. lopez-Perez *et al.*, "OFDMA Femtocells: A Roadmap on Interference Avoidance," *IEEE Communications Magazine,* vol. 47, no. 9, pp. 41-48, Sept. 2009.

[56] D. Lopez-Perez *et al.,* "Enhanced Intercell Interference Coordination Challenges in Heterogeneous Networks," *IEEE Wireless Communications Magazine*, vol. 18, no.3, pp. 22-30, June 2011.

[57] D. Aziz, M. Mazhar, and A. Weber, "Interference Management Through Interference Alignment Based Transmit Precoding in Multi User Heterogeneous Cellular Networks," in *Proceedings of 20th European Wireless Conference,* 2014, pp. 1-6.

[58] S. Singh and J.G. Andrews, "Joint Resource Partitioning and Offloading in Heterogeneous Cellular Networks," *IEEE Transactions on Wireless Communications,* vol. 13, no. 2, pp. 888-901, Feb. 2014.

[59] A.H. Sakr and E. Hossain, "Location-Aware Cross-Tier Coordinated Multipiont Transmission in Two-Tier Cellular Networks," *IEEE Transactions on Wireless Communications,* vol. 13, no. 11, pp. 6311-6325, Nov. 2014.

[60] Y. Wui, Y. Cui, and B. Clerckx, "Analysis and Optimisation of Interference Nulling in Downlink Multi-Antenna HetNets with Offloading," in *IEEE International Conference on Communications (ICC),* 2015, pp. 2457-2462.

[61] O.E. Ayach, S.W. Peters, and R.W. Heath, "The Practical Challenges of Interference Alignment," *IEEE Wireless Communications Magazine*, vol. 20, no. 1,pp. 35-42, Feb. 2013.

[62] T. Akitaya and T. Saba, "Hierachical Multi-Stage Interference Alignment for Downlink Heterogeneous Networks," *Signal and Processing Association Annual Summit and Conference (APSIPA),* 2013, pp. 1-5.

[63] A. Adhikary, J. Nam, J.-Y. Ahn, and G. Caire, "Joint Spatial Division and Multiplexing: The Large-Scale Array Regime," *IEEE Transactions on Information Theory,* vol. 59, no. 10, pp. 6441-6463, Oct. 2013.

[64] L. Sanguinetti, A. Moustakas, and M. Debbah, "Interference Management in 5G Reverse TDD HetNets: A large System Analysis," *IEEE Journal on Selected Areas in Communications,* vol. 33, no. 6, pp. 1187-1200, Mar. 2015.

[65] G. Xu, C-H Lin, W. Ma, S. Chen, and C-Y Chi, "Outage Constrained Robust Hybrid Coordinated Beamforming for Massive MIMO Enabled Heterogeneous Cellular Networks," *IEEE Access,* vol. 5, pp. 13601-13616, Mar. 2017.

[66] D. Castanheira, P. Lopes, A. Silva, A. Gameiro, "Hybrid Beamforming Designs for Massive MIMO Millimetre-Wave Heterogeneous Systems," *IEEE Access*, vol. 5, pp. 21806-21817, Oct. 2017.

[67] L.N. Tran, M.F. Hanif, A. Tolli, and M. Junti, "Fast Converging Algorithm for Weighted Sum Rate Maximization in Multicell MISO Downlink," *IEEE Signal Processing Letters,* vol. 19, no. 12, pp. 872-875, Dec. 2012.

[68] S. Joshi, P. Weeraddana, M. Codreanu, and M. latva-aho, "Weighted sum rate Maximization for MISO Downlink Cellular Networks via Branch and Bound," *IEEE Transactions on Signal Processing*, vol. 60, no. 4, pp. 2090-2095, Apr. 2012.

[69] C.T.K. Ng and H. Huang, "Linear Precoding in Cooperative MIMO Cellular Networks with Limited Coordination Clusters," *IEEE Journal of Selected Areas in Communication,* vol. 28, no.9, pp. 1446-1454, Dec. 2010.

[70] S.S. Christensen, R. Argawal, E. de Carrvalho, and J.M. Cioffi, "Weighted Sum-Rate Maximization Using Weighted MMSE for MIMO-BC Beamforming Design," *IEEE Transactions on Wireless Communications,* vol. 7, no. 12, pp. 4792-4800, Dec. 2008.

[71] M.F. Hanif, L. Tran, A. tolli, and M. Junti, "Computationally Efficient Robust Beamforming for SINR Balancing in Multicell Downlink with Applications to Large Antenna Array Systems," *IEEE Transactions on Communications*, vol. 62, no. 6, pp. 1908-1920, June 2014.

[72] A. Alfa, B.T. Maharaj, S. Lall, and S. Pal, "Mixed-Integer Programming Based Techniques for Resource Allocation in Underlay Cognitive Radio Networks: A Survey," *Journal of Communications and Networks*, vol. 18, no.5, pp. 744-761, Oct. 2016.

[73] F. Alizadeh and D. Goldfarb, "Second-Order Cone Programming," *Mathematical Programming*, vol. 95, no. 1, pp. 3-51, Jan. 2003.

[74] T. Yoo and A. Goldsmith, "Capacity and Power Allocation for Fading MIMO Channels with Channel Estimation Error," *IEEE Transactions on Information Theory*, vol. 52, no. 5, pp. 2203-2214, May 2006.

[75] P. Zhao, M. Zhang, H. Yu, H. Luo, and W. Chen, "Robust beamforming Design for Sum Secrecy Rate Optimisation in MU-MISO Networks," *IEEE Transactions on Information Forensics and Security*, vol. 10, no. 9, Sept. 2015.

[76] A. Tajer, N. Prasad, and X. Wang, "Robust Linear Precoder Design for Multi-Cell Downlink Transmission," *IEEE Transactions on Signal Processing*, vol. 59, no. 1, pp. 235-251, Jan. 2011.

[77] A. Ben-Tal and A. Nemirovski, "Robust Solutions of Uncertain Linear Programs," *Operations Research Letters*, vol. 25, no. 1, pp. 1-13, Aug. 1999.

[78] D. Bertsimas and M. Sim, "The Price of Robustness," *Operations Research*, vol. 52, no. 1, pp. 35-53, Jan. 2004.

[79] D. Bertsimas, D. Pachamanova, and M. Sim, "Robust Linear Optimisation under General Norms," *Operations Research Letters*, vol. 32, no. 6, pp. 510-516, Nov. 2004.

[80] J. Lofberg, "YALMIP: A Toolbox for Modeling and Optimisation in MATLAB," in *IEEE International Conference on Robotics and Automation*, 2004, pp. 284-289.

[81] J.F. Sturm, "Using SeDuMi 1.02, a MATLAB Toolbox for Optimisation over Symmetric Cones," *Optimisation Methods and Software*, vol. 11, no. 1-4, pp. 625-653, 1999.

[82] J. Mattingley, and S. Boyd, "CVXGEN: A Code Generator for Embedded Convex Optimisation," *Optimisation and Engineering*, vol. 13, no. 1, pp. 1-27, Mar. 2012.

[83] E. Chu, N. Parikh, A. Domahidi, and S. Boyd, "Code Generation for Embedded Second-Order Cone Programming," in *European Control Conference (ECC)*, 2013, pp. 1547-1552.

[84] A. Domahidi, "FORCES: Fast Optimisation for Real-Time Control on Embedded Systems," Available at forces.ethz.ch, Oct. 2012.

[85] B. Houska, H. Ferreau, and M. Diehl, "ACADO Toolkit – An Open Source Framework for automatic Control and Dynamic Optimisation," *Optimal Control Applications and Methods*, vol. 32, no. 3, pp. 298-312, May 2011.

[86] Y. Shi, J. Zhang, and K.B. Letaief, "Scalable Coordinated Beamforming for Dense Wireless Cooperative Networks," in *IEEE Global Communications Conference (GLOBECOM)*, 2014, pp. 3603-3608.

[87] S. Zarei, W. Gerstarcker, and R. Schober, "Uplink/Downlink Duality in Massive MIMO Systems with Hardware Impairments," in *IEEE International Conference on Communications (ICC)*, 2016, pp. 1-7.

[88] I. Telatar, "Capacity of Multi-Antenna Gaussian Channels," Bell Labs Technical Memorandum, June 1995.

[89] S.I.A. Ahmed and K.K. Wong, "On the MIMO Capacity with Imperfect CSI," *London Communications Symposium*, 2007, pp. 1-4.

[90] D. Bertsimas and M. Sim, "Tractable Approximations to Robust Conic Optimization Problems," *Mathematical Programming*, vol. 107, no. 1, pp. 5-36, Jun. 2006.

[91] L.S. Liberti, "Reformulation and Convex Relaxation Techniques for Global Optimisation," PhD. Dissertation, Imperial College London (University of London), 2004.

[92] M.M. Sande, B.T. Maharaj, and S. Hamouda, "Fast Convergence for Efficient Beamforming in Massive MIMO Heterogeneous Networks," in *IEEE 12th International Conference on Wireless and Mobile Computing, Networking and Communications (WiMob)*, 2016, pp. 1-7.

[93] B. O'Donoghue, E. Chu, N. Parikh, and S. Boyd, "Operator Splitting for Conic Optimisation via Homogeneous Self-Dual Embedding," *Journal of Optimisation Theory and Applications*, vol. 168, no. 2, pp. 1-27, Feb. 2016.

[94] E.M.B. Smith and C.C. Pantelides, "A Symbolic Reformulation/Spatial Branch-and-Bound Algorithm for the Global Optimisation of Nonconvex MINLPs," *Computers and Chemical Engineering*, vol. 23, no. 4-5, pp. 457-478, May 1999.

[95] Y. Shi, J. Zhang, B. O'Donoghue, and K.B. Letaief, "Large-Scale Convex Optimisation for Dense Wireless Cooperative Networks," *IEEE Transactions on Signal Processing*, vol. 63, no. 18, pp. 4729-4743, Sept. 2015.

[96] Y. Ye, M. Todd, and S. Mizuno, "An O(√*n*L)-Iteration Homogeneous and Self-Dual Linear Programming Algorithm," *Mathematics of Operations Research*, vol. 19, no. 1, pp. 53-67, Feb. 1994.

[97] S. Boyd, N. Parikh, E. Chu, B. Peleato, and J. Eckstein, "Distributed Optimisation and Statistical Learning via the Alternative Direction Method of Multipliers," *Foundations and Trends in machine Learning*, vol. 3, no.1, pp. 1-122, 2011.

[98] O. Goldreich, *Computational Complexity: A Conceptual Perspective*, Cambridge University Press, 2010.

[99] Further Advancements for E-UTRA Physical Layer Aspect (Release 9). 3GPP TS 36.814, Mar. 2010.

[100] A Tremba *et al.*, "RACT: Randomized Algorithms Control Toolbox for MATLAB," *IFAC Proceedings Volumes*, vol. 41, no. 2, pp. 390-395, July 2008.

ADDENDUM A PROOF OF SELF-DUAL PROPERTY

This section shows that the system in (4.37), given in (A.1) below, is self-dual.

$$\begin{aligned} &\text{find } (p, r) \\ &\text{subject to } r = Qp \\ &(p, r) \in \mathbb{C} \times \mathbb{C}^*. \end{aligned} \tag{A.1}$$

The Lagrangian of problem (A.1) can be written as

$$L(p, r, v, \lambda, \mu) = v^T(Qu - r) - \lambda^T u - \mu^T r, \tag{A.2}$$

where v, λ, μ are the dual variables, with $\lambda \in \mathbb{C}^*$, and $\mu \in \mathbb{C}$. By minimising the Lagrangian over the primal variables, *p*, *r*, one sees that

$$Q^T v - \lambda = 0, \tag{A.3}$$

and

$$-v - \mu = 0. \tag{A.4}$$

Using $v = -\mu$ from (A.4) to eliminate v, and $Q^T = -Q$, the dual problem is given as

$$\begin{aligned} &\text{find } (\lambda, \mu) \\ &\text{subject to } \lambda = Q\mu \\ &(\lambda, \mu) \in \mathbb{C} \times \mathbb{C}^*, \end{aligned} \tag{A.5}$$

which is identical to (A.1) with the variables λ, μ instead of p, r.